DOI:10.14753/SE.2022.2766

SEMMELWEIS EGYETEM

DOKTORI ISKOLA

Ph.D. értekezések

2766.

PALCSÓ BARNABÁS

A gyógyszerészeti tudományok korszerű kutatási irányai
című program

Programvezető: Dr. Antal István, egyetemi tanár

Témavezető: Dr. Zelkó Romána, egyetemi tanár

DOI:10.14753/SE.2022.2766

FORMULATION AND CHARACTERIZATION OF CHLORINE-DIOXIDE-RELEASING, POLYMER-BASED DELIVERY SYSTEMS

PhD thesis

Barnabás Palcsó

Doctoral School of Pharmaceutical Sciences

Semmelweis University

Supervisor: Romána Zelkó, D.Sc., professor

Official reviewers: Rita Ambrus, Ph.D., associate professor
Krisztina Ludányi, Ph.D., associate professor

Head of the Complex Examination Committee:
István Antal, Ph.D., professor

Members of the Complex Examination Committee:
Piroska Szabó-Révész, D.Sc., professor
Imre Klebovich, D.Sc., professor

Budapest
2022

DOI:10.14753/SE.2022.2766

TABLE OF CONTENTS

DOI:10.14753/SE.2022.2766

DOI:10.14753/SE.2022.2766

LIST OF ABBREVIATIONS

CFU	colony forming unit
ClO_2	chlorine dioxide
Cys	cysteine
FTIR	Fourier transform infrared spectroscopy
FWHM	full width at half maximum
GSH	glutathione
MRSA	Methicillin-resistant *Staphylococcus aureus*
$NaClO_2$	sodium chlorite
NAR	no adverse reaction
NR	not reported
o-Ps	ortho-positronium
PAA	poly(acrylic acid)
PALS	positron annihilation lifetime spectroscopy
PEO	poly(ethylene oxide)
SEM	scanning electron microscopy
T3	triiodothyronine
T4	thyroxine
TNTC	too numerous to count
Trp	tryptophan
Tyr	tyrosine
UV-VIS	ultraviolet–visible spectroscopy

DOI:10.14753/SE.2022.2766

1. INTRODUCTION

Over the past few decades and especially in the last 2 and a half years a greater emphasis is put on antiseptic agents in public health. Antiseptics possess general mechanisms of action by which they are able to eliminate a great variety of pathogens. Such agents could aid the fight against widespread antimicrobial resistance and slow down the escalation of an epidemic. Polymer-based formulations are suitable carriers for such agents as they enable their application under multiple circumstances.

1.1. The main characteristics of chlorine dioxide

1.1.1. Physical and chemical properties of chlorine dioxide

Chlorine dioxide (ClO_2) is a greenish-yellow gas at room temperature with a boiling point of 11°C and a chlorine-like odor. (1). The oxidation number of the chlorine atom in the molecule is +4, the 3 atoms share a total number of 19 valence electrons, thus the ClO_2 molecule is neutral and exists as a free radical (2). Figure 1 shows two possible states of electron distribution in the molecule.

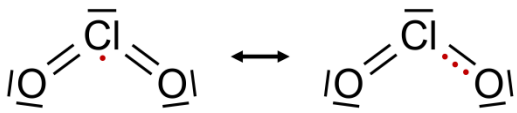

Figure 1 Molecular geometry and two of the possible Lewis structures of ClO_2.

One of the unusual properties of ClO_2 is the stability despite the unpaired electron present in the molecule. Under normal conditions, no reaction occurs between ClO_2 molecules. However, the storage of the substance still represents a considerable difficulty. Upon exposure to light, ClO_2 undergoes a rapid photodecomposition reaction (3). If the concentration of the gas is higher than 10% (v/v) in the storage tank, an explosive decomposition takes place in the presence of air (4). Due to the restrictions regarding the transportation of gaseous ClO_2, the substance is usually generated *in situ* at the site of use (5).

DOI:10.14753/SE.2022.2766

Chlorine dioxide is highly soluble in water and does not react upon dissolution. Due to its volatility, it liberates rapidly from the aqueous solution (1). When protected from light, the neutral aqueous solution of ClO_2 can be stored for long periods of time at cool temperatures, especially in fully filled amber glass bottles. Some of the commercially available aqueous ClO_2 products are fitted with a special two-piece cap that is impermeable to ClO_2. When there is a headspace above the aqueous solution, ClO_2 is distributed between the two phases. The concentration of the aqueous and gaseous form is determined by the temperature and can be calculated with an equilibrium ratio (6). The concentration of ClO_2 is usually given in ppm, which stands for mg/L in aqueous solutions or μL/L in the gas phase.

1.1.2. Methods for ClO_2 production

The main source of ClO_2 generation is usually sodium chlorite ($NaClO_2$). Chlorite ion has to undergo oxidation to form ClO_2. One of the common methods uses chlorine in the form of an aqueous solution or moist gas. The chlorite ion – chlorine reaction can be described by Eq. 1 (gaseous) and 2 (aqueous) (7).

$$2\ ClO_2^- + Cl_2 \rightarrow 2\ ClO_2 + 2\ Cl^- \qquad \text{(Eq. 1)}$$

$$2\ ClO_2^- + HOCl \rightarrow 2\ ClO_2 + 2\ Cl^- + OH^- \qquad \text{(Eq. 2)}$$

Water treatment facilities usually use this method to generate ClO_2. Chlorine water and chlorite solution are introduced simultaneously into the reaction chamber, while the generated ClO_2 is discharged into the water system (8).

Chlorite ions can undergo protonation and self-decomposition reaction in the presence of acid. In this reaction ClO_2, chloride and chlorate ions are produced. Chloride ion functions as a catalyzer, thus ClO_2 is formed more effectively as the reaction proceeds. In the beginning, only half of the chlorite ions produce ClO_2. As the concentration of chloride increases, the stoichiometry changes and 80% of the chlorite ion forms ClO_2. The actual stoichiometry is a linear combination of the two limiting cases. Eq. 3 describes the protonation of the chlorite ion, while Eq. 4 and 5 show the uncatalyzed and catalyzed reactions, respectively (9).

$$H^+ + ClO_2^- \rightleftharpoons HClO_2 \quad \text{(Eq. 3)}$$

$$4\ HClO_2 \rightarrow 2\ ClO_2 + ClO_3^- + Cl^- + 2\ H^+ + H_2O \quad \text{(Eq. 4)}$$

$$5\ HClO_2 \rightarrow 4\ ClO_2 + Cl^- + H^+ + 2\ H_2O \quad \text{(Eq. 5)}$$

The major drawback of this system is that chlorate ion is produced and the yield of ClO_2 is lower due to the formation of chlorate and chloride ions. This method is often used in the paper industry.

An electrochemical method can be also used to oxidize chlorite ions. The reaction is described by Eq. 6.

$$2\ ClO_2^- + 2H_2O \rightarrow 2\ ClO_2 + 2\ OH^- + H_2 \quad \text{(Eq. 6)}$$

This reaction uses only one starting material and generates no chlorate or chloride ion, thus the yield is at maximum. The electrochemical generator is suitable for lab-scale production of ClO_2.

It is possible to produce ClO_2 from chlorate ions and hydrogen peroxide. A strong acidic media is required for the reduction of chlorate. In the reaction, oxygen is generated as a by-product. The shortcoming of the system is that chlorate ion and hydrogen peroxide is generated via electrolysis and the optimum operation conditions of these methods are not yet established (10).

1.1.3. Reactivity and mechanism of action of ClO_2

Chlorine dioxide is regarded as a strong oxidizing agent, transferring one electron from its reaction partner in most cases. In the first step ClO_2 forms chlorite ion (ClO_2^-), while under suitable conditions, further reduction leads to the formation of chloride ion. Despite its reactive nature, ClO_2 is rather a selective oxidant. In its reactions with organic molecules, ClO_2 does not break the carbon-carbon bonds, thus chlorination does not occur. The reactions of ClO_2 with carbohydrates, alcohols, primary and secondary amines and carbonyl groups have been examined several decades ago (11). These reactions are considered to be slow compared to the oxidation

DOI:10.14753/SE.2022.2766

of the thiol group, phenolic compounds, and tertiary amines, that react with ClO_2 rapidly (12).

Experiments investigating the mechanism of the antimicrobial activity of ClO_2 revealed that the inactivation of pathogens by ClO_2 relies on its reactions with proteins. An early examination showed that the reaction with the viral capsid proteins leads to the elimination of the bacterial virus f2, while the viral RNA is mostly unaffected (13). Since then, a deeper understanding of the ClO_2 – protein reactions have been acquired. It has been found that three amino acids, cysteine, containing a thiol group, tyrosine, a phenolic compound, and tryptophan with an indole side chain are the most reactive components of the viral peptides (14-18). The rapid oxidative modification of these amino acids by ClO_2 leads to the denaturation of the protein and the subsequent elimination of the pathogen (19). Figure 2 shows the three fast-acting amino acids and the products formed in the reaction with ClO_2. The oxidation leads to the formation of covalent bonds between thiol groups of cysteine and changes in the capability for secondary interactions in the case of tyrosine and tryptophan, thus modifications of the tertiary and quaternary protein structure occur.

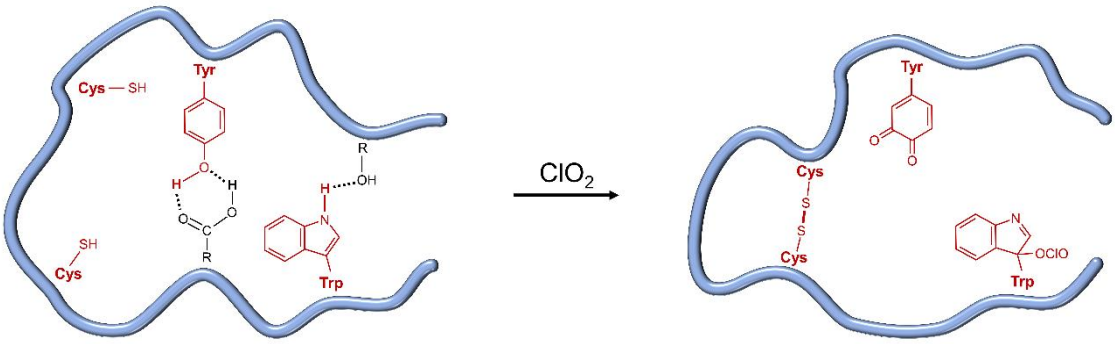

Figure 2 Oxidation of amino acids in the presence of ClO_2 and illustration of the subsequent changes in the protein structure.

1.1.4. Antimicrobial spectrum of ClO_2

The antimicrobial activity of ClO_2 relies on the inhibition of proteins which results in loss of function and inhibition of vital functions of the pathogens. Since proteins are universal macromolecules across cells and viruses, ClO_2 is potentially effective against all kinds of pathogens, including viruses, bacteria, fungi, and protozoa.

As mentioned above, the reaction between ClO_2 and viral peptides has been in the focus of investigations for a long time. The effectiveness of ClO_2 gas against influenza A virus has been proven in an experiment where ClO_2 was administered simultaneously with the aerosol of the virus. A very low concentration of the gas was able to decrease mortality to zero among mice (20). The strong inactivation of influenza A was due to the inhibition of the receptor-binding ability of the virus via the oxidation of a tryptophan in the hemagglutinin spike protein (21). The effectiveness of ClO_2 against a great variety of viruses, such as polio, rotavirus, hepatitis A and H1N1 has been confirmed (22-26). In these experiments, ClO_2 aqueous solutions of different concentrations were used. A 4-log removal of viruses was achieved in the 0.2 - 1.0 ppm concentration range, depending on the species. The contact time during which the given magnitude of reduction was achieved, varied between 2 and 60 minutes. Influenza A H1N1, an enveloped virus was among the more species with an above 4.5-log reduction under 5 minutes in the presence of 0.5 ppm ClO_2 solution, while 0.4 ppm ClO_2 reached a 4-log reduction of the non-enveloped hepatitis A virus under 20 minutes.

The volatility of ClO_2 plays a significant role in its antimicrobial effectiveness. It is able to reach and kill pathogens in the gas phase and areas where regular antiseptics have no access. However, it has been shown that ClO_2 gas itself has lower effectiveness against viruses in a ‘dry state’ compared to when moisture is present, thus a certain level of humidity is desired when gaseous ClO_2 is used (27).

Bacteria are a magnitude larger in size, have more complex cell functions and contain a higher concentration of substrates for ClO_2, thus higher concentrations are required for bacterial inactivation. An aqueous ClO_2 concentration of 5 ppm was found to be suitable for the elimination of *Pseudomonas aeruginosa* and *Staphylococcus aureus*. The investigation of bacterial cell morphology revealed that ClO_2 is likely to kill the pathogen by diffusing through the cell wall to deactivate its substrates proteins. An increased cytoplasmic and outer membrane permeability and release of the vital cell structures lead to the death of bacteria (28). A number of nosocomial pathogens, including MRSA were isolated from sources such as blood, urine and wound infection and were exposed to sub-toxic levels of ClO_2 and chlorine gas. No survival could be observed in the ClO_2 group. However, partial growth was seen with chlorine gas. The amount of the two oxidizing agents was similar, unfortunately, exact data on the

concentrations are not available (29). Highly prevalent nosocomial pathogens (Pseudomonas spp., Stenotrophomonas spp. and non-tuberculotic mycobacteria) were eliminated from the water of a hospital after the introduction of 0.3-0.5 ppm ClO_2 into the system (30). Chlorine dioxide shows strong inactivating effect against high-resistance bacterial structures, such as *Bacillus anthracis* spores and biofilms (31-33). As the main structural elements and macromolecules are the same across organisms, ClO_2 is effective against a wide range of species. Inactivation of fungi, algae, zooplankton, and larvae has been reported (34-37).

1.1.5. Applications of ClO_2

After its discovery in 1814, ClO_2 served mostly as a water purifying agent in Europe and later in the US (38). It replaced chlorine in water treatment plants due to its ability to eliminate pathogens effectively and remove phenolic odors and tastes from water over a wide pH range without forming chlorinated organic compounds (39, 40). The maximum concentration of the oxidizing agent allowed in municipal water treatment is 0.8 ppm, while 4 ppm can be used in surface water treatment. Later ClO_2 supplanted chlorine also in the paper industry. With the use of ClO_2 as a bleaching agent, durable and white fibers can be produced without the unwanted by-products associated with chlorine. The ClO_2 concentration for wood pulp bleaching is usually above 5000 ppm. Recently, ClO_2 was approved as a disinfectant and bleaching agent in the food industry. The maximum ClO_2 concentration can be 3 ppm when it is used as a bleaching agent for flour or as an antimicrobial agent in poultry processing (41).

Despite being approved as antiseptic, the use of ClO_2 has not been widespread in the medical field as topical disinfectant. Among the factors restricting its use are the transportation and storage requirements of ClO_2. It should be generated at the site of use with one of the methods mentioned above. The continuous and large-scale production of ClO_2 at the site of application can be efficient and sustainable in water plants or in the paper industry, however, these methods are hard to implement in a clinical setting. The presence of impurities and by-products in the produced ClO_2 solution, such as acid or chlorate are also matters of concern. However, decontamination of surfaces and air in medical facilities have been successfully carried out. A number of hospitals uses ClO_2 to reduce microbial colonization in their water systems (42-44). In the past few years,

decontamination of ambulance vehicles and hospital rooms with gaseous ClO_2 has also been reported (45-48).

So far, the application of ClO_2 in human medicine has been mostly on an experimental level. There are commercially available ClO_2-containing products on the market, such as mouthwashes, however, these are mostly two-part products containing a $NaClO_2$ solutions and an acidic solution separately. The use of ClO_2 in healthcare is burdened by pseudoscience, which proposes ClO_2 as an ultimate solution to serious illnesses and suggests the oral administration of high-concentration ClO_2 solutions. In these cases, usually an acidic $NaClO_2$ solution is used instead of pure ClO_2 aqueous solution (49). The potential use of ClO_2 as topical disinfectant is supported by several studies. When applied on an infected human skin simulant, ClO_2 was able to eliminate *Bacillus anthracis* spores successfully. In addition, the toxicity of ClO_2 was significantly lower than that of $NaClO_2$ (32). In a randomized controlled trial, ClO_2 showed substantial antibacterial effect as a wound irrigant and caused no skin-related adverse effects (50). Chlorine dioxide shows promising results in oral and dental infections. When used as a mouth rinse in chronic candidiasis of the oral mucosa, it reduced the total CFU significantly after 10 days of treatment, without any major side effects (51). Similarly, ClO_2 was able to reduce tongue coat and dental plaque formation substantially when administered as a mouthwash (35, 52). High purity ClO_2 aqueous solution was more effective against intracanal biofilm than other conventional antiseptics used in dental care (53). In conclusion, data support the topical use of ClO2 in infections, however, caution is required regarding the concentration and purity of the applied aqueous solution.

1.2. Toxicological profile and the safety of ClO_2

Chlorine dioxide is a strong oxidizing agent that exists in gaseous and aqueous forms, therefore its potential adverse reactions after inhalation and oral administration have to be evaluated. Data on its toxicity in humans is derived mainly from reports of occupational accidents and unintentional self-poisonings with unspecified ClO_2 products. Designed studies are available about the effects of acute and chronic ClO_2 administration in animals. A hindering factor in the evaluation of the safety of ClO_2 is that in a number of studies about the effectiveness of ClO_2 and the adverse reactions

related to the treatment, ‘activated’ or ‘stabilized’ ClO_2 is used, indicating that ClO_2 is generated via the reaction between $NaClO_2$ and acid. In case reports discussing ClO_2 intoxication, such ClO_2 product is usually mentioned as the source of poisoning. In these cases, the ClO_2 solution is prepared by mixing (‘activating’) the aqueous $NaClO_2$ solution (the ‘stabilized ClO_2’) upon application with the other component, which is the aqueous solution of a weak acid, such as lactic or citric acid. As discussed before, such a mixture contains starting materials and by-products from the chlorite – acid reaction that can affect the biocompatibility and toxicity of the ClO_2 solution.

1.2.1. Inhalation

Gaseous ClO_2 and aqueous ClO_2 mist act as a respiratory tract irritants. The main clinical signs of respiratory toxicity include pulmonary oedema, bronchitis and alveolar lesions. One case report has been published regarding death in humans due to gaseous ClO_2. According to the report, a bleach tank worker died after being exposed to ClO_2 vapor for an unspecified amount of time (4). In another case, 13 water purification plant workers suffered from chronic nasal inflammation after being exposed to ClO_2 gas from a leak in the pipe system (54). A woman experienced coughing and pharyngeal irritation after inhaling the vapor of a ClO_2-containing bleaching agent. Tachycardia and leukocytosis were also diagnosed after hospitalization (55). A great amount of data is available regarding the respiratory effect of ClO_2 on animals. Table 1 is a non-exhaustive summary of the available reported data. The extent of damage caused by the inhaled gas is determined by the concentration of ClO_2 and the exposure time. To help the comparison of the administration schedules and the total ClO_2 intake, a concentration – time value was calculated by multiplying the concentrations with the total number of hours during which the animals were exposed to the gas. If the exposure time is below 14 days, the treatment is regarded as acute. The exposure time is intermediate when the duration of administration is between 15 and 364 days (4). The effect of ClO_2 on the respiratory system ranges from slight bronchitis to pulmonary inflammation, lesions and nasal bleeding, depending on the concentrations and exposure times. Considering the concentration – time values and outcomes, it is hard to set up a dose-response correlation for the respiratory effects of ClO_2.

1.2.2. Oral administration

The probability of producing systemic toxicity in humans is low due to the reactive nature of ClO_2. After oral intake, ClO_2 reacts with its substrates, mostly proteins present in the digestive system. In these reactions chlorite is formed, thus the effect of chlorite has to be considered. As mentioned before, the presence of chlorite in the various ClO_2 products also hinders the evaluation of adverse reactions associated with ClO_2. To this date, no death associated with the oral intake of ClO_2 was reported in the literature. The evidence on the nature and severity of adverse reactions following the oral administration of ClO2 is sporadic and small in number. A case study reports the formation of acute and reversible kidney injury due to acute tubular necrosis after the oral administration of 250 ml of 'stable ClO_2' in a 20-year-old male (56). After drinking a nonspecified form and amount of ClO_2 solution, a 55-year-old male was hospitalized with nausea, vomiting and altered mental state (57). To evaluate the effect of ClO2 on the development during pregnancy, the data from two groups of women were compared. The first group lived in an area where tap water was disinfected with ClO_2 and chlorite, the second group got access only to drinking water from wells. Higher risk for neonatal jaundice, smaller cranial circumference and body length was found in infants from the first group. However, no other factors, as differences in exposure to chemicals or nutritional habits were considered (58).

Another study found no congenital malformations, neonatal jaundice or lower Apgar scores in children how lived in an area where drinking water was treated with ClO_2 (59). No adverse reactions were observed in male volunteers after acute and intermediate intake of ClO_2 solution (60, 61). More data is available on the systemic effects of ClO_2 in animals. Table 2 shows the clinical outcomes of the administration of the given doses. The most common adverse reactions associated with the oral intake of ClO_2 were the damage of the mucosa in digestive system, change in thyroid hormone levels (T3, T4) and haematological alterations. However, most alterations in serum levels were temporary and the dose-response correlations were not significant. Methemoglobinemia, a serious consequence of chlorite intake could not be observed in the case of ClO_2.

DOI:10.14753/SE.2022.2766

Table 1 Clinical outcome of acute and intermediate exposure of ClO_2 inhalation in animals. NAR: no adverse reaction, NR: not reported.

Concentration (ppm)	Exposure time/ frequency/ duration	Concentration – time value (ppm h)	Species	Death rate (%)	Clinical signs of toxicity	Ref.
Acute exposure						
10	4 h/day for 9 of 13 days	360	rat	60	rhinorrhea, altered respiration, secondary liver congestion	(62)
20	24 h	480	mouse	0	NAR	(63)
150	0.25 h	12.5 – 37.5	guinea pig	0	NR	(64)
150	0.75 h	110	guinea pig	100	NR	
260	2 h	520	rat	25	pulmonary oedema, nasal bleeding, circulatory engorgement	(62)
Intermediate exposure						
0.1	24 h/day for 6 months	432	rat	0	NAR	(65)
0.1	5 h/day for 2.5 months	35	rat	0	NAR	(62)
1	5 h/day, 5 days/week for 2 months	212.5	rat	0	vascular congestion, peribronchiolar oedema	(66)
2.5	7 h/day for 1 month	525	rat	0	bronchial inflammation, alveolar congestion and haemorrhage	(67)
2.5	4 h/day for 1.5 months	450	rabbit	0	slight pulmonary irritation	
15	1 h/day for 1 month	450	rat	7	nasal and ocular inflammation, bronchitis, alveolar lesions	(68)

DOI:10.14753/SE.2022.2766

Table 2 Clinical outcome of oral administration of ClO_2 solution in human and animal subjects. NAR: no adverse reaction.

Dose (mg/kg/day)	Exposure time	Species	Clinical signs of toxicity	Ref.
0.04	3 months	human	NAR	(60)
0.0014 - 0.34	5 in 16 days	human	NAR	(61)
9	2-3 months	African green monkey	oral erythema, ulceration, reduced serum T4	(69)
13	52 days (10 days prior mating, under gestation and lactation)	rat (female)	T3 uptake decreased temporarily, temporarily decreased locomotor activity (in pups)	(70)
13	56 days (14 days prior mating, under gestation and lactation)	rat (female)	decreased T4, elevated T3 levels (in pups)	(71)
14	16 days postnatal	rat (pup)	decreased T4, lower bodyweight	
14	20 days postnatal	rat (pup)	lower bodyweight, decreased forebrain weights	(72)
40	3 months	mouse	NAR	(63)
80	13 weeks	rat	ulceration, chronic inflammation, oedema, hyperkeratosis, epithelial hyperplasia	(73)
0.1 – 100	12 months	rat	decreased osmotic fragility – at 2 months; decreased testicular DNA synthesis - at 3 months; increased haematocrit – at 7 months; decreased erythrocyte, haematocrit, haemoglobin levels - at 9 months; reduced bodyweight	(74)

1.2.3. Protective factors against ClO_2 in organisms

When rats were exposed to various concentrations of ClO_2 (1-100 ppm) during a 2-month period, changes in the GSH reductase and peroxidase levels could be measured and blood GSH levels decreased. Glutathione was identified as the main protective factor in the cells (75). Antioxidants, such as glutathione have an important role in the protection of cells against oxidizing agents. The rate of the reaction between glutathione and ClO_2 is higher than the rate of the cysteine – ClO_2 reaction, which is known to be the fastest reacting amino acid (15). On a cellular level, pure ClO_2 showed significantly lower toxicity in periodontal ligament stem cells, compared to chlorhexidine and hydrogen peroxide (76).

Cells have access to continuous exchange of nutrients and waste through tissue fluid and blood flow. The oxidized substrates can be transported, and a permanent supply of protective factors is provided. Besides the GSH content of the cells and the protective role of blood flow, the relative safety of ClO_2 relies also on its size selectivity. If we assume that ClO_2 needs to enter and fill up the cell or pathogen in order to be able to eliminate it, the size of the target organism is crucial. Animal and human cells are much larger in size and contain a larger amount of substrate for ClO_2. The time required for ClO_2 to permeate through tissue via diffusion is several magnitudes larger than the amount of time needed to fill up and kill bacteria. In addition, the concentrations used in disinfection processes are below the tolerability levels for humans (12).

1.3. Polymer-based formulations of antiseptics

1.3.1. Antimicrobial resistance and the need for antiseptics

The widespread of drug-resistant pathogens became one of the most serious challenges in modern medicine. The combination of several concurrent factors, such as over-prescription and misuse of antibiotics in public healthcare, their extensive use in agriculture along with a decrease in the development of new antimicrobials led to a major socio-economic issue (77, 78). To address these problems, it is crucial to minimize all kinds of non-adequate antibiotic use but also to find safe and effective alternatives in the elimination of pathogens. Disinfectants and antiseptics are considered less susceptible to microbial resistance, as their mechanisms of action are more ‘general’ than in the case of antibiotics. Biocides eliminate pathogens by destroying the cell wall and/or macromolecules essential for the microorganism. Due to the way of

action, biocides are universal in the sense that they are effective against a broad spectrum of pathogens, but the susceptibility of microorganisms can vary considerably (79, 80). Both groups of antimicrobial substances are in the focus of prevention of nosocomial and community-acquired infections (81-83). Although antiseptic agents are effective against a wide range of pathogens, they do not cover the whole spectrum. Relative resistance against widely used biocides has also been reported (84-87).

A great advantage of ClO_2 is its insusceptibility to microbial resistance mechanisms as the mutations in the amino acid sequence do not change the general susceptibility of the proteins to the denaturalizing effect of ClO_2. However, it was found that different serotypes of the same viral species show different susceptibility to ClO_2 depending on the amino acid sequence of the viral protein (26, 88). Considering the various reaction rates of the oxidation of amino acids, it can be presumed that the actual inactivation efficiency of a given species depends on the number and position of the fast-reacting moieties present in the crucial protein regions. By adjusting the concentration of ClO_2, effective antimicrobial activity can be achieved (89).

1.3.2. Antiseptic hydrogels and viscous solutions

Polymer-based viscous solutions and hydrogels have an extensive application in topical antimicrobial therapy and wound management. By selecting the suitable monomer and the molecular weight of the polymer, the physicochemical properties of the solution or hydrogel can be easily optimized. Complexes, copolymers and blends consisting of two or more types of polymers increase the possibilities even further when choosing a material that meets our needs. Depending on the polymer type, concentration and cross-linking, polymeric solutions can be used as spreadable gels or coatings with a stable three-dimensional matrix. The antimicrobial activity of a polymer-based formulation can be designed via several methods. Hydrogels can be prepared from polymers with intrinsic antiseptic properties, or an antimicrobial substance can be added to the formulation (90, 91).

Polymers can possess intrinsic antimicrobial activity by mimicking the structure of host-defense peptides. Upon contact with the bacterial surface, the macromolecules form pores in the membrane of the pathogen which leads to disruption and elimination. The presence of cationic monomers can provide selective interaction with negatively charged bacterial surfaces. Due to the similar nature of cell membranes across the organisms, the human blood cells are also subjected to the membrane-damaging effect

of these polymers. An important aspect of polymer synthesis is to achieve an optimum between hydrophobic and cationic monomers to minimize hemolytic and increase antimicrobial effects (92). Fitted with suitable sidechains, polymers such as polynorbornene, polyoxanorbornene, polymethacrylate, polycarbonate and nylon-based poly(β-lactam) represent such antimicrobial activity (93-96). Polymaleimide was found to have a strong biofilm-disrupting property and was able to eliminate *Acinetobacter baumannii* biofilms (33).

Hydrogels formed by certain polymers are able to kill pathogens upon contact. Natural chitosan is a well-known polymer that forms hydrogels with antimicrobial activity. Synthetic modifications, such as the attachment of cationic groups, can enhance the biocide character of the formulation (97). Polymers made from cationic amino acids and polycarbonate-based hydrogels also show a substantial antimicrobial effect (98, 99).

By the incorporation of an antimicrobial agent in the polymer matrix, a great variety of combinations can be achieved. The polymer hydrogel can be formed from a number of macromolecules, however, a crucial element of the selection of the ingredients is the potential incompatibilities occurring between them. In the first part of my work, polyacrylic acid was selected as a biocompatible polymer that is able to withstand the oxidizing effect of ClO_2. The incorporated antimicrobial agent is usually an antibiotic or a metal ion, such as silver or gold (100-103). Polymer-based viscous solutions and hydrogels containing povidone-iodine, chlorhexidine, silver sulfadiazine and octenidine as antimicrobial agents are available on the market.

1.3.3. Preparation of antimicrobial nanofibers by electrospinning

Electrospinning is a long-known but rapidly developing and versatile method for nanofiber production. Fibers can be obtained from polymer solutions without major applying extreme conditions, thus the incorporation of sensitive substances is possible. Figure 3 shows the basic setup of a laboratory instrument. Electrospinning is carried out from a polymer viscous solution. The polymer is squeezed out from the tip of a needle by the syringe pump. High voltage is connected to the needle, while the collector is grounded. Due to the electric field, charged particles appear on the surface of the polymer droplet. After surpassing a threshold, the droplet gets elongated and ejected onto the collector. Between the needle and collector, the solvent evaporates thus solid polymer fibers are formed.

DOI:10.14753/SE.2022.2766

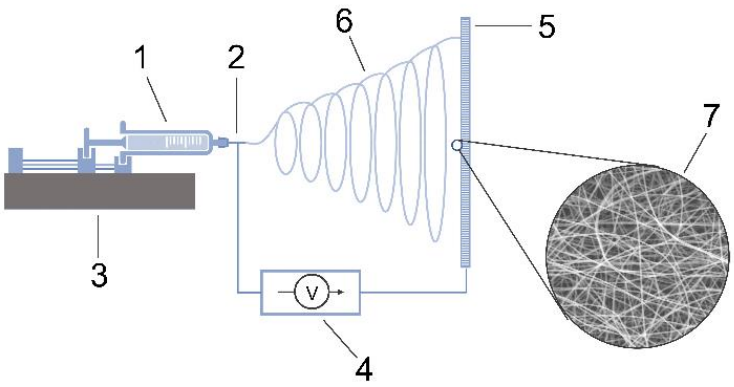

Figure 3 Basic electrospinning setup. Polymer solution in syringe (1), metal needle (2), syringe pump (3), voltage supply (4), collector (5), ejected jet (6), nanofibrous mesh (7).

Due to their unique physicochemical and morphological properties and the great number of polymers available for electrospinning, nanofibrous polymer scaffolds became a focus of tissue engineering and drug delivery studies. By selecting a suitable polymer or incorporating antimicrobial agents into the fibers, various polymer-based nanofibrous compositions can be attained for the elimination of pathogens (104). The average fiber diameter is usually between 100 and 1000 nm, which results in high porosity and surface-to-volume ratio. These characteristics provide improved attachment and inhibition of pathogens of similar magnitude of size (e.g., bacteria) (105, 106). On the other hand, the nanofiber matrix is able to change the dissolution profile and increase the apparent solubility of the antimicrobial drug upon incorporation (107).

As discussed before, some polymers, such as chitosan, possess inherent antimicrobial activity. With the help of an auxiliary polymer, an antibacterial nanofibrous scaffold can be electrospun from chitosan (108). The electrospinning of polymers derived from cationic amino acids, such as ε-poly-lysine, is also feasible, thus antimicrobial scaffolds can be obtained (98, 109). Encapsulation of antimicrobial molecules, such as metal particles, antibiotics, graphene oxide and antimicrobial peptides can be achieved with a great number and combination of polymers (110, 111).

Regarding my work, $NaClO_2$ was incorporated into poly(ethylene oxide) (PEO) nanofibers. Despite $NaClO_2$ possessing an antimicrobial effect, the nanofibrous mesh was not designed for direct contact, rather it was the starting material and a generator for ClO_2.

DOI:10.14753/SE.2022.2766

2. OBJECTIVES

The purpose of my work was to prepare polymer-based formulations that are capable of extending the residence time and subsequent antibacterial activity of ClO_2. To achieve this goal, my work consisted of the following elements:

- Formulation and evaluation of ClO_2-loaded hydrogels. Poly(acrylic acid) (PAA) was chosen as the gel-forming polymer of the viscous solutions.
    - Investigation of the ClO_2-loading capacity of the different compositions.
    - Evaluating the effect of the PAA and ClO_2 concentrations on the ClO_2-loading capacity of the viscous solutions. We applied a two-factor, three-level face-centered composite design to construct a second-order polynomial model as a description of the effect of the formulation factors.
    - Microstructural characterization of the formulations to examine the relationship between the supramolecular structure and the ClO_2-loading capacity.
    - Evaluation of the antibacterial activity of ClO_2-loaded viscous solutions.
- Formulation and evaluation of PEO-based, ClO_2-generating nanofibrous mesh via electrospinning. The fibers contained $NaClO_2$ as a starting material for ClO_2 production.
    - Solid-state characterization of the starting materials and electrospun samples.
    - Morphological characterization of the fibrous mesh.
    - Evaluation of the ClO_2-generating ability of the $NaClO_2$-loaded fibers with particular regard to the initial weight of the sample. The results were compared to the theoretical ClO_2 production values.
    - The effect of the environmental parameters in the reaction chamber on the ClO_2 production was also evaluated.
    - Investigation of the antibacterial activity of the ClO_2 generating fibers under conditions modelling the exhaled human breath in terms of CO_2 concentration, temperature, and humidity. The experiments were carried out in sealed containers, and the antimicrobial activity was evaluated in the gas phase.

DOI:10.14753/SE.2022.2766

3. RESULTS

3.1. ClO_2-loading capacity, microstructure, and antibacterial activity of PAA based viscous solutions

3.1.1. Analytical measurement of the ClO_2-loading capacity of the polymer- and aqueous control solutions

The PAA-based, ClO_2-loaded viscous solutions along with aqueous ClO_2 control solutions were stored in open amber glasses at room temperature for 14 days. Samples were taken from the gels and aqueous control solutions every second day until the 8th day, and lastly, on the 14th day. The residual ClO_2 concentration was measured by iodometric titration. The acidic (pH 2) reaction media contained excess potassium iodide, sulfuric acid, starch indicator and were titrated with sodium thiosulfate.

A rapid decrease in ClO_2 concentration can be observed in the case of aqueous control solutions. Control samples containing 0.05 mg/g and 0.15 mg/g of initial ClO_2 lost their ClO_2 content after 2 days (Figures 4A and B). The control solution with the highest initial ClO_2 concentration (0.25 mg/g) could store ClO_2 for 4 days (Figure 4C). PAA-based viscous solutions retained their ClO_2 content for 14 days. Samples of 0.05, 0.15, and 0.25 mg/g initial ClO_2 concentrations show similar rate of ClO_2 concentration decrease (Figures 4A-C). The slopes of the ClO_2 concentration decrease are also similar among samples with different PAA concentrations, however, gels containing 0.2%, w/w PAA result in higher residual ClO_2 concentration than 0.1 and 0.3%, w/w PAA samples (Figure 5). In the case of the samples with initial ClO_2 concentration of 0.15 and 0.25 mg/g, the residual ClO_2 concentration of the PAA 0.2%, w/w sample was more than 30% higher than of the PAA 0.1 and 0.3%, w/w samples. Based on the residual ClO_2 concentration measurements, the ClO_2-loading capacity of the PAA 0.1%, w/w samples with initial ClO_2 concentration of 0.05, 0.15 and 0.25 mg/g was 15, 13.4 and 14.7%, respectively. Viscous solutions of 0.05, 0.15 and 25 mg/g of initial ClO_2 concentration and PAA 0.2%, w/w stored 23.6, 18.7 and 20.3%, while PAA 0.3%, w/w samples retained 19.6, 13.9 and 14.7% of their ClO_2 content, respectively.

DOI:10.14753/SE.2022.2766

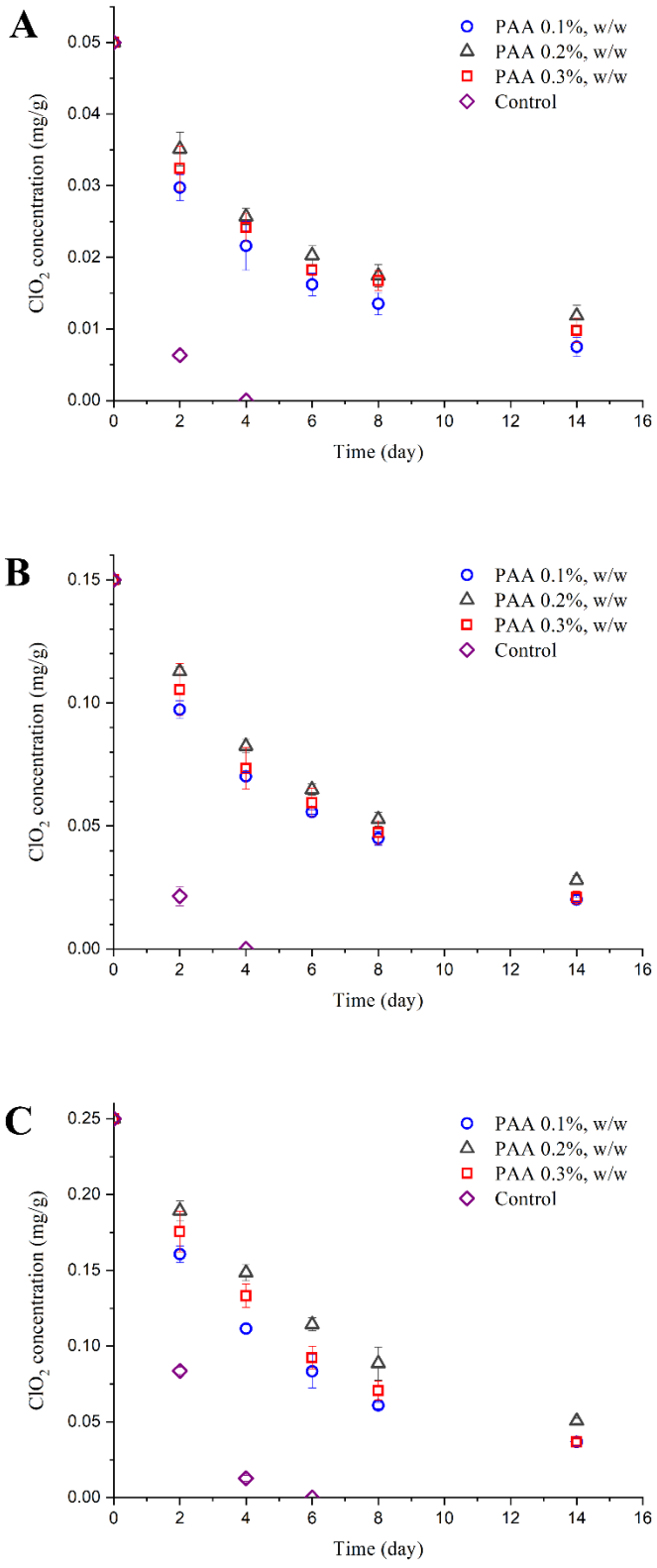

Figure 4 ClO_2 concentration decrease in PAA 0.1, 0.2 and 0.3%, w/w hydrogels and aqueous control solutions of different initial ClO_2 concentrations: 0.05 mg/g (A), 0.15 mg/g (B), 0.25 mg/g (C) (mean ± SD, n = 3).

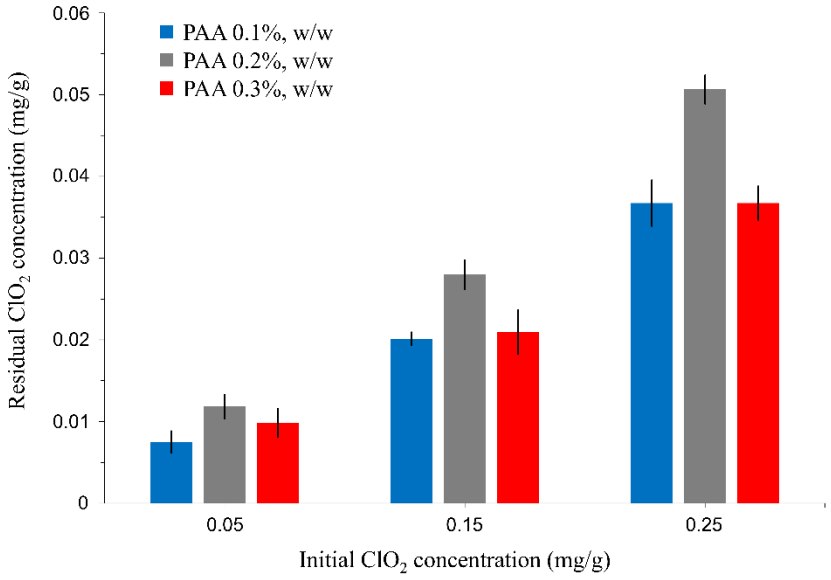

Figure 5 Residual ClO_2 concentrations of PAA-based viscous solutions (mean ± SD, n = 3).

3.1.2. Statistical experimental design

To evaluate the effect of the formulation parameters on the ClO_2-storage capacity of the viscous solutions, a second-order polynomial model was constructed using a two-factor, three-level, face-centered central composite design. The two formulation parameters represented in our model were the polymer concentration (factor 1) and initial ClO_2 concentration (factor 2). The residual ClO_2 concentration was selected as the response parameter. The levels of each parameter are shown in Table 3.

Table 3 Experimental design with formulation parameters and their levels.

Levels	Factor 1 (x): PAA concentration (%, w/w)	Factor 2 (y): ClO_2 concentration (mg/g)
Lower (-)	0.1	0.05
Base (0)	0.2	0.15
Higher (+)	0.3	0.25

The second-order polynomial model is described by the following equation:

$$z = a + bx + cy + dx^2 + ey^2 + fxy \qquad \text{(Eq. 7)}$$

where *z* is the response parameter, *x* denotes factor 1, *y* denotes factor 2, *a* is a constant, *b* and *c* parameters refer to the main, *d* and *e* to the quadratic, and *f* to the interaction effects. The estimated residual ClO_2 concentration of the viscous solutions was calculated. The measured and estimated values are summarized in Table 4.

Table 4 Matrix of the three-level full factorial design (mean ± SD, $n = 3$).

Factor		Response parameter	
x	y	z measured (mg/g)	z predicted (mg/g)
0.1	0.05	0.0075	0.0059
0.1	0.15	0.0201	0.0198
0.1	0.25	0.0367	0.0387
0.2	0.05	0.0118	0.0152
0.2	0.15	0.0280	0.0284
0.2	0.25	0.0507	0.0468
0.3	0.05	0.0098	0.0081
0.3	0.15	0.0210	0.0208
0.3	0.25	0.0367	0.0386

After performing a significance test at 95% confidence level, the obtained equation (Eq. 8) represents the effect of the formulation parameters on the ClO_2 storage capacity of the viscous solutions:

$$z = -0.025 + 0.314x + 0.094y - 0.818x^2 + 0.252y^2 - 0.058xy \qquad \text{(Eq. 8)}$$

3.1.3. Characterization of the supramolecular structure by o-Ps lifetime measurement

In polymer-based hydrogels, free volume holes are formed by the randomly oriented macromolecules. The size and distribution of the vacancies can be measured by positron annihilation lifetime spectroscopy (PALS). Ortho-positronium (o-Ps) lifetime values ranged between 1.1 and 1.4 ns in the ClO_2-loaded, PAA-based viscous solutions. The addition of ClO_2 shifted the lifetime distributions in the samples (Figure 6). Compared to the unloaded PAA 0.2%, w/w hydrogel, adding 0.05 mg/g ClO_2 to the viscous solution resulted in higher o-Ps lifetime values, shifting from 1.15-1.35 to 1.20-1.40 ns. The lifetime distribution of the sample containing 0.15 mg/g ClO_2 overlapped

with the unloaded PAA hydrogel. Higher ClO_2 concentration resulted in lower lifetime values, shifting to 1.10-1.27 ns in the case of samples containing 0.25 mg/g ClO_2.

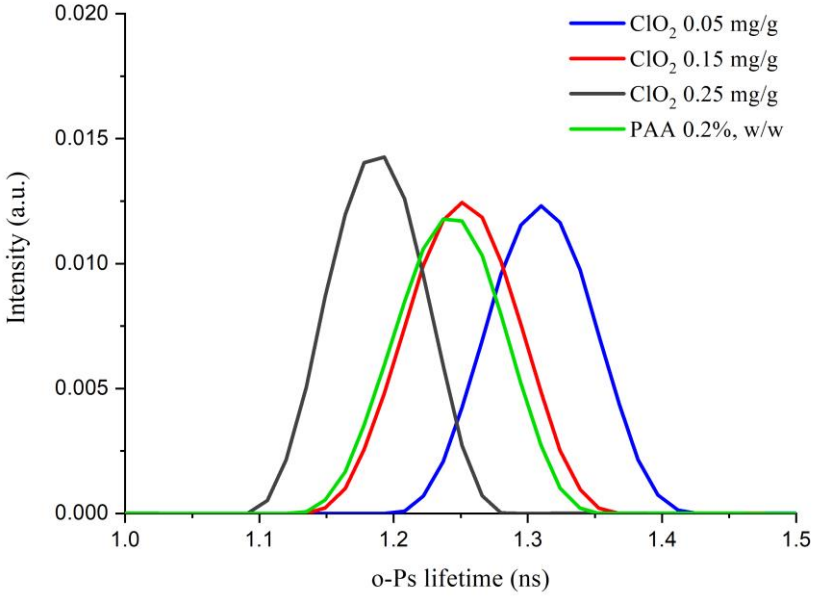

Figure 6 o-Ps lifetime distributions of PAA 0.2%, w/w viscous solutions containing 0.5, 0.15 and 0.25 mg/g ClO_2.

Examination of the hydrogels containing 0.25 mg/g ClO2 and various PAA concentrations showed that PAA 0.1 and 0.3%, w/w samples result in overlapping o-Ps lifetime distribution curves ranging from 1.1 to 1.3 ns with 0.096 and 0.107 of bandwidth, respectively. The lifetime distribution curve of the sample containing 0.2%, w/w PAA shifted to lower values, ranging from 1.10 to 1.27 ns and the full width at half maximum (FWHM) was 0.088 (Figure 7).

DOI:10.14753/SE.2022.2766

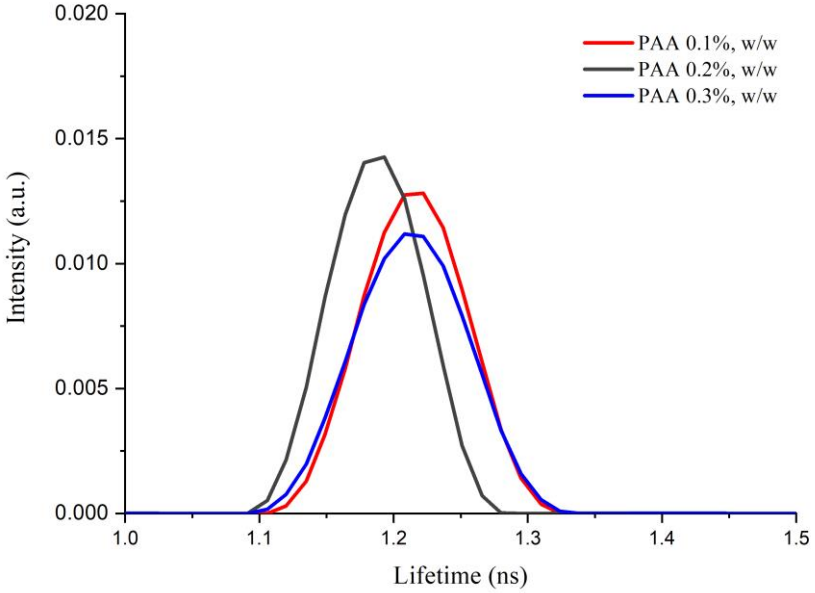

Figure 7 o-Ps lifetime distributions of PAA 0.1, 0.2 and 0.3%, w/w viscous solutions containing 0.25 mg/g ClO_2.

3.1.4. Antimicrobial efficacy of the ClO_2-loaded viscous solutions

Figure 8A shows that PAA-based viscous solutions containing 0.05 mg/g of initial ClO_2, showed distinct antibacterial activity depending on the concentration of the polymer. After 14 days of storage, substantial bacterial growth could be observed when adding 100 µL of 6.8×10^8 CFU *Enterococcus faecalis* suspension to PAA 0.1%, w/w samples. In the case of PAA 0.1%, w/w, the number of surviving colonies was too numerous to count in the further cycles. In the first cycle, after contaminating with 100 µL of bacterial suspension, only a few colonies could survive in one of the 3 parallels of PAA 0.3%, w/w hydrogel, other parallels showed no bacterial growth. The number of surviving colonies increased after the second and was TNTC after the third cycle in PAA 0.3%, w/w. The PAA 0.2%, w/w samples eliminated all bacteria in the first cycle. Only a few surviving colonies could be observed after the second cycle, and the surviving colonies were TNTC after adding a total amount of 300 µL of *E. faecalis* suspension to the PAA 0.2%, w/w samples.

DOI:10.14753/SE.2022.2766

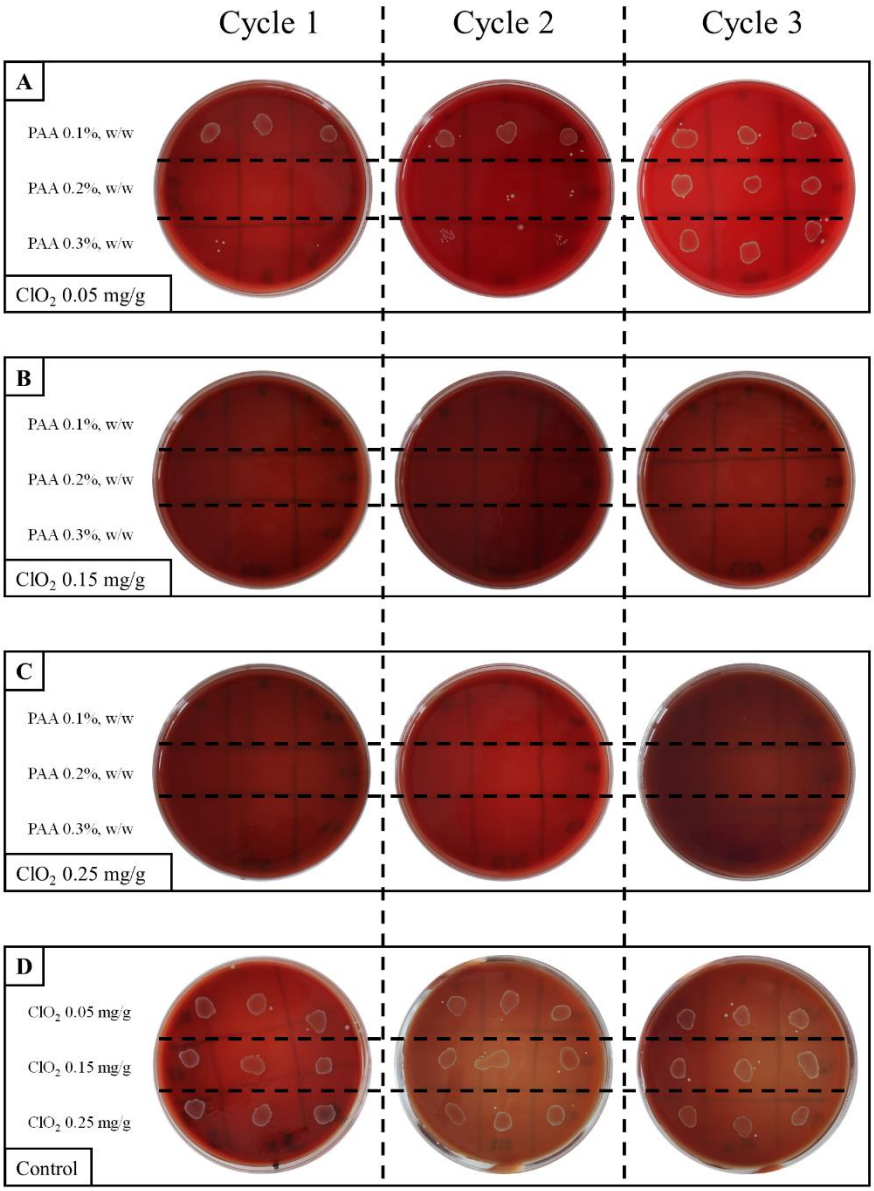

Figure 8 Surviving colonies in ClO_2-loaded viscous solutions and control solutions inoculated with 6.8×10^8 CFU *E. faecalis* suspension after 14 days of storage. 0.05 mg/g initial ClO_2 concentration (A), 0.15 mg/g initial ClO_2 concentration (B), 0.25 mg/g initial ClO_2 concentration (C), control solution (D).

Inoculation of samples of 0.15 and 0.25 mg/g initial ClO_2 concentration with *E. faecalis* suspension resulted in complete elimination of the bacteria, regardless of the concentration of PAA. In the case of samples of 0.15 and 0.25 mg/g initial ClO_2 concentrations, no bacterial growth could be observed on the blood agar plates after the third cycle (Figure 8B, 8C). Control samples containing 0.05, 0.15 and 0.25 mg/g initial ClO_2 concentration, could not eliminate bacteria after 14 days of storage (Figure 8D).

The number of surviving colonies was TNTC after the first cycle and throughout the experiment, regardless of the initial concentration of the active ingredient.

3.2. Morphology and microstructural characterization of the fibers

3.2.1. Morphology of the $NaClO_2$-loaded and unloaded electrospun samples

Scanning electron microscopy images of unloaded PEO samples showed smooth-surfaced, randomly oriented polymer fibers. The average fiber diameter was 315±27 nm and showed normal distribution. Bead-like structures and non-fibrous elements could not be observed (Figure 9A). Due to the addition of $NaClO_2$ to the precursor polymer solution, the process parameters of electrospinning changed substantially, thus higher voltage and lower flowrate were required. Samples containing $NaClO_2$ resulted in uniform, nanoscale fibers with an average diameter value of 193±23 nm. The fiber diameter values of $NaClO_2$-loaded PEO samples also showed normal distribution (Figure 9B).

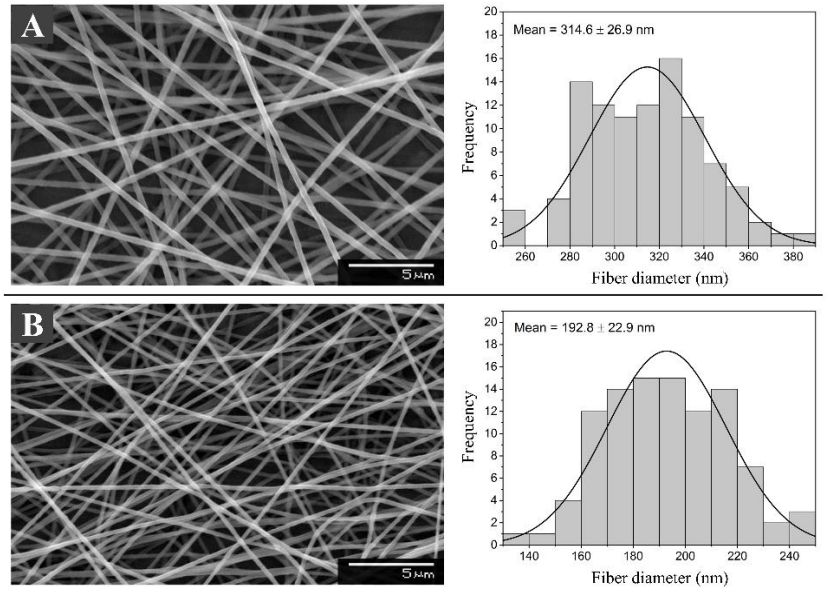

Figure 9 Morphology by SEM imaging and fiber diameter histograms of the unloaded PEO (A) and $NaClO_2$-loaded PEO fibers (B) (n = 100).

3.2.2. FTIR analysis of the fibers

FTIR spectra were recorded and analyzed to investigate the potential changes in the functional groups and subsequently, the structural alterations of PEO macromolecules. On the spectrum of unloaded PEO fibers, the wide peak at 2890 cm^{-1} corresponds to the symmetrical stretching of C-H bond (Figure 10B). The bands at 1467, 1341, 1280 and 842 cm^{-1} were assigned to the scissoring, wagging, twisting, and rocking of the CH_2 group. The most intense peak on the unloaded PEO spectrum observed at 1095 cm^{-1} along with the bands at 1145 and 1061 cm^{-1} belong to the asymmetric stretching vibration of the C-O-C bond. The sharp peak at 960 cm^{-1} corresponds to the C-C skeletal stretching vibrations. The spectrum of $NaClO_2$ shows two smaller peaks at 1438 and 1157 cm^{-1}, and two strong peaks merged together at 823 and 800 cm^{-1} (Figure 10C). The peaks and intensities on the spectrum of the $NaClO_2$-loaded fibers are similar to that of the unloaded PEO fibers (Figure 10A). A slight broadening can be observed at the base of the peak at 842 cm^{-1} on the spectrum of the $NaClO_2$-loaded PEO fibers, where $NaClO_2$ has its characteristic peaks.

DOI:10.14753/SE.2022.2766

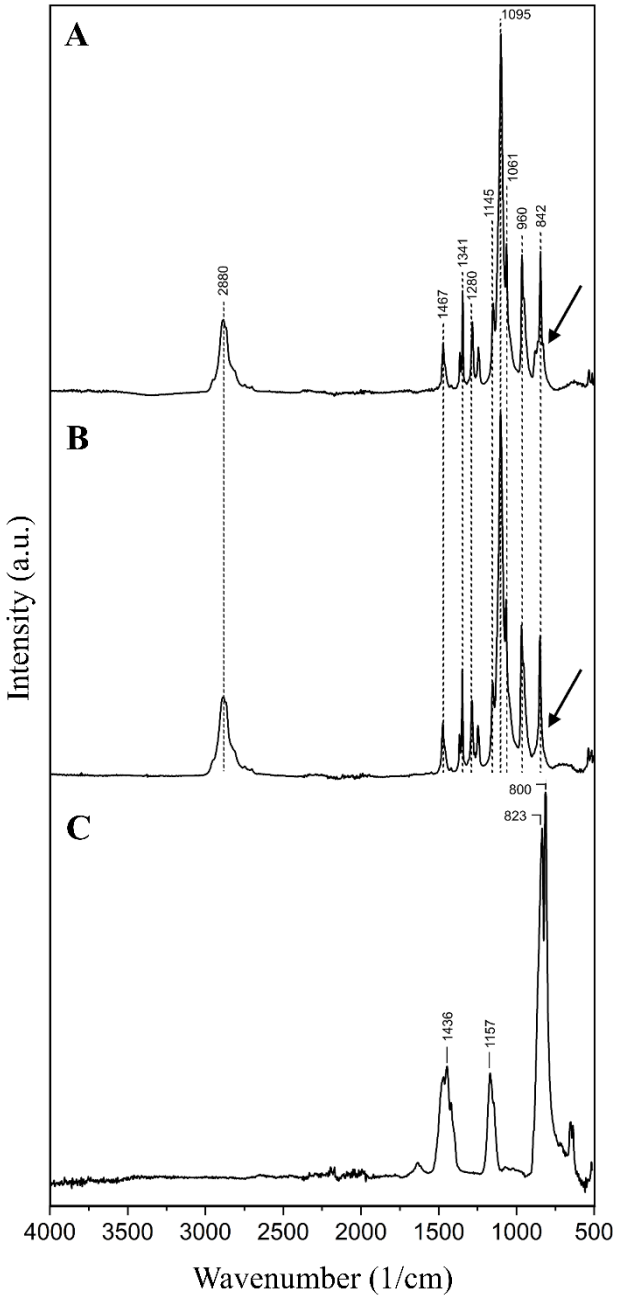

Figure 10 FTIR spectra of $NaClO_2$-loaded PEO fibers (A), unloaded PEO fibers (B) and $NaClO_2$ (C).

3.3. ClO_2 production from $NaClO_2$-loaded PEO fibers

3.3.1. Concentration and yield of the generated ClO_2 gas

To determine the concentration of the generated ClO_2 in the gas phase, sample was taken from the small water container placed into the reaction chamber and measured via UV-VIS spectroscopy. To calculate the concentration of the gaseous ClO_2 from the concentration values of the aqueous form, the following equation was used:

DOI:10.14753/SE.2022.2766

$$[ClO_2]_g\ (\mu L/L) = k \times K_\theta \times V_m \times [ClO_2]_{aq}\ (M) \qquad \text{(Eq. 9)}$$

where V_m is the molar volume of the gas, K_θ is the distribution constant of ClO_2, and k=10^6 is a constant. The experiment was carried out at 37°C, thus the value of the distribution constant needed to be determined. To construct an equation for the calculation of the distribution constant, we used the following data from Ishi's work (Table 5) (112):

Table 5 Value of the $[ClO_2]_g$(M)/$[ClO_2]_{aq}$(M) distribution constant at different temperatures (K_θ).

Temperature (°C)	K_θ distribution constant
0	0.0155
5	0.0189
10	0.0222
15	0.0267
20	0.0316
30	0.0428
40	0.0578

Figure 11 shows the distribution constant values at different temperatures and Eq. 10 describes the fitted polynomial equation:

$$y = 0.0157 \times 5.281x + 1.299x^2 \qquad \text{(Eq. 10)}$$

The R-squared value (R^2) of the linear regression was 0.9997 and the distribution constant at 37°C was found to be 0.053.

DOI:10.14753/SE.2022.2766

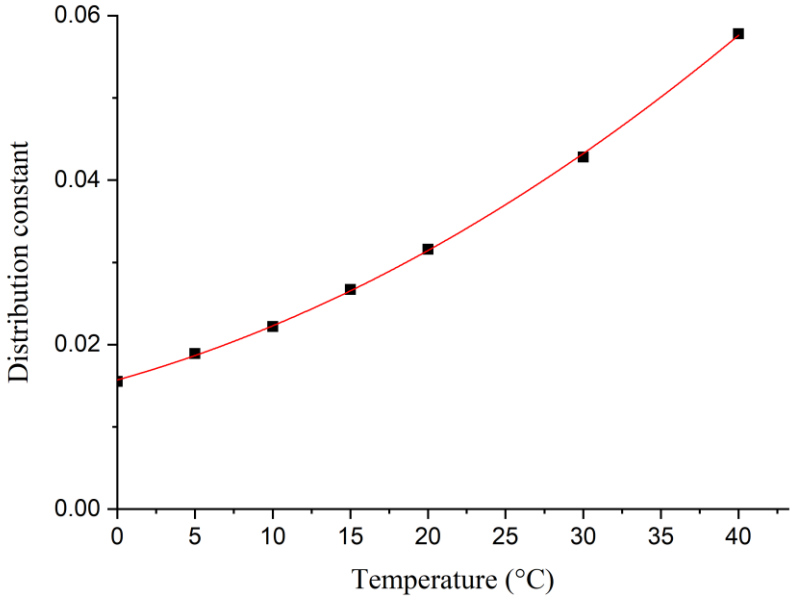

Figure 11 Distribution constant of $[ClO_2]_g$(M)/$[ClO_2]_{aq}$(M) at different temperatures and the fitted polynomial equation.

Using the K_θ distribution constant value corresponding to the equilibrium of the gaseous and aqueous form of ClO_2 at 37°C, the concentration of the gas produced by the $NaClO_2$-loaded fibers were calculated. Figure 12 represents the ClO_2 concentration reached in the reaction chamber after 24 hours along with the produced gas-per-weight values. Under humid (RH>95%) and CO_2-rich (c_{CO2}=5%, v/v) conditions, the concentration of ClO_2 generated by 1 mg of $NaClO_2$-loaded sample reached 65.8 ppm. The concentrations of ClO_2 produced by the 5 and 10 mg sample were 115.5 and 134.9 ppm, respectively. Higher weights of samples did not result in significantly higher concentrations of ClO_2, thus the ClO_2 production-per-weight data show gradual decrease with increasing sample weights. The ClO_2 generating ability of the 30 mg sample resulted in 145.2 ppm gas concentration in the reaction chamber, however, the ClO_2 production-per-weight value reached only 4.8 ppm/mg.

DOI:10.14753/SE.2022.2766

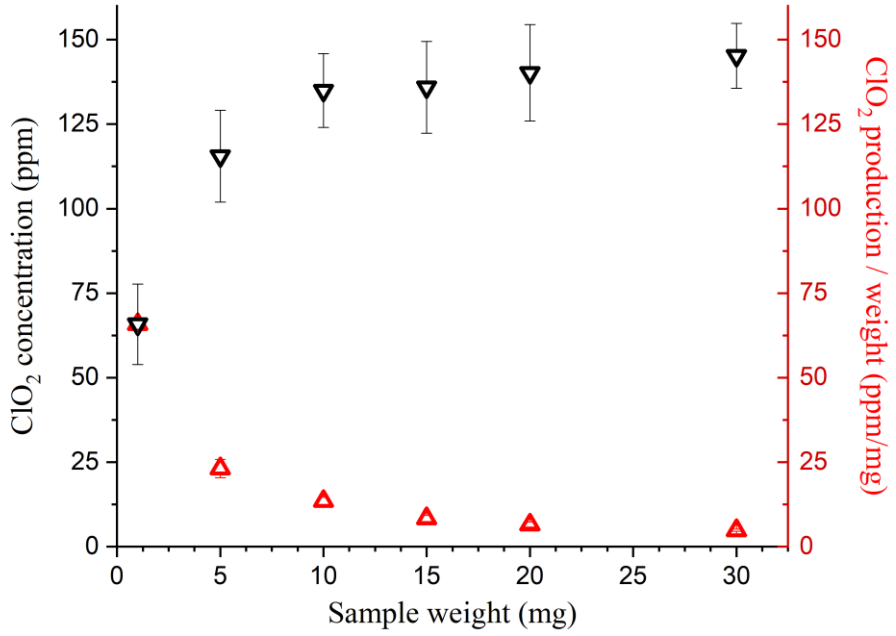

Figure 12 ClO_2 production ability and production-per-weight values of $NaClO_2$-loaded PEO fibers of 1, 5, 10, 15, 20 and 30 mg (mean ± SD, n = 3).

Using the equations of the chemical transformation of $NaClO_2$ under acidic conditions, a theoretical maximum of ClO_2 production from the samples of given weights was calculated. The measured and theoretical concentrations along with the yield of production are presented in Table 6. The concentration of the generated ClO_2 reached by 1 mg of $NaClO_2$-loaded PEO fibers resulted in a yield of 89.4%, compared to the potential ClO_2 production value. As the ClO_2 generating ability-per-weight data decreased with increasing sample weight, the yield of ClO_2 production declined substantially. In the 24-hour experiment, the 10 mg sample produced 18.4% of the potential ClO_2 concentration, while the 30 mg sample reached 6.6% of the maximal ClO_2 yield.

DOI:10.14753/SE.2022.2766

Table 6 Yield of ClO_2 production from $NaClO_2$-loaded PEO fibers using the theoretical maximum of the $NaClO_2$ – ClO_2 transformation under acidic conditions (mean ± SD, *n* = 3).

m_{sample} (mg)	n_{NaClO2} (mmol)	$[ClO_2]_g$ (ppm)	$[ClO_2]_g$ (ppm, theoretical)	Yield (%)
1	0.217	65.79	73.57	89.43
5	1.084	115.54	367.85	31.41
10	2.168	134.93	735.69	18.34
15	3.252	135.91	1103.54	12.32
20	4.336	141.16	1471.38	9.59
30	6.504	145.23	2207.07	6.58

3.3.2. Effect of environmental parameters on the ClO_2 production ability

The ClO_2 production ability of $NaClO_2$-loaded PEO fibers of 5 mg was tested in humid (RH>95%) environment, while temperature was kept at 37°C. We placed the samples into the reaction chamber containing 5, 10 and 15% (v/v) carbon dioxide. Figure 13A shows that the concentration of CO_2 did not have a significant effect on the ClO_2 production ability of the fibers. To evaluate the effect of time of exposure to the acidic environment, samples were placed into the reaction chamber for 24, 48 and 72 hours, while c_{CO2} was kept at 5%. The residence time of the fibers had a substantial impact on the ClO_2 generating ability, resulting in higher concentration values with increasing exposure times (Figure 13B).

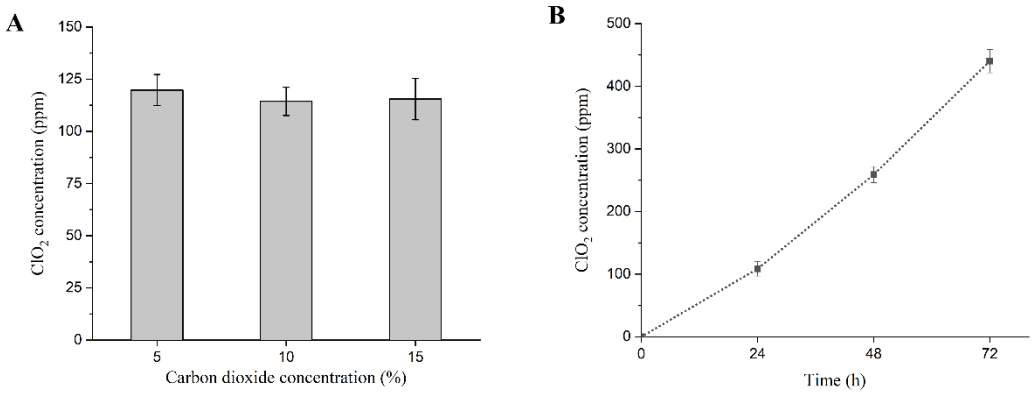

Figure 13 Effect of environmental parameters of the ClO2 generating ability of 5 mg $NaClO_2$-loaded PEO fibers: carbon dioxide concentration (A), time of exposure (B) (mean ± SD, *n* = 3).

3.4. Antibacterial effect of the $NaClO_2$-loaded PEO fibers

The setup of the reaction chamber and the environmental parameters are presented in Figure 14. Carbon dioxide concentration was 5% (v/v), humidity was of RH>95% and the temperature was set to 37°C. Figure 15 shows the blood agar plates after incubation and counting along with the average value of surviving colonies-per-plate. In our experiment, the antibacterial activity of 1, 5, 10 mg fibers and unloaded PEO fibers was tested using three parallels of each weight.

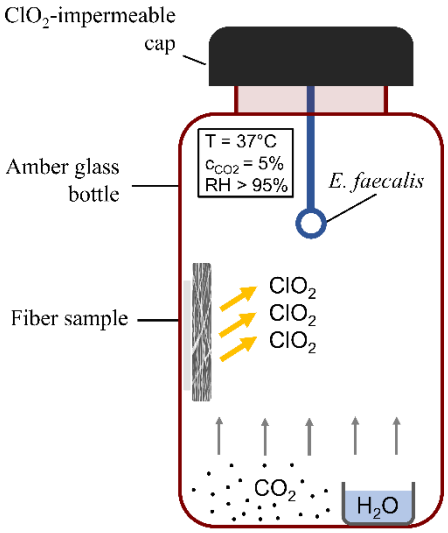

Figure 14 Reaction chamber for bacterial inactivation study and ClO_2 production.

The unloaded PEO control fibers could not eliminate the bacteria, resulting in a high number of surviving colonies on the blood agar plates (Figure 15A). The CFU/plate value for unloaded PEO samples was above 250, indicating, that the environmental conditions were suitable for bacterial growth (Figure 15B). The $NaClO_2$-loaded fibers of different weights decreased the number of surviving colonies successfully. After 24 hours, only 5 and 3 surviving colonies could be counted on one of the plates of the 1 and 5 mg samples, resulting in 1.7 and 1.0 CFU/plate values, respectively. In the case of the 10 mg sample, bacteria were completely eliminated; the CFU/plate value was zero.

DOI:10.14753/SE.2022.2766

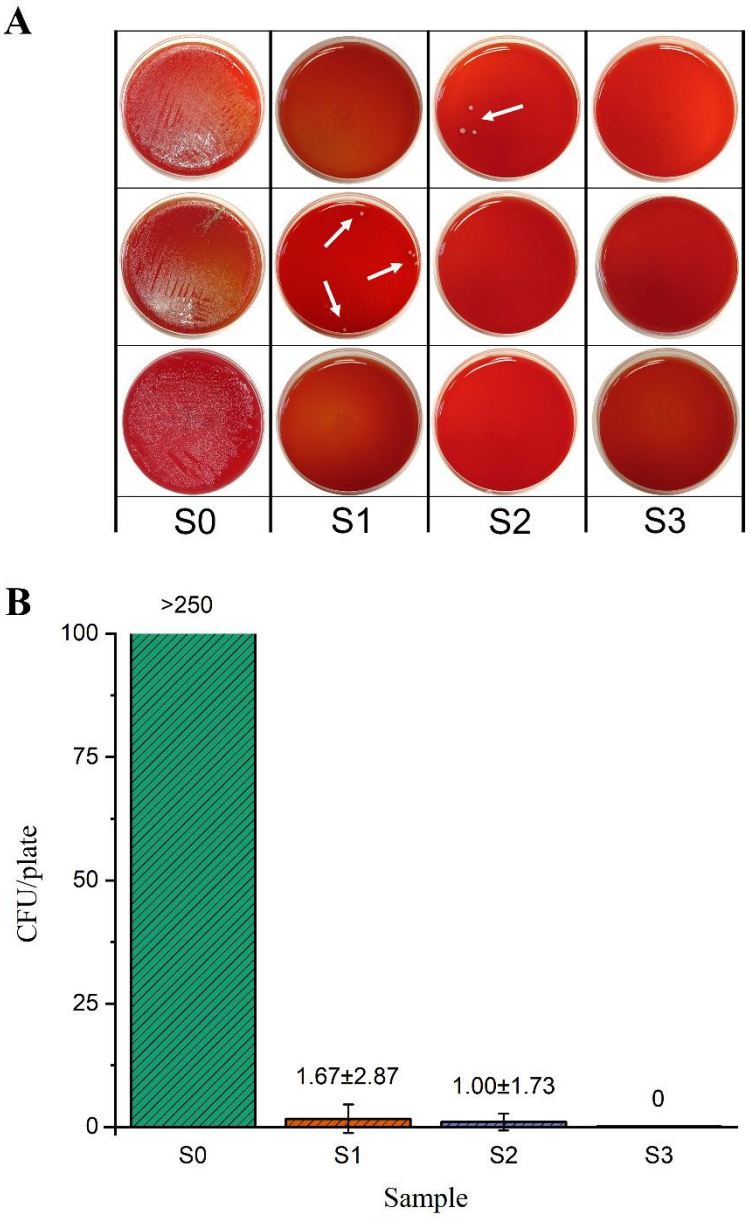

Figure 15 Surviving colonies on blood agar plates after incubation (A) and the number of colonies after counting (B): unloaded PEO control fibers (S0), 1 mg $NaClO_2$-loaded PEO fibers (S1), 5 mg $NaClO_2$-loaded PEO (S2) fibers, 10 mg $NaClO_2$-loaded PEO (S3) fibers.

DOI:10.14753/SE.2022.2766

4. DISCUSSION

4.1. ClO_2-storage capacity, microstructure, and antibacterial activity of PAA based viscous solutions

4.1.1. Analytical measurement of ClO_2-loading capacity and the effect of formulation parameters

Aqueous ClO_2 control solutions lost their sodium chloride content in 48-96 hours, while PAA-based viscous solutions retained ClO_2 up to 14 days. Dissolved ClO_2 molecules are removed by diffusion from the solution. The rapid ClO_2 loss from the control samples is driven by the high volatility of ClO_2 and the convection of the solvent. Even under steady-state conditions, there is a slight difference between the temperature and thus, the density of the upper and lower parts of the aqueous solution due to the evaporation of the solvent, generating a continuous circulation of the fluid. A constant flow of water, driven by temperature equalization, facilitates the diffusion and the liberation of ClO_2 from the solution.

In a viscous solution the matrix, formed by polymer macromolecules acts as a diffusion barrier for the dissolved gas and blocks the convection of water, resulting in a smaller rate of ClO_2 loss. Samples of 0.1%, w/w PAA concentration did not form hydrogels, rather they had an oil-like liquid texture, however, their ClO_2-loading capacity reached 14 days. PAA 0.2%, w/w samples demonstrated a more viscous and gel-like behavior with the ability to flow under gravity, while PAA 0.3%, w/w hydrogels had the most rigid texture, withstanding flow under gravity. If the ClO_2-loading capacity of the viscous solutions is based on the ability of the polymer matrix to act as a diffusion barrier, higher PAA concentrations should result in increased residual ClO_2 content, however, analytical measurement of the residual ClO_2 concentrations showed that PAA 0.2%, w/w samples had the highest ClO_2-loading capacity. The results suggest that the ClO_2-loading capacity of the polymer matrix is based not solely on the diffusion barrier function of the polymer matrix, but additional secondary interactions should occur between the polymer macromolecules and the aqueous form of ClO_2. Initial ClO_2 concentration had no substantial impact on the rate of the ClO_2 loss, as the slopes of the concentration decrease are similar among 0.05, 0.15 and 0.25 mg/g samples.

The results of the statistical experimental design give an insight into the effect of the PAA and the initial ClO_2 concertation on the residual ClO_2 content of the samples.

The positive sign of the main coefficients of the *x* and *y* factors shows that both the polymer and ClO_2 concentration increase the residual ClO_2 concentration of the viscous solutions. The main coefficient of the PAA concentration (b = 0.341) is more than three times higher than that of the ClO_2 (c = 0.094), indicating that the polymer concentration has a significant impact on the ClO_2-loading capacity of the samples. The results of the analytical measurement have shown that the PAA concentration is not directly proportional to the residual ClO_2 content of the samples, which is confirmed by the negative coefficient of the quadratic effect of the *x* parameter (d = -0.818). The negative coefficient of the interaction effect (f = -0.058) also indicates a reduction in the corresponding response parameter.

4.1.2. Macrostructural aspects of the ClO_2-loading capacity

PALS is a useful tool in the evaluation of the supramolecular structure of polymer-based nanosystems. The gel matrix, formed by randomly oriented polymer chains contains vacancies. The size of these holes is determined by the distance and relative position of the macromolecules. The level of entanglement of the chains is influenced by the secondary interactions occurring in the matrix. PALS results suggest that the addition of ClO_2 alters the supramolecular structure of the viscous solutions. According to the o-Ps lifetime distribution measurement of the ClO_2-loaded PAA 0.2%, w/w hydrogels, a low concentration of ClO_2 results in larger free volume holes, indicating that the original arrangement of the PAA macromolecules changes in the presence of the active ingredient. As the concentration of ClO_2 increases, more secondary bonds emerge between the hydrated form of ClO_2 and PAA, thus a more compact structure is formed, causing the o-Ps distribution to shift to lower values. However, the differences in the o-Ps lifetime distribution values of the ClO_2-loaded PAA 0.1, 0.2, and 0.3%, w/w viscous solutions indicate that an optimum PAA concentration and subsequent ideal supramolecular arrangement exists. Samples containing 0.25 mg/g of ClO_2 and 0.2%, w/w of PAA resulted in lower o-Ps lifetime and thus smaller free volume holes than in the case of the 0.1 and 0.3%, w/w samples. The FWHM values of the o-Ps lifetime distribution curves indicate the uniformity of the free volume hole sizes. There is an 8.6 and 17.8% decrease in the FWHM value of the PAA 0.2%, w/w sample compared to the bandwidths measured in the curves of the PAA 0.1 and 0.3%, w/w samples, suggesting that at 0.2%, w/w polymer concentration, a more arranged supramolecular structure is formed with the hydrated form of ClO_2,

thus more active ingredient is loaded in the matrix. This phenomenon is confirmed by the results of the analytical measurement of the residual ClO_2 concentration and the subsequent statistical evaluation.

4.1.3. Antimicrobial efficacy of the ClO_2-loaded viscous solutions

The antimicrobial evaluation of the polymer-based viscous solutions was carried out after storing the samples for 14 days under conditions similar to the ClO_2-loading capacity experiment. A total volume of 300 μL of bacterial suspension was added to the polymer solutions in 3 cycles. The sample was taken and plated on blood agar after each cycle. The residual ClO_2 concentration of the PAA-based viscous solutions with initial ClO_2 concentrations of 0.15 and 0.25 mg/g in these samples ranged between 0.02-0.028 and 0.037-0.051 mg/g, respectively and was sufficient to eliminate bacteria after 3 cycles of inoculation, regardless of the PAA content of the sample. The antibacterial activity was distinguishable only among samples with 0.05 mg/g of initial ClO_2 concentration. The ability to eliminate the inoculated pathogens in the different cycles correlated with the residual ClO_2 concentration of the viscous solutions. PAA 0.1%, w/w samples retained 15% of the initial ClO_2 and could not prevent bacterial growth after the first cycle of inoculation. PAA 0.2 and 0.3%, w/w samples with ClO_2-loading capacity of 23.6 and 19.6% showed sufficient antibacterial activity to eliminate *E. faecalis* in the first cycle. As their ClO_2 content was gradually depleted, bacteria could grow in the following cycles.

4.2. Formulation and characterization of $NaClO_2$-loaded PEO nanofibers

4.2.1. Morphology of the electrospun samples

Neat and $NaClO_2$-loaded PEO nanofibers were prepared via electrospinning. Scanning electron microscopy was used to investigate the morphology and size range of the fibrous samples. Both the electrospinning of the unloaded and $NaClO_2$-loaded precursor solutions resulted in smooth, nanoscale fibers. While PEO nanofibers generally have good spinnability and are relatively easy to formulate, the addition of $NaClO_2$ altered and limited the range of optimal process parameters. Unloaded PEO precursor solutions were spinned at 10.5 kV, however, the applied voltage had to be increased to 14.8 kV during the formulation of $NaClO_2$-loaded fibers. The average fiber diameter of the $NaClO_2$-loaded fibers also differed substantially than that of the unloaded sample. Generally, higher applied voltage decreases the average fiber diameter

by increasing the applied force on the precursor solution ejecting from the needle. Stronger electrical field results in the stretching and thinning of the fiber jet. Inorganic salt dissolved in the precursor solution also have a significant impact on the fiber formation by increasing the conductivity and surface density of the polymer solution. Charged particles increase the coulombic and electrostatic forces acting on the electrospun jet, usually resulting in stretching and thinning. The overall effect of the presence of an inorganic salt in the precursor polymer solution depends on the properties of the macromolecule and the concentration and characteristics of the salt. Our results showed that $NaClO_2$ dissolved in the polymer solution along with the higher applied voltage decreased the average fiber diameter from 315 to 193 nm. The concentration of $NaClO_2$ in the precursor solution was selected as the maximum salt concentration where a stable electrospinning process could be sustained.

4.2.2. Microstructural characterization of the $NaClO_2$-loaded PEO fibers

A major concern emerging with the addition of $NaClO_2$ to the precursor solution was the stability of the formulation regarding the potential oxidation of PEO by the active ingredient. FTIR spectra were collected to detect the possible changes in the functional groups of the polymer macromolecule. Unloaded and $NaClO_2$-loaded nanofibers show identical peaks and intensities, except in the region between 800 and 850 cm^{-1}, where a minor broadening can be observed on the spectrum of the $NaClO_2$-loaded PEO fibers. The strongest peaks of $NaClO_2$ are located at 800 and 823 cm^{-1}. Due to the concentration differences of the components, the characteristic bands of the active ingredient do not appear on the $NaClO_2$-loaded PEO spectrum, rather they cause a slight broadening at the base of the peak at 842 cm^{-1}. The similarities in the loaded and unloaded PEO spectra suggest that the functional groups of PEO were unaffected and unwanted chemical reactions did not occur in the $NaClO_2$-loaded precursor solution.

4.3. ClO_2 production and antibacterial activity of the samples

4.3.1. Concentration measurement and yield of the produced ClO_2

The ClO_2 production of the $NaClO_2$-loaded PEO fibers was tested in sealed reaction chambers. The environmental parameters for ClO_2 generation were set to imitate the exhaled human breath, thus humidity was above 95%, CO_2 was 5% and the temperature was set to 37°C. In the presence of water vapor, carbonic acid is formed by carbon dioxide *in situ* and reacts with $NaClO_2$ to form ClO_2 in a protonation and self-

decomposition reaction. In equilibrium, a given portion of ClO_2 is dissolved in the water, and placed in the reaction chamber, thus its concentration can be measured. After 24 hours of incubation, the concentration of ClO_2 produced by the 1 mg sample was 65.8 ppm, which resulted in a yield of 89.4%. The concentration of ClO_2 generated by larger weights of samples was higher, however, the rate of growth of the generated ClO_2 remained substantially lower than expected. Samples weighing 20 and 30 mg reached only 9.6 and 6.6% of the theoretical ClO_2 concentration in the same experiment. To assess the potential limiting factors in the production of ClO_2, different reaction parameters were set.

To evaluate the limiting effect of the low concentration of carbon dioxide in the reaction chamber, ClO_2 production was tested in the presence of 10 and 15% of CO_2. Results showed that a two- and threefold increase in the concentration of the reactant did not alter the concentration of the generated ClO_2. However, when samples were incubated for 42 and 72 hours, the concentration of ClO_2 increased, indicating that the time of exposure has a substantial effect on the ClO_2 production. Data suggests that there are factors outside the concentration of the reactants that determine the rate of production and the maximal concentration of ClO_2. One key element influencing the rate of ClO_2 production is the polymer structure and the changes regarding the porosity of the fibrous mesh during incubation. When samples are put in the reaction chamber, fibers contact with water molecules rapidly, thus a gradual swelling and disintegration of the mesh occur in the outer layers of the sample, resulting in a gel-like structure. As fibers swell and merge in the humid environment, the number of reaction sites available for ClO_2 generation decreases. The gel-like outer layer acts as a diffusion barrier and the diffusion of CO_2 and ClO_2 through the layer becomes a determining factor of the rate of ClO_2 generation and liberation. The other essential component influencing the ClO_2 producing ability of the samples is the thickness of the electrospun mesh. Larger weighing samples were prepared under longer spinning time, resulting in thicker fiber mesh. Throughout the experiments, similar sizes were cut from the samples, thus the different weights of samples varied particularly in their thickness. The decrease in the surface-to-volume ratio due to swelling and the formation of a gel-like outer layer had a more substantial hindering effect on the ClO_2 producing ability of larger weighing samples compared to smaller samples. This phenomenon is due to the greater diffusion barrier thickness of these samples and the higher ratio of unreacted $NaClO_2$ that is difficult for the reactant to access.

DOI:10.14753/SE.2022.2766

4.3.2. Antibacterial activity of the $NaClO_2$-loaded fibers

In our experiment evaluating the antibacterial activity of $NaClO_2$-loaded PEO fibers, samples were tested under conditions similar to the exhaled human breath (RH>95%, C_{CO2} = 5%, T = 37°C). *Enterococcus faecalis* was selected as a model organism due to its undemanding nature in terms of growth requirements and resilience. Different weights of samples were placed into the reaction chamber to determine the sufficient amount of fiber required to eliminate the pathogens. The number of the surviving bacteria was TNTC in the case of unloaded PEO fibers, and decreased significantly when 1 mg of $NaClO_2$-loaded PEO fiber was placed into the reaction chamber. The CFU/plate value of the 1 mg sample was 1.7, meaning that only 5 colonies survived from the potential $2.8x10^6$ CFUs in one parallel experiment, and no bacteria was found on the other parallel plates. When 5 and 10 mg of fiber were placed into the reaction chamber, the CFU/plate value decreased to 1 and 0, respectively. Results suggest that small weights of $NaClO_2$-loaded PEO fiber are able to produce and liberate a sufficient amount of ClO_2 to eliminate bacteria from the gas phase in the presence of humidity and carbon dioxide.

DOI:10.14753/SE.2022.2766

5. CONCLUSIONS

ClO_2 is an effective and safe gaseous antiseptic, however, its rapid liberation from aqueous solution and the cumbersome handling of the gas form hinders its application in the medical field. Solid and liquid polymer-based formulations can form arranged supramolecular systems with advantageous drug-delivering capabilities and tunable drug release profiles. With a polymer-based formulation, a number of issues regarding the applicability of ClO_2 can be addressed.

The first approach to achieve prolonged ClO_2-release was to prepare polymer-based viscous solutions. PAA was chosen due to its considerable gel-forming ability at low concentrations and insusceptibility to the oxidizing effect of ClO_2. An essential element of the preparation and a novelty of the work was to use ClO_2 in the form of a hyper pure aqueous solution, containing solely water and ClO_2 to avoid impurities being present in the formulation. Using a two-factor, three-level central composite design, 9 different combinations were formulated by altering the PAA and ClO_2 concentrations. The ClO_2-loading capacity of the polymer-based viscous solutions was compared with that of the aqueous ClO_2 solution. The ClO_2 concentration decrease was significantly slower in the PAA-based samples compared to the control solutions. The difference in the ClO_2-loading capacity of the aqueous control solutions and the PAA-based solutions showed that the presence of PAA and the subsequent formation a polymer matrix is the key factor in the determination of the rate of the ClO_2 loss.

Besides the aim to formulate an applicable polymer-based ClO_2 formulation, my purpose was to investigate the role of the polymer matrix in ClO_2 retention and to understand the underlying mechanism of the ClO_2-loading capacity of the polymer. Statistical examination showed that the differences in the ClO_2-loading capacity of the PAA hydrogels of various concentrations were due to the dual role of the polymer in the mechanism of ClO_2 retention. On one hand, the polymer matrix acts as a diffusion barrier and thus inhibits the transport of the hydrated gas in the solution. On the other hand, a substantial difference could be observed in the residual ClO_2 concentration of the polymer solutions depending on the concentration of PAA, however, the ClO_2-loading capacity was not directly proportionate with the PAA concentration of the samples. PAA 0.2%, w/w samples showed the best ClO_2-loading capacity among the viscous solutions.

PALS measurements gave an insight into the macrostructural properties influencing the ClO_2 retention. The o-Ps lifetime distribution curves of the samples showed that the size and distribution of the free-volume holes were minimum in PAA 0.2%, w/w samples. It can be stated that there exists a PAA concentration where the degree of the secondary interactions between the macromolecule and hydrated form of ClO_2 and the supramolecular arrangement of the ClO_2-loaded polymer matrix shows optimum. The results of the microbiological study confirmed the analytical, statistical, and macrostructural examinations since the ClO_2-loading capacity and the antimicrobial properties of the PAA-based viscous solutions are closely related.

The second approach for ClO_2 release was based on the self-disproportionation reaction of $NaClO_2$ in an acidic environment. PEO-based nanofibers were chosen for the formulation of $NaClO_2$. The reaction between $NaClO_2$ and weak acids, such as citric or carbonic acid is a widely used method for ClO_2 production, however, to the best of our knowledge, it was the first time when the ClO_2 production from nanofibers was tested under conditions similar to the human exhaled breath. The large surface-to-volume ratio of the nanofibrous mesh is a key element in the generation of ClO_2, as fibers provide a sufficient reaction site for carbonic acid and chlorite ions to form ClO_2. The fibrous structure of the samples was proven via SEM imaging. Due to the oxidizing effect of $NaClO_2$ it was important to examine the potential changes in the polymer microstructure after the loading of the active ingredient. FTIR spectra did not show any undesirable changes in the functional groups of the macromolecule.

In my work, the primary focus was put on the examination of the parameters influencing the ClO_2 production of the $NaClO_2$-loaded nanofibrous sheets. Sample weight had a significant impact on the ClO_2 producing ability and yield of the generated gas. Fibrous sheet with larger weights had lower ClO_2 producing ability and resulted in smaller yield. Environmental parameters, such as CO_2 concentration did not alter the productivity of the samples, however, exposure time increased the final ClO_2 concentration significantly. An essential finding of my work was that swelling and gelation of the outer layers of the fibrous sheets decrease the rate of ClO_2 production, and the diffusion of reactants through this barrier becomes a rate determining mechanism. As the surface-to-volume ratio decreased due to swelling in the outer layers of the samples of higher weights, the surface density of reaction sites for CO_2 decreased and the protonation-disproportionation of the chlorite ions took place in a dissolved polymer matrix. A necessary condition and also a novelty of our work was to measure

DOI:10.14753/SE.2022.2766

ClO_2 production in a reaction chamber fitted with a sealing that is completely impermeable for ClO_2, in order to reduce its loss during the experiment.

My primary assumption is that $NaClO_2$-loaded nanofibers can liberate ClO_2 in the gas phase under the given conditions and thus show antibacterial activity, which was proven by the microbiological experiment. Even 1 mg of the fibrous sample was able to eliminate the bacteria placed in the upper region of the reaction chamber. Considering the ClO_2-producing ability and yield of the samples of different weights, a fibrous sheet of lower thickness and higher surface is desirable for antibacterial application, however, a tunable rate of swelling on the surface of the sample could provide a controlled release for ClO_2.

Based on the findings presented in my dissertation, it can be stated that polymer-based viscous solutions and nanofibrous meshes are promising alternatives in the formulation of ClO_2-releasing systems. My work contributes to a better understanding of the potential methods by which the limitations of the applicability of ClO_2 can be addressed.

DOI:10.14753/SE.2022.2766

6. SUMMARY

ClO_2-containing polymer formulations were prepared with the aim of improving ClO_2 loading and residence time in the formulation and thus extending the potential applications of the antimicrobial agent. Poly(acrylic acid)-based viscous solutions of different polymer concentrations were formulated and their ClO_2 loading capacity was compared with aqueous ClO_2 control solutions. PAA-based viscous solutions retained ClO_2 after 14 days of storage, however, control solutions lost their ClO_2 content. In terms of ClO_2-loading capacity, the PAA concentration of the hydrogels showed an optimum at 0.2%, w/w. The investigation of the supramolecular structure of the polymer matrix confirmed the relationship between the polymer concentration and the residual ClO_2 concentrations. The size of the free-volume holes was the smallest and the size distribution was the most homogenous in the case of the samples with medium PAA content. The statistical examination of the PAA and residual ClO_2 concentrations supported the findings of the PALS measurement. ClO_2-loaded viscous solutions showed a substantial antimicrobial effect and the results of the microbiological experiment supported the findings of the analytical and macrostructural examinations.

$NaClO_2$-containing, ClO_2 emitting PEO nanofibers were prepared via electrospinning. Due to the addition of $NaClO_2$ to the precursor solution, the average fiber diameter decreased substantially. Major changes in the FTIR spectrum of the fibers could not be observed after $NaClO_2$-loading. ClO_2 production of samples of different weights was tested under conditions similar to the exhaled human breath. The ClO_2 production along with the yield of ClO_2 decreased with increasing sample weights. The 1 mg sample produced 66 ppm of ClO_2 with 89% of yield. The changes in carbon dioxide concentration in the reaction chamber did not alter the ClO_2 production of the samples. A longer exposure time, however, increased the final ClO_2 concentration. Due to the humid environment, swelling and disintegration of the fibrous structure was observed in the PEO-based sheets, thus a gel-like layer was formed in the presence of moisture. The presence of such layer decreased the surface-to-volume ratio and limited the diffusion of the reactants in higher weights of fibers. $NaClO_2$-loaded fibers were able to liberate ClO_2 into the gas phase and eliminate bacteria effectively. The antibacterial efficacy was influenced by the $NaClO_2$-loading of the sample and the subsequent maximal ClO_2 concentration reached.

7. REFERENCES

1. Hoehn RC, Shorney-Darby H, Neemann J. Chlorine Dioxide. In: Wallis-Lage C (Ed.), White's Handbook of Chlorination and Alternative Disinfectants. John Wiley & Sons, Inc., Hoboken, NJ, 2009: 703-755. https://doi.org/10.1002/9780470561331.ch14
2. Gordon G, Kieffer RG, Rosenblatt DH. The Chemistry of Chlorine Dioxide. In: Lippard S (Ed.), Progress in Inorganic Chemistry. John Wiley & Sons, Inc., New York, NY, 1972: 201-286. https://doi.org/10.1002/9780470166161.ch3
3. Cosson H, Ernst WR. (1994) Photodecomposition of Chlorine Dioxide and Sodium Chlorite in Aqueous Solution by Irradiation with Ultraviolet Light. Ind. Eng. Chem. Res., 33: 1468-1475. https://doi.org/10.1021/ie00030a006
4. ATSDR. (2004) Toxicological Profile for Chlorine Dioxide and Chlorite. Atlanta, GA: U.S. Department of Health and Human Services, Public Health Service. https://doi.org/10.15620/cdc:37580
5. Qi M, Yi T, Mo Q, Huang L, Zhao H, Xu H, Huang C, Wang S, Liu Y, Hui Z. (2020) Preparation of High-Purity Chlorine Dioxide by Combined Reduction. Chem Eng Technol, 43: 1850-1858. https://doi.org/10.1002/ceat.202000121
6. Kály-Kullai K, Wittmann M, Noszticzius Z, Rosivall L. (2020) Can chlorine dioxide prevent the spreading of coronavirus or other viral infections? Medical hypotheses. Physiol Int, 107: 1-11. https://doi.org/10.1556/2060.2020.00015
7. Körtvélyesi Zs. (2004). Analytical Methods for the Measurement of Chlorine Dioxide and Related Oxychlorine Species in Aqueous Solution. (PhD Dissertation). Miami University, Oxford, OH. Retrieved from http://rave.ohiolink.edu/etdc/view?acc_num=miami1088030135 (Access date: 10.03.2022.)
8. Gordon G, Rosenblatt AA. (2005) Chlorine Dioxide: The Current State of the Art. Ozone Sci Eng, 27: 203-207. https://doi.org/10.1080/01919510590945741
9. Kieffer RG, Gordon G. (1968) Disproportionation of Chlorous Acid. I. Stoichiometry. Inorg Chem, 7: 235-239. https://doi.org/10.1021/ic50060a013
10. Sales Monteiro MK, Sales Monteiro MM, de Melo Henrique AM, Llanos J, Saez C, Dos Santos EV, Rodrigo MA. (2021) A review on the electrochemical production of chlorine dioxide from chlorates and hydrogen peroxide. Curr Opin Electrochem, 27: 100685. https://doi.org/10.1016/j.coelec.2020.100685

11. Hull LA, Davis GT, Rosenblatt DH, Williams HKR, Weglein RC. (1967) Oxidations of Amines. III. Duality of Mechanism in the Reaction of Amines with Chlorine Dioxide. J Am Chem Soc, 89: 1163-1170. https://doi.org/10.1021/ja00981a023
12. Noszticzius Z, Wittmann M, Kály-Kullai K, Beregvári Z, Kiss I, Rosivall L, Szegedi J. (2013) Chlorine dioxide is a size-selective antimicrobial agent. PLoS One, 8: e79157. https://doi.org/10.1371/journal.pone.0079157
13. Noss CI, Hauchman FS, Olivieri VP. (1986) Chlorine dioxide reactivity with proteins. Water Res, 20: 351-356. https://doi.org/10.1016/0043-1354(86)90083-7
14. Tan H, Wheeler WB, Wei C. (1987) Reaction of chlorine dioxide with amino acids and peptides: Kinetics and mutagenicity studies. Mutat Res, 188: 259-266. https://doi.org/10.1016/0165-1218(87)90002-4
15. Ison A, Odeh IN, Margerum DW. (2006) Kinetics and Mechanisms of Chlorine Dioxide and Chlorite Oxidations of Cysteine and Glutathione. Inorg Chem, 45: 8768-8775. https://doi.org/10.1021/ic0609554
16. Napolitano MJ, Green BJ, Nicoson JS, Margerum DW. (2005) Chlorine Dioxide Oxidations of Tyrosine, N-Acetyltyrosine, and Dopa. Chem Res Toxicol, 18: 501-508. https://doi.org/10.1021/tx049697i
17. Stewart DJ, Napolitano MJ, Bakhmutova-Albert EV, Margerum DW. (2008) Kinetics and Mechanisms of Chlorine Dioxide Oxidation of Tryptophan. Inorg Chem, 47: 1639-1647. https://doi.org/10.1021/ic701761p
18. Napolitano MJ, Stewart DJ, Margerum DW. (2006) Chlorine Dioxide Oxidation of Guanosine 5‘-Monophosphate. Chem Res Toxicol, 19: 1451-1458. https://doi.org/10.1021/tx060124a
19. Ogata N. (2007) Denaturation of Protein by Chlorine Dioxide: Oxidative Modification of Tryptophan and Tyrosine Residues. Biochemistry, 46: 4898-4911. https://doi.org/10.1021/bi061827u
20. Ogata N, Shibata T. (2008) Protective effect of low-concentration chlorine dioxide gas against influenza A virus infection. J Gen Virol, 89: 60-67. https://doi.org/10.1099/vir.0.83393-0
21. Ogata N. (2012) Inactivation of influenza virus haemagglutinin by chlorine dioxide: oxidation of the conserved tryptophan 153 residue in the receptor-binding site. J Gen Virol, 93: 2558-2563. https://doi.org/10.1099/vir.0.044263-0

22. Tachikawa M, Saita K, Tezuka M, Sawamura R. (1993) Inactivation of Poliovirus with Chlorine Dioxide. Eisei kagaku, 39: 572-576. https://doi.org/10.1248/jhs1956.39.6_572

23. Xue B, Jin M, Yang D, Guo X, Chen Z, Shen Z, Wang X, Qiu Z, Wang J, Zhang B, Li J. (2013) Effects of chlorine and chlorine dioxide on human rotavirus infectivity and genome stability. Water Res, 47: 3329-3338. https://doi.org/10.1016/j.watres.2013.03.025

24. Zoni R, Zanelli R, Riboldi E, Bigliardi L, Sansebastiano G. (2007) Investigation on virucidal activity of chlorine dioxide. experimental data on feline calicivirus, HAV and Coxsackie B5. J Prev Med Hyg, 48: 91-95.

25. Lénès D, Deboosere N, Ménard-Szczebara F, Jossent J, Alexandre V, Machinal C, Vialette M. (2010) Assessment of the removal and inactivation of influenza viruses H5N1 and H1N1 by drinking water treatment. Water Res, 44: 2473-2486. https://doi.org/10.1016/j.watres.2010.01.013

26. Sanekata T, Fukuda T, Miura T, Morino H, Lee C, Maeda KEN, Araki K, Otake T, Kawahata T, Shibata T. (2010) Evaluation of the Antiviral Activity of Chlorine Dioxide and Sodium Hypochlorite against Feline Calicivirus, Human Influenza Virus, Measles Virus, Canine Distemper Virus, Human Herpesvirus, Human Adenovirus, Canine Adenovirus and Canine Parvovirus. Biocontrol Sci, 15: 45-49. https://doi.org/10.4265/bio.15.45

27. Morino H, Fukuda T, Miura T, Lee C, Shibata T, Sanekata T. (2009) Inactivation of Feline Calicivirus, a Norovirus Surrogate, by Chlorine Dioxide Gas. Biocontrol Sci, 14: 147-153. https://doi.org/10.4265/bio.14.147

28. Ofori I, Maddila S, Lin J, Jonnalagadda SB. (2018) Chlorine dioxide inactivation of Pseudomonas aeruginosa and Staphylococcus aureus in water: The kinetics and mechanism. J Water Process Eng, 26: 46–54. https://doi.org/10.1016/j.jwpe.2018.09.001

29. Al-Sa'ady AT, Nahar HS, Saffah FF. (2020) Antibacterial activities of chlorine gas and chlorine dioxide gas against some pathogenic bacteria. Eurasia J Biosci, 14.

30. Hsu MS, Wu MY, Huang YT, Liao CH. (2016) Efficacy of chlorine dioxide disinfection to non-fermentative Gram-negative bacilli and non-tuberculous mycobacteria in a hospital water system. J Hosp Infect, 93: 22-28. https://doi.org/10.1016/j.jhin.2016.01.005

31. Lowe JJ, Gibbs SG, Iwen PC, Smith PW, Hewlett AL. (2013) Decontamination of a Hospital Room Using Gaseous Chlorine Dioxide: Bacillus anthracis, Francisella tularensis, and Yersinia pestis. J Occup Environ Hyg, 10: 533-539. https://doi.org/10.1080/15459624.2013.818241

32. Stratilo CW, Crichton MK, Sawyer TW. (2015) Decontamination Efficacy and Skin Toxicity of Two Decontaminants against Bacillus anthracis. PLoS ONE, 10: e0138491. https://doi.org/10.1371/journal.pone.0138491

33. Uppu DS, Samaddar S, Ghosh C, Paramanandham K, Shome BR, Haldar J. (2016) Amide side chain amphiphilic polymers disrupt surface established bacterial bio-films and protect mice from chronic Acinetobacter baumannii infection. Biomaterials, 74: 131-143. https://doi.org/10.1016/j.biomaterials.2015.09.042

34. Wen G, Xu X., Huang T, Zhu H, Ma J. (2017) Inactivation of three genera of dominant fungal spores in groundwater using chlorine dioxide: Effectiveness, influencing factors, and mechanisms. Water Res, 125: 132-140. https://doi.org/10.1016/j.watres.2017.08.038

35. Yadav SR, Kini VV, Padhye A. (2015) Inhibition of Tongue Coat and Dental Plaque Formation by Stabilized Chlorine Dioxide Vs Chlorhexidine Mouthrinse: A Randomized, Triple Blinded Study. J Clin Diagn Res, 9: Zc69-74. https://doi.org/10.7860/jcdr/2015/14587.6510

36. Junli H, Li W, Nenqi R, Li L.X, Fun SR, Guanle Y. (1997) Disinfection effect of chlorine dioxide on viruses, algae and animal planktons in water. Water Res, 31: 455-460.

37. Venkatnarayanan S, Sriyutha Murthy P, Kirubagaran R, Venugopalan VP. (2017) Chlorine dioxide as an alternative antifouling biocide for cooling water systems: Toxicity to larval barnacle Amphibalanus reticulatus (Utinomi). Mar Pollut Bull, 124: 803-810. https://doi.org/10.1016/j.marpolbul.2017.01.023

38. Benarde MA, Israel BM, Olivieri VP, Granstrom ML. (1965) Efficiency of chlorine dioxide as a bactericide. Appl Microbiol, 13: 776-780. https://doi.org/10.1128/am.13.5.776-780.1965

39. Grunert A, Frohnert A, Selinka HC, Szewzyk R. (2018) A new approach to testing the efficacy of drinking water disinfectants. Int J Hyg Environ Health, 221: 1124-1132. https://doi.org/10.1016/j.ijheh.2018.07.010

40. Gray NF. Chlorine dioxide. In: Percival S, Yates M, Williams D, Chalmers R, Gray N (Eds.), Microbiology of Waterborne Diseases, 2nd ed. Academic Press, New York, 2014.
41. Liester MB. (2021) The chlorine dioxide controversy: A deadly poison or a cure for COVID-19? Int J Med Med Sci, 13: 13-21. https://doi.org/10.5897/IJMMS2021.1461
42. Vincenti S, de Waure C, Raponi M, Teleman AA, Boninti F, Bruno S, Boccia S, Damiani G, Laurenti P. (2019) Environmental surveillance of Legionella spp. colonization in the water system of a large academic hospital: Analysis of the four-year results on the effectiveness of the chlorine dioxide disinfection method. Sci Total Environ, 657: 248-253. https://doi.org/10.1016/j.scitotenv.2018.12.036
43. Walker JT, Mackerness CW, Mallon D, Makin T, Williets T, Keevil CW. (1995) Control ofLegionella pneumophila in a hospital water system by chlorine dioxide. J Ind Microbiol, 15: 384-390. https://doi.org/10.1007/BF01569995
44. Zhang Z, McCann C, Stout JE, Piesczynski S, Hawks R, Vidic R, Yu VL. (2007) Safety and Efficacy of Chlorine Dioxide for Legionella Control in a Hospital Water System. Infect Control Hosp Epidemiol, 28: 1009-1012. https://doi.org/10.1086/518847
45. Lowe JJ, Hewlett AL, Iwen PC, Smith PW, Gibbs SG. (2013) Evaluation of ambulance decontamination using gaseous chlorine dioxide. Prehosp Emerg Care, 17: 401-408. https://doi.org/10.3109/10903127.2013.792889
46. Trinh VM, Yuan MH, Chen YH, Wu CY, Kang SC, Chiang PC, Hsiao TC, Huang HP, Zhao YL, Lin JF, Huang CH, Yeh JH, Lee DM. (2021) Chlorine dioxide gas generation using rotating packed bed for air disinfection in a hospital. J Clean Prod, 320: 128885. https://doi.org/10.1016/j.jclepro.2021.128885
47. Lowe JJ, Gibbs SG, .Iwen PC, Smith PW, Hewlett AL. (2013) Impact of Chlorine Dioxide Gas Sterilization on Nosocomial Organism Viability in a Hospital Room. Int J Environ Res Public Health, 10: 2596–2605. https://doi.org/10.3390/ijerph10062596
48. Ogata N, Sakasegawa M, Miura T, Shibata T, Takigawa Y, Taura K, Taguchi K, Matsubara K, Nakahara K, Kato D, Sogawa K, Oka H. (2016) Inactivation of Airborne Bacteria and Viruses Using Extremely Low Concentrations of

Chlorine Dioxide Gas. Pharmacology, 97: 301-306. https://doi.org/10.1159/000444503

49. Mostajo-Radji MA. (2021) Pseudoscience in the Times of Crisis: How and Why Chlorine Dioxide Consumption Became Popular in Latin America During the COVID-19 Pandemic. Front Polit Sci, 3. https://doi.org/10.3389/fpos.2021.621370

50. Valente JH, Jay GD, Zabbo CP, Reinert SE, Bertsch K. (2014) Activated chlorine dioxide solution can be used as a biocompatible antiseptic wound irrigant. Adv Skin Wound Care, 27: 13-19. https://doi.org/10.1097/01.ASW.0000439060.79822.b3

51. Mohammad AR, Giannini PJ, Preshaw PM, Alliger H. (2004) Clinical and microbiological efficacy of chlorine dioxide in the management of chronic atrophic candidiasis: an open study. Int Dent J, 54: 154-158. https://doi.org/10.1111/j.1875-595X.2004.tb00272.x

52. Shinada K, Ueno M, Konishi C, Takehara S, Yokoyama S, Zaitsu T, Ohnuki M, Wright FAC, Kawaguchi Y. (2010) Effects of a mouthwash with chlorine dioxide on oral malodor and salivary bacteria: a randomized placebo-controlled 7-day trial. Trials, 11: 14. https://doi.org/10.1186/1745-6215-11-14

53. Herczegh A, Ghidan A, Friedreich D, Gyurkovics M, Bendő Z, Lohinai Z. (2013) Effectiveness of a high purity chlorine dioxide solution in eliminating intracanal Enterococcus faecalis biofilm. Acta Microbiol Immunol Hung, 60: 63-75. https://doi.org/10.1556/amicr.60.2013.1.7

54. Meggs WJ, Elsheik T, Metzger WJ, Albernaz M, Bloch RM. (1996) Nasal pathology and ultrastructure in patients with chronic airway inflammation (RADS and RUDS) following an irritant exposure. J Toxicol Clin Toxicol, 34: 383-396. https://doi.org/10.3109/15563659609013808

55. Exner-Freisfeld H, Kronenberger H, Meier-Sydow J, Nerger KH. (1986) Bleaching agent poisoning with sodium chlorite. The toxicology and clinical course. Dtsch Med Wochenschr, 111: 1927-1930. https://doi.org/10.1055/s-2008-1068737

56. Bathina G, Yadla M, Burri S, Enganti R, Prasad Ch R, Deshpande P, Ch R, Prayaga A, Uppin M. (2013) An unusual case of reversible acute kidney injury due to chlorine dioxide poisoning. Ren Fail, 35: 1176-1178. https://doi.org/10.3109/0886022X.2013.819711

57. Medina-Avitia E, Tella-Vega P, García-Estrada C. (2021) Acute kidney injury secondary to chlorine dioxide use for COVID-19 prevention. Hemodial Int, 25: E40-E43. https://doi.org/10.1111/hdi.12941

58. Kanitz S, Franco Y, Patrone V, Caltabellotta M, Raffo E, Riggi C, Timitilli D, Ravera G. (1996) Association between drinking water disinfection and somatic parameters at birth. Environ Health Perspect, 104: 516-520. https://doi.org/10.1289/ehp.96104516

59. Källén BA, Robert E. (2000) Drinking water chlorination and delivery outcome-a registry-based study in Sweden. Reprod Toxicol, 14: 303-309. https://doi.org/10.1016/s0890-6238(00)00086-1

60. Lubbers JR, Chauhan S, Bianchine JR. (1981) Controlled clinical evaluations of chlorine dioxide, chlorite and chlorate in man. Fundam Appl Toxicol, 1: 334-338. https://doi.org/10.1016/s0272-0590(81)80042-5

61. Lubbers JR, Bianchine JR. (1984) Effects of the acute rising dose administration of chlorine dioxide, chlorate and chlorite to normal healthy adult male volunteers. J Environ Pathol Toxicol Oncol, 5: 215-228.

62. Dalhamn T. (1957) Chlorine dioxide toxicity in animal experiments and industrial risks. AMA Arch Ind Health, 15: 101-107.

63. Ma JW, Huang BS, Hsu CW, Peng CW, Cheng ML, Kao JY, Way TD, Yin HC, Wang SS. (2017) Efficacy and Safety Evaluation of a Chlorine Dioxide Solution. Int J Environ Res Public Health, 14: 329. https://doi.org/10.3390/ijerph14030329

64. Haller JF, Northgraves WW. (1955) Chlorine Dioxide and Safety. TAPPI, 38: 199-202.

65. Akamatsu A, Lee C, Morino H, Miura T, Ogata N, Shibata T. (2012) Six-month low level chlorine dioxide gas inhalation toxicity study with two-week recovery period in rats. J Occup Med Toxicol, 7: 2. https://doi.org/10.1186/1745-6673-7-2

66. Paulet G, Desbrousses S. (1972) On the toxicology of chlorine dioxide. Arch Mal Prof, 33: 59-61.

67. Paulet G, Desbrousses S. (1970) On the action of ClO2 at low concentrations on laboratory animals. Arch Mal Prof, 31: 97-106.

68. Paulet G, Desbrousses S (1974) Action of a discontinuous exposure to chlorine dioxide (ClO2) on the rat. Arch Mal Prof, 35: 797-804.

69. Bercz JP, Jones L, Garner L, Murray D, Ludwig DA, Boston J. (1982) Subchronic toxicity of chlorine dioxide and related compounds in drinking water in the nonhuman primate. Environ Health Perspect, 46: 47-55. https://doi.org/10.1289/ehp.824647

70. Mobley SA, Taylor DH, Laurie RD, Pfohl RJ. Chlorine dioxide depresses T3 uptake and delays development of locomotor activity in young rats. In: Jolley R, Bull R, Davis W (Eds.), Water chlorination: chemistry, environmental impact and health effects. Lewis Publications,, Chelsea, MI, 1990: 347-358.

71. Orme J, Taylor DH, Laurie RD, Bull RJ. (1985) Effects of chlorine dioxide on thyroid function in neonatal rats. J Toxicol Environ Health, 15: 315-322. https://doi.org/10.1080/15287398509530657

72. Toth GP, Long RE, Mills TS, Smith MK. (1990) Effects of chlorine dioxide on the developing rat brain. J Toxicol Environ Health, 31: 29-44. https://doi.org/10.1080/15287399009531435

73. Harrington RM, Romano RR, Gates D, Ridgway P. (1995) Subchronic toxicity of sodium chlorite in the rat. J Am Coll Toxicol, 14: 21-33.

74. Abdel-Rahman MS, Couri D, Bull RJ. (1984) Toxicity of Chlorine Dioxide in Drinking Water. J Am Coll Toxicol, 3: 277-284. https://doi.org/10.3109/10915818409009082

75. Abdel-Rahman MS, Couri D, Bull RJ. (1979) Kinetics of Cl02 and effects of Cl02, Cl02-, and Cl03- in drinking water on blood glutathione and hemolysis in rat and chicken. J Environ Pathol Toxicol, 3: 431-449.

76. Láng O, Nagy KS, Láng J, Perczel-Kovách K, Herczegh A, Lohinai Z, Varga G, Kőhidai L. (2021) Comparative study of hyperpure chlorine dioxide with two other irrigants regarding the viability of periodontal ligament stem cells. Clin Oral Investig, 25: 2981-2992. https://doi.org/10.1007/s00784-020-03618-5

77. da Cunha BR, Fonseca LP, Calado CRC. (2019) Antibiotic Discovery: Where Have We Come from, Where Do We Go? Antibiotics-Basel, 8: 21. https://doi.org/10.3390/antibiotics8020045

78. Cassini A, Hogberg LD, Plachouras D, Quattrocchi A, Hoxha A, Simonsen GS, Colomb-Cotinat M, Kretzschmar ME, Devleesschauwer B, Cecchini M, Ouakrim DA, Oliveira TC, Struelens MJ, Suetens C, Monnet DL. (2019) Attributable deaths and disability-adjusted life-years caused by infections with antibiotic-resistant bacteria in the EU and the European Economic Area in 2015:

a population-level modelling analysis. Lancet Infect Dis, 19: 56-66. https://doi.org/10.1016/s1473-3099(18)30605-4

79. Beier RC, Franz E, Bono JL, Mandrell RE, Fratamico PM, Callaway TR, Andrews K, Poole TL, Crippen TL, Sheffield CL, Anderson RC, Nisbet DJ. (2016) Disinfectant and Antimicrobial Susceptibility Profiles of the Big Six Non-0157 Shiga Toxin-Producing Escherichia coli Strains from Food Animals and Humans. J Food Prot, 79: 1355-1370. https://doi.org/10.4315/0362-028x.Mp-15-600

80. Capita R, Riesco-Pelaez F, Alonso-Hernando A, Alonso-Calleja C. (2014) Exposure of Escherichia coli ATCC 12806 to Sublethal Concentrations of Food-Grade Biocides Influences Its Ability To Form Biofilm, Resistance to Antimicrobials, and Ultrastructure. Appl Environ Microbiol, 80: 1268-1280. https://doi.org/10.1128/aem.02283-13

81. Lemmen SW, Lewalter K. (2018) Antibiotic stewardship and horizontal infection control are more effective than screening, isolation and eradication. Infection, 46: 581-590. https://doi.org/10.1007/s15010-018-1137-1

82. Kohler AT, Rodtoff AC, Labahn M, Reinhardt M, Truyen U, Speck S. (2018) Efficacy of sodium hypochlorite against multidrug-resistant Gram-negative bacteria. J Hosp Infect, 100: E40-E46. https://doi.org/10.1016/j.jhin.2018.07.017

83. Messler S, Klare I, Wappler F, Werner G, Ligges U, Sakka SG, Mattner F. (2019) Reduction of nosocomial bloodstream infections and nosocomial vancomycin-resistant Enterococcus faecium on an intensive care unit after introduction of antiseptic octenidine-based bathing. J Hosp Infect, 101: 264-271. https://doi.org/10.1016/j.jhin.2018.10.023

84. Beier RC, Duke SE, Ziprin RL, Harvey RB, Hume ME, Poole TL, Scott HM, Highfield LD, Alali WQ, Andrews K, Anderson RC, Nisbet DJ. (2008) Antibiotic and disinfectant susceptibility profiles of vancomycin-resistant Enterococcus faecium (VRE) isolated from community wastewater in texas. Bull Environ Contam Toxicol, 80: 188-194. https://doi.org/10.1007/s00128-007-9342-0

85. Kampf G. (2019) Antibiotic Resistance Can Be Enhanced in Gram-Positive Species by Some Biocidal Agents Used for Disinfection. Antibiotics, 8: 15. https://doi.org/10.3390/antibiotics8010013

86. Zhang YZ, Zhao YJ, Xu CQ, Zhang XC, Li JH, Dong GF, Cao JM, Zhou TL. (2019) Chlorhexidine exposure of clinical Klebsiella pneumoniae strains leads to acquired resistance to this disinfectant and to colistin. Int J Antimicrob Agents, 53: 864-867. https://doi.org/10.1016/j.ijantimicag.2019.02.012

87. Liu WJ, Fu L, Huang M, Zhang JP, Wu Y, Zhou YS, Zeng J, Wang GX. (2017) Frequency of antiseptic resistance genes and reduced susceptibility to biocides in carbapenem-resistant Acinetobacter baumannii. J Med Microbiol, 66: 13-17. https://doi.org/10.1099/jmm.0.000403

88. Sigstam T, Gannon G, Cascella M, Pecson BM, Wigginton KR, Kohn T. (2013) Subtle Differences in Virus Composition Affect Disinfection Kinetics and Mechanisms. Appl Environ Microbiol, 79: 3455-3467. https://doi.org/10.1128/AEM.00663-13

89. Ge Y, Zhang X, Shu L, Yang X. (2021) Kinetics and Mechanisms of Virus Inactivation by Chlorine Dioxide in Water Treatment: A Review. Bull Environ Contam Toxicol, 106: 560-567. https://doi.org/10.1007/s00128-021-03137-3

90. Konai MM, Bhattacharjee B, Ghosh S, Haldar J. (2018) Recent Progress in Polymer Research to Tackle Infections and Antimicrobial Resistance. Biomacromolecules, 19: 1888-1917. https://doi.org/10.1021/acs.biomac.8b00458

91. Ng VW, Chan JM, Sardon H, Ono RJ, Garcia JM, Yang YY, Hedrick JL. (2014) Antimicrobial hydrogels: a new weapon in the arsenal against multidrug-resistant infections. Adv Drug Deliv Rev, 78: 46-62. https://doi.org/10.1016/j.addr.2014.10.028

92. Colak S, Nelson CF, Nüsslein K, Tew GN. (2009) Hydrophilic modifications of an amphiphilic polynorbornene and the effects on its hemolytic and antibacterial activity. Biomacromolecules, 10: 353-359. https://doi.org/10.1021/bm801129y

93. Sgolastra F, Deronde BM, Sarapas JM, Som A, Tew GN. (2013) Designing mimics of membrane active proteins. Acc Chem Res, 46: 2977-2987. https://doi.org/10.1021/ar400066v

94. Palermo EF, Vemparala S, Kuroda K. (2012) Cationic spacer arm design strategy for control of antimicrobial activity and conformation of amphiphilic methacrylate random copolymers. Biomacromolecules, 13: 1632-1641. https://doi.org/10.1021/bm300342u

95. Chakraborty S, Liu R, Lemke JJ, Hayouka Z, Welch RA, Weisblum B, Masters KS, Gellman SH. (2013) Effects of Cyclic vs. Acyclic Hydrophobic Subunits on the Chemical Structure and Biological Properties of Nylon-3 Co-Polymers. ACS Macro Lett, 2. https://doi.org/10.1021/mz400239r

96. Chin W, Yang C, Ng VWL, Huang Y, Cheng J, Tong YW, Coady DJ, Fan W, Hedrick JL, Yang YY. (2013) Biodegradable broad-spectrum antimicrobial polycarbonates: Investigating the role of chemical structure on activity and selectivity. Macromolecules, 46: 8797-8807. https://doi.org/10.1021/ma4019685

97. Aziz MA, Cabral JD, Brooks HJ, Moratti SC, Hanton LR. (2012) Antimicrobial properties of a chitosan dextran-based hydrogel for surgical use. Antimicrob Agents Chemother, 56: 280-287. https://doi.org/10.1128/AAC.05463-11

98. Zhou C, Li P, Qi X, Sharif AR, Poon YF, Cao Y, Chang MW, Leong SS, Chan-Park MB. (2011) A photopolymerized antimicrobial hydrogel coating derived from epsilon-poly-L-lysine. Biomaterials, 32: 2704-2712. https://doi.org/10.1016/j.biomaterials.2010.12.040

99. Li Y, Fukushima K, Coady DJ, Engler AC, Liu S, Huang Y, Cho JS, Guo Y, Miller LS, Tan JPK, Ee PLR, Fan W, Yang YY, Hedrick JL. (2013) Broad-spectrum antimicrobial and biofilm-disrupting hydrogels: stereocomplex-driven supramolecular assemblies. Angew Chem Int Ed, 52: 674-678. https://doi.org/10.1002/anie.201206053

100. Bu Y, Zhang L, Liu J, Zhang L, Li T, Shen H, Wang X, Yang F, Tang P, Wu D. (2016) Synthesis and Properties of Hemostatic and Bacteria-Responsive in Situ Hydrogels for Emergency Treatment in Critical Situations. ACS Appl Mater Interfaces, 8: 12674-12683. https://doi.org/10.1021/acsami.6b03235

101. Zhang Y, Zhang J, Chen M, Gong H, Thamphiwatana S, Eckmann L, Gao W, Zhang L. (2016) A Bioadhesive Nanoparticle-Hydrogel Hybrid System for Localized Antimicrobial Drug Delivery. ACS Appl Mater Interfaces, 8: 18367-18374. https://doi.org/10.1021/acsami.6b04858

102. Kojic N, Pritchard EM, Tao H, Brenckle MA, Mondia JP, Panilaitis B, Omenetto F, Kaplan DL. (2012) Focal Infection Treatment using Laser-Mediated Heating of Injectable Silk Hydrogels with Gold Nanoparticles. Adv Funct Mater, 22: 3793-3798. https://doi.org/10.1002/adfm.201200382

103. GhavamiNejad A, Park CH, Kim CS. (2016) In Situ Synthesis of Antimicrobial Silver Nanoparticles within Antifouling Zwitterionic Hydrogels by Catecholic

Redox Chemistry for Wound Healing Application. Biomacromolecules, 17: 1213-1223. https://doi.org/10.1021/acs.biomac.6b00039

104. Shahriar SMS, Mondal J, Hasan MN, Revuri V, Lee DY, Lee YK. (2019) Electrospinning Nanofibers for Therapeutics Delivery. Nanomaterials, 9: 532. https://doi.org/10.3390/nano9040532
105. Abrigo M, Kingshott P, McArthur SL. (2015) Electrospun polystyrene fiber diameter influencing bacterial attachment, proliferation, and growth. ACS Appl Mater Interfaces, 7: 7644-7652. https://doi.org/10.1021/acsami.5b00453
106. Guarino V, Cruz-Maya I, Altobelli R, Abdul Khodir WK, Ambrosio L, Alvarez Pèrez MA, Flores AA. (2017) Electrospun polycaprolactone nanofibres decorated by drug loaded chitosan nano-reservoirs for antibacterial treatments. Nanotechnology, 28: 505103. https://doi.org/10.1088/1361-6528/aa9542
107. Topuz F, Kilic ME, Durgun E, Szekely Gy. (2021) Fast-dissolving antibacterial nanofibers of cyclodextrin/antibiotic inclusion complexes for oral drug delivery. J Colloid Interface Sci, 585: 184-194. https://doi.org/10.1016/j.jcis.2020.11.072
108. Martínez-Camacho AP, Cortez-Rocha MO, Castillo-Ortega MM, Burgos-Hernández A, Ezquerra-Brauer JM, Plascencia-Jatomea M. (2011) Antimicrobial activity of chitosan nanofibers obtained by electrospinning. Polym Int, 60: 1663-1669. https://doi.org/10.1002/pi.3174
109. Lin L, Gu Y, Cui H. (2018) Novel electrospun gelatin-glycerin-ε-Poly-lysine nanofibers for controlling Listeria monocytogenes on beef. Food Packag Shelf Life, 18: 21-30. https://doi.org/10.1016/j.fpsl.2018.08.004
110. Heidari M, Bahrami SH, Ranjbar-Mohammadi M, Milan PB. (2019) Smart electrospun nanofibers containing PCL/gelatin/graphene oxide for application in nerve tissue engineering. Mater Sci Eng C Mater Biol Appl, 103: 109768. https://doi.org/10.1016/j.msec.2019.109768
111. Yang J, Wang K, Yu DG, Yang Y, Bligh SWA, Williams GR. (2020) Electrospun Janus nanofibers loaded with a drug and inorganic nanoparticles as an effective antibacterial wound dressing. Mater Sci Eng C, 111: 110805. https://doi.org/10.1016/j.msec.2020.110805
112. Ishi G. (1958) Solubility of chlorine dioxide. Chem Eng Japan, 22: 153-114.

8. BIBLIOGRAPHY OF THE CANDIDATE'S PUBLICATIONS

8.1. Publication relevant to the dissertation

I. Palcsó B, Kazsoki A, Herczegh A, Ghidán Á, Pinke B, Mészáros L, Zelkó R. (2022) Formulation of Chlorine-Dioxide-Releasing Nanofibers for Disinfection in Humid and CO2-Rich Environment. Nanomaterials, 12(9): 1481. IF(2021): 5.719. https://doi.org/10.3390/nano12091481

II. Palcsó B, Moldován Zs, Süvegh K, Herczegh A, Zelkó R. (2019) Chlorine dioxide-loaded poly(acrylic acid) gels for prolonged antimicrobial effect. Mater Sci Eng C, 98: 782-788. IF(2019): 5.88. https://doi.org/10.1016/j.msec.2019.01.043

8.2. Further related publications

III. Kazsoki A, Palcsó B, Omer SM, Kovacs Z, Zelkó R. (2022) Formulation of Levocetirizine-Loaded Core–Shell Type Nanofibrous Orally Dissolving Webs as a Potential Alternative for Immediate Release Dosage Forms. Pharmaceutics, 14(7): 1442. IF: 6.525. https://doi.org/10.3390/pharmaceutics14071442

IV. Kazsoki A, Palcsó B, Alpár A, Snoeck R, Andrei G, Zelkó R. (2022). Formulation of acyclovir (core)-dexpanthenol (sheath) nanofibrous patches for the treatment of herpes labialis. Int J Pharm, 611: 121354. IF(2021): 6.51. https://doi.org/10.1016/j.ijpharm.2021.121354

V. Herczegh A, Palcso B, Lohinai Zs, Zelko R. (2019). Tracking of the degradation process of chlorhexidine digluconate and ethylenediaminetetraacetic acid in the presence of hyper-pure chlorine dioxide in endodontic disinfection. J Pharm Biomed Anal, 164: 360–364. IF(2019): 3.209. https://doi.org/10.1016/j.jpba.2018.11.005

8.3. Other, not related publications

VI. Palcsó B, Zelkó R. (2018). Different types, applications and limits of enabling excipients of pharmaceutical dosage forms. Drug Discov Today Technol, 27: 21–39. IF:-

VII. Kovács A, Palcsó B, Zelkó R. (2018) Elektrosztatikus szálképzéssel előállított szálas hatóanyag-hordozó rendszerek vizsgálatának lehetőségei. Acta Pharm Hung, 88: 1 pp. 27-43. , 17 p. IF:-

DOI:10.14753/SE.2022.2766

9. ACKNOWLEDGEMENTS

I would like to express my sincere gratitude to my supervisor, Professor Romána Zelkó for her guidance, encouragement, ideas, and endless patience that did not fade throughout my Ph.D. studies.

I could not have undertaken this journey without my colleague, Dr. Adrienn Kazsoki, who helped me selflessly, from whom I could learn and received countless pieces of practical advice.

I am also grateful for my co-authors, Dr. Anna Herczegh and Dr. Ágoston Ghidán for helping me design and carry out the microbiological experiments.

Special thanks to Dr. Zoltán Noszticzius for his guidance and ideas on the analytical measurements and for providing me equipment whenever I needed.

I am also indebted to Károly Süvegh, Balázs Pinke and László Mészáros for providing me their expertise during my work.

I am grateful to my colleagues at the University Pharmacy Department of Pharmacy Administration.

I am more than grateful to my wife, Dr. Zsófia Palcsó-Moldován and my daughter, Eliza for patiently enduring my overtimes, late-night works and holding our family and household together when I had no capacity for it.

Last, but not least I would like to thank God Almighty for leading me on His way.

DOI:10.14753/SE.2022.2766
Materials Science & Engineering C 98 (2019) 782–788

Contents lists available at ScienceDirect

Materials Science & Engineering C

journal homepage: www.elsevier.com/locate/msec

Chlorine dioxide-loaded poly(acrylic acid) gels for prolonged antimicrobial effect

Barnabás Palcsó[a], Zsófia Moldován[b], Károly Süvegh[c], Anna Herczegh[b], Romána Zelkó[a,*]

[a] University Pharmacy Department of Pharmacy Administration, Semmelweis University, Hőgyes Endre utca 7-9, H-1092 Budapest, Hungary
[b] Department of Conservative Dentistry, Semmelweis University, Szentkirályi utca 47, H-1088 Budapest, Hungary
[c] Laboratory of Nuclear Chemistry, Eötvös Loránd University/HAS Chemical Research Center, P.O. Box 32, H-1518 Budapest 112, Hungary

ARTICLE INFO

Keywords:
Chlorine dioxide
Poly(acrylic acid)
Gel
Ortho-positronium lifetime
Factorial design
Antimicrobial activity

ABSTRACT

Chlorine dioxide, the so-called "ideal biocide", can be successfully applied as an antiseptic agent based on its rapid and safe antimicrobial property. One of the significant limitations of its topical or oral use is that the chlorine dioxide residence time in aqueous solution is very short due to the volatility of the gas. Therefore, the primary purpose of the present study was to increase the duration of chlorine dioxide effect by creating a system capable of loading the gas for a prolonged time and gradually releasing it at the site of action. Poly(acrylic acid) gels of various chlorine dioxide and polymer concentrations were formulated to achieve this goal. A two-factor, three-level face-centred central composite design was applied for the formulation. The microstructure of the gels was tracked by positron annihilation lifetime spectroscopy based on the ortho-positronium (o-Ps) lifetime distributions with the residual chlorine concentrations, determined by iodometric titration and their antibacterial effects. The results indicate that the polymer possesses two functions. On the one hand, as a diffusion barrier inhibits the fugacity of the gaseous chlorine dioxide but on the other side, the polymer chains form an arranged supramolecular structure with the hydrated forms of chlorine dioxide thus resulting in its sustained fugacity. The latter showed optimum as a function of the polymer concentration in the investigated range (0.1–0.3% w/w). The o-Ps lifetime distributions confirmed the microstructural changes of the formulations and were in good agreement with the analytical and microbiological evaluation. The application of chlorine dioxide-loaded bioadhesive gels could be a promising alternative for the effective and safe treatment of topical infections.

1. Introduction

Chlorine dioxide is traditionally a water-soluble, gaseous disinfectant used in industry, which, through its beneficial properties, also gains an increasing role in healthcare. They often refer to chlorine dioxide as an "ideal" antiseptic, which does not seem to be exaggerated when examining the antimicrobial properties and relative harmlessness of the compound [1]. Chlorine dioxide is an effective compound capable of destroying bacteria, viruses, fungi and other cellular pathogens and is therefore widely used as a disinfectant for the purification of drinking water and the disinfection of fruits in the food industry [2–6]. The broad spectrum of effects is based on the fact that chlorine dioxide damages the life functions of the microorganism, which can be found in all living organisms regardless of species. The compound exerts its effect mainly through the oxidation of sulfhydryl (SH) groups of proteins essential to the cell. The individual antimicrobial compounds of the human body, hypo-halogenic acids, work with a similar mechanism as chlorine dioxide, they inhibit the ATP synthesis of pathogens by oxidation their SH-groups [7]. Since chlorine dioxide destroys pathogens by eliminating vital proteins, the microorganisms cannot resist it by either of their resistance mechanisms. Its broad spectrum and protection to resistance made the chlorine dioxide an effective mean for fighting nosocomial infections. It is known that one of the major health challenges of today is the spread of resistant bacteria, which is an increasingly urgent problem with the decreasing number of new types of antibiotics. By the use of surface disinfectants and antiseptics, the formation of nosocomial infections can be prevented, and antibiotic use can be reduced [8]. Despite their efficacy, the main limit of the currently applied disinfectants (e.g. ozone, hydrogen peroxide, peracetic acid) is that they are toxic even at low concentrations. The health-damaging effect of such compounds was investigated and confirmed on workers under hospital circumstances [9]. The other pillar of the ideal property of chlorine dioxide is its safety. Based on its mechanism of action, human and animal cells are not free from the cell-killing effect

* Corresponding author.
E-mail address: zelko.romana@pharma.semmelweis-univ.hu (R. Zelkó).

https://doi.org/10.1016/j.msec.2019.01.043
Received 16 August 2018; Received in revised form 13 December 2018; Accepted 10 January 2019
Available online 11 January 2019

DOI:10.14753/SE.2022.2766

of chlorine dioxide, but it can be observed that it is not harmful to the animal organism even at adequate antibacterial, antifungal and antiviral activity [10]. According to the results of a recent study, the background of the unexpected selectivity and safety is not in the different biochemical processes but the difference in size [11]. While destroying bacteria by the fraction of a second, chlorine dioxide cannot cause real damage to the human or animal body. The background of the protection against toxicity is multifactorial. Chlorine dioxide selectively reacts with a few amino acids, while other macromolecules can only be oxidised in a few orders of magnitude slower reactions. The size of the mammalian cell exceeds its bacteria by order of magnitude, so higher exposure is required to damage the cell. A part of the protection function consists of the mammalian SH-group storage depot (glutathione), which serves as a substrate for chlorine dioxide. The blood circulation of the mammalian tissue can eliminate a significant amount of potentially damaging substances from the cells. As a result, the penetration depth of the chlorine dioxide in the mammalian organism is small, and the concentration required for the bactericide effect is well below the toxic level. Accordingly, it can be advantageously applied under hospital conditions, as well as in aqueous solution and a gas form [12,13]. The use of chlorine dioxide as an antiseptic agent has so far been limited by the fact that the most commonly used manufacturing methods resulted in contaminants. A method has been developed to help scientists successfully produce a high purity chlorine dioxide solution to open the way for a wide range of therapeutic applications [14]. Compared with other disinfectants, it can be stated that antimicrobial activity and biofilm dissolution ability of chlorine dioxide reach or even exceed those of popular antiseptics such as sodium hypochlorite or chlorhexidine [15]. Considering its safe application, it is therefore ideal for treating various infections caused by bacterial, fungal or other, even resistant pathogens, as well. One of the major limitations of topical or oral use is that the chlorine dioxide residence time in aqueous solution is little more than 1 min due to the volatility of the gas. Chlorine dioxide needs only a few milliseconds to the bactericide effect, so this time is sufficient for disinfection [11]. However, in the body or other therapeutic applications, the time available for the effect may be reduced considerably if the aqueous solution flows out or diffuse from the site of application. Along with the excessive fugacity of chlorine dioxide, the latter can disadvantageously influence its bactericide efficacy. Due to the short residence time of chlorine dioxide dissolved in water, it may be necessary to rinse or wash several times during the treatment. The safe application of chlorine dioxide is based on the fact that the penetration depth during little contact is small (a few tenths of a millimetre), so that the oxidant does not pose a risk to a larger organism, but it can destroy infectious agents on the surface. However, there may be a case in which an increase in the residence time of chlorine dioxide on the body surface or in the body cavity becomes necessary. For example, a long-lasting (at least a few minutes) effects may be needed to treat a highly infected, pustulous or deep wound, and inflamed root canal, which the aqueous solution cannot provide. The residence time of chlorine dioxide can be increased by creating a system capable of loading the gas for a prolonged time and gradually releasing it at the site of action.

The primary purpose of the present study was to formulate a bioadhesive gel capable of increasing the effect of chlorine dioxide. Another aim was to investigate the relationship between the microstructure of the gel and the chlorine dioxide loading ability and thus the following antimicrobial activity of the composition.

2. Materials and methods

2.1. Materials

For the formulation of gels, poly(acrylic acid) with an apparent viscosity of 47,000 mPa·s (trade name: ACRYPOL ELT-10), chlorine dioxide (ClO_2), sodium hydroxide (NaOH) and distilled water were used. Poly(acrylic acid) was donated from Corel Pharma Chem (Gujarat, India). Chlorine dioxide was purchased from Zoltán Noszticzius (Budapest University of Technology and Economics) in the form of 1000 ppm Solumium and 3000 ppm Solvocid. The 3000 ppm Solvocid was diluted to 1000 ppm with distilled water, and only 1000 ppm of chlorine dioxide was used in the experiments. The NaOH required for the gelling was of analytical reagent grade.

2.2. Formulation of gels

Gels containing 0.1, 0.2 and 0.3% w/w of poly(acrylic acid) (PAA) powder were prepared. We used three different chlorine dioxide concentrations: 0.05, 0.15 and 0.25 mg/g (or 50, 150 and 250 ppm). The total weight of the chlorine dioxide-containing gel samples was 80 g, thus 0.1, 0.2 and 0.3% w/w gels contained 0.08 g, 0.16 g and 0.24 g of PAA powder, respectively. In the preparation of the gels, PAA powder was measured into a 100 ml brown bottle and a sufficient amount of distilled water was added. NaOH was added to neutralise the polymer and the samples were placed on a shaker. The gels were homogenized for 4 h and allowed to stand at 6 °C overnight. The next day, the chlorine dioxide solution stored at 6 °C was also added, and the glass was closed with a unique chlorine dioxide-resistant cap. The active ingredient was added to the samples in 1000 ppm aqueous solution. When determining the total volume of water necessary for the preparation of gels, the amounts of water added along with the chlorine dioxide solution and with the dissolved NaOH were also taken to consideration. To minimise the fugacity of chlorine dioxide, Solumium was injected at a slow rate into the gel with a 10 or 20 ml syringe of 1.2 × 50 mm (18 G, 2″) needles depending on the volume of the chlorine dioxide solution. To test the chlorine dioxide loading ability of the gels, the samples were stored at room temperature in the same glass containers with open caps. We prepared control samples according to the gels. The control samples were aqueous solutions of chlorine dioxide, and the concentrations were 0.05, 0.15 and 0.25 mg/g, respectively.

2.3. Analytical measurements

The chlorine dioxide content of the gels was determined by iodometric titration. After preparation, the gels were stored at room temperature without cover for two weeks, and the remaining chlorine dioxide concentration was measured to determine the 'ClO_2-storing capacity' of the gels. The chlorine dioxide concentration was measured every second day following the preparation until the 8th day, and finally, the chlorine dioxide residue was determined on day 14. The titration was based on the measurement of iodine generated in the reduction-oxidation reaction between chlorine dioxide and the excess of potassium iodide. The reaction is carried out in acidic medium (pH 2) according to the following equation:

$$2\,ClO_2 + 10\,I^- + 8\,H^+ = 5\,I_2 + 2\,Cl^- + 4\,H_2O \quad (1)$$

1 g of the gels were taken with a 10 ml syringe and placed in the reaction medium containing 10 ml of distilled water, 2 ml of 1 M sulfuric acid and 1 ml of 1 M potassium iodide solution. The potassium iodide solution was added directly to the medium before addition of the gels. The sample was then placed in a dark place for 5 min, and the resulting iodine was titrated with a 0.01 N sodium thiosulfate solution in the presence of a starch indicator. Three parallel measurements were carried out for each composition. We measured the control samples similarly.

2.4. Statistical experimental design

A two-factor, three-level face-centred central composite design was applied to construct a second-order polynomial model describing the effect of formulation factors (x: polymer concentration, y: chlorine

DOI:10.14753/SE.2022.2766

Table 1
Experimental design with factors and their levels.

Levels	x: PAA concentration (% w/w)	y: ClO_2 concentration (mg/g)
Lower (−)	0.1	0.05
Base (0)	0.2	0.15
Higher (+)	0.3	0.25

dioxide concentration) on the residual chlorine dioxide concentration of the gels (z) [16]. The two factors, as well as their levels, are shown in Table 1. The levels for each parameter are represented by a (−) sign for the lower level, a (+) sign for the higher level and by (0) for the base level.

Table Curve 3D V4.0 software was applied for the multiple regression analysis. The expected form of the polynomial equation is as follows in Eq. (2):

$$z = a + bx + cy + dx^2 + ey^2 + fxy \quad (2)$$

where z is the response, x and y are the factors, a is a constant, b and c parameters denote the coefficients characterizing the main, d and e the quadratic, and f the interaction effects.

2.5. Positron annihilation lifetime spectroscopy (PALS)

The ortho-positronium lifetime (o-Ps) values were determined according to Szabó et al. [17]. For positron lifetime measurements, a positron source made of carrier-free 22NaCl was used. Its activity was around 105 Bq, and the active material was sealed between two very thin Kapton foils. Lifetime spectra were measured with a fast–fast coincidence system based on BaF2/XP2020Q detectors and Ortec electronics [18]. Every spectrum was recorded in 4096 channels of an analyser card and each contained 105 coincidence events. Vertical array detectors were used, and the sample was located on the aluminium plate between the two detectors. 7 ml of the gels were taken with a syringe and placed in a glass cylinder of which bottom was closed with Kapton foil. In the sample cylinder, a thickness of 5 mm was achieved. The positron source was placed on the aluminium sheet under the glass cylinder.

The upper detector was located 2 mm from the surface of the gel. Five consecutive spectra were taken from each sample, and the first recorded was used to compare the different gels. The remaining four spectra were used to determine whether any changes occurred during the measurement of the structure of the samples. All the lifetime spectra were evaluated individually by the RESOLUTION computer code [19]. Lifetime distributions were calculated with the MELT code according to Shukla et al. [20].

2.6. Microbiological evaluation

The antibacterial effect of the chlorine dioxide-containing gels was investigated by infection and quenching with a bacterial suspension. The study was carried out after the 2-week storage on the 14th day. 1 ml of the samples was measured by a syringe into a 2 ml Eppendorf tube and 100 µl of 6.8×10^8 CFU *Enterococcus faecalis* (*E. faecalis*) strain was pipetted to the samples and mixed with a syringe. After the tube was closed, the samples were shaken and were placed in a dark place for 3 min and then cultured on blood agar plates. The infection was repeated every 10 min for three times. The plates were placed in a 37 °C incubator for a night, and the cultured colonies were tested on the next day. During the experiment, three parallels of each of the nine different

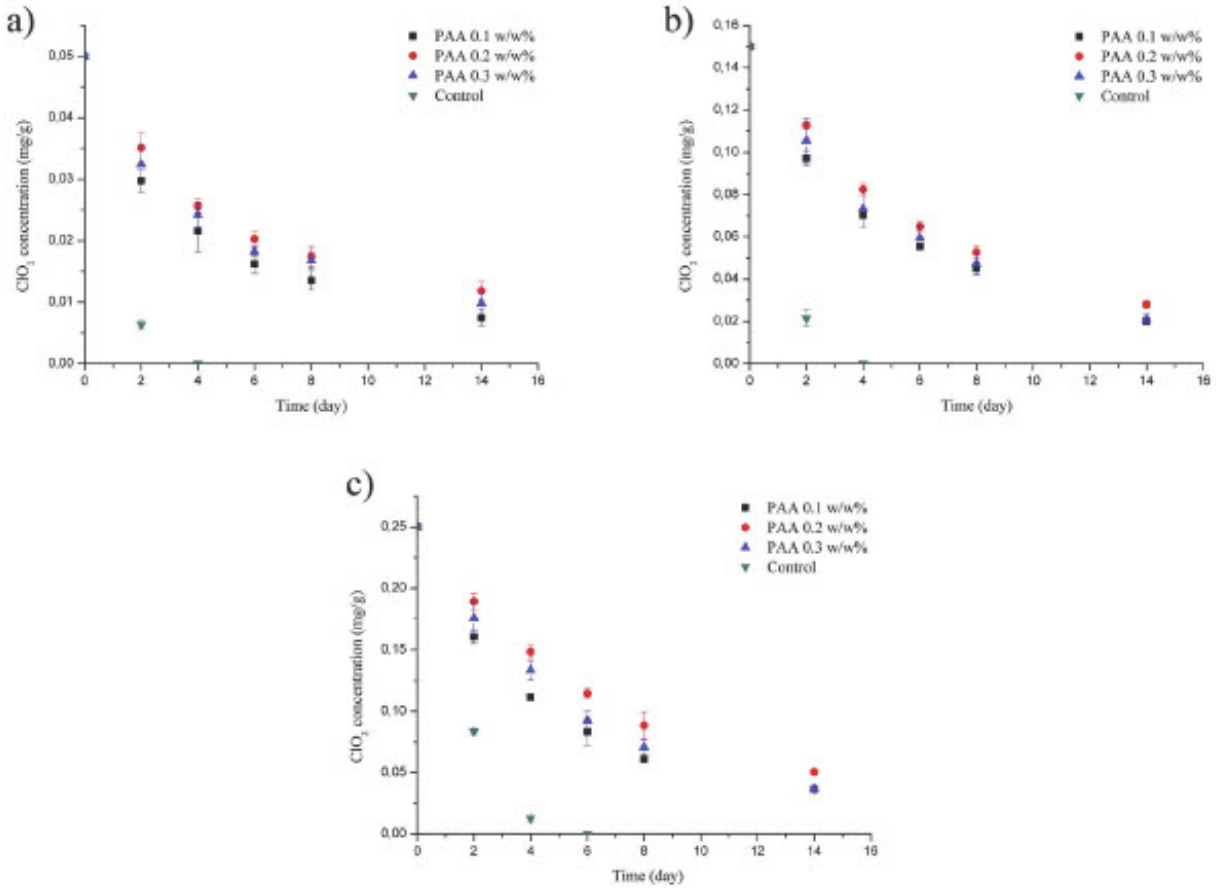

Fig. 1. ClO_2 concentration of PAA gels measured on every second day until day 8 and on day 14. Samples with distinct initial ClO_2 concentrations are shown separately: (a) 0.05 mg/g, (b) 0.15 mg/g, (c) 0.25 mg/g.

DOI:10.14753/SE.2022.2766

gel and three control samples were examined.

3. Results and discussion

3.1. Analytical measurements

Results of the titration of the samples stored for 14 days at room temperature without covers are shown in Fig. 1. The slopes of the chlorine dioxide concentration decrease of aqueous solutions of different polymer concentrations as a function of storage time seem to be similar. It is apparent from the results that the values differ from expectations. The dissolved gas molecule is removed by diffusion from the gel formed by the polymer. If only the diffusion barrier formed by the polymer matrix is taken into account in the characterization of the chlorine dioxide loading capacity of the gels, there should be a straight proportionality between the poly(acrylic acid) concentration of the gel and the amounts of the residual chlorine dioxide. In such a case, the gels containing 0.3% w/w poly(acrylic acid) should, of course, hold the highest amounts of chlorine dioxide.

However, it is apparent from the titration results that the concentration data are the highest in PAA 0.2% w/w, and after two weeks of storage, these gels contain significantly higher amounts of active ingredient (Fig. 2). Based on the results it can be stated that the role of the polymer matrix in the influencing of the chlorine dioxide loading capacity is double. On the one hand, it exists as a diffusion barrier by increasing the diffusion layer, thus inhibiting the fugacity of the gaseous chlorine dioxide. On the other side, the polymer chains form an arranged supramolecular matrix that interacts with the hydrated forms of chlorine dioxide via secondary hydrogen bonds thus resulting in its sustained fugacity. The latter showed optimum as a function of the polymer concentration. By examining the titration curves of the control samples, it can be seen that aqueous solutions have been able to retain chlorine dioxide for only a few days, due to high volatility and significant diffusion of the drug.

3.2. Statistical evaluation

To indicate the influence of formulation factors on the chlorine dioxide loading capacity of the polymer gels the residual chlorine dioxide content was selected as a response parameter. Table 2 summarises the measured and the estimated chlorine dioxide contents of gels. The resultant equation (Eq. (3)) obtained after significance test at 95% confidence level represents the effect of formulation factors (x, y) on the residual chlorine dioxide content (z) of the gels.

Table 2
Randomized matrix of the two-factor, three-level face-centred central composite factorial design (average of three parallels ± SD).

Controlled factors			Response parameter	
Trial	x	y	z measured (mg/g)	z predicted (mg/g)
1	+	0	0.0210	0.0208
2	−	−	0.0075	0.0059
3	0	−	0.0118	0.0152
4	−	+	0.0367	0.0387
5	0	0	0.0280	0.0284
6	+	−	0.0098	0.0081
7	0	+	0.0507	0.0468
8	+	+	0.0367	0.0386
9	−	0	0.0201	0.0198

$$z = -0.025 + 0.341x + 0.094y - 0.818x^2 + 0.252\,y^2 - 0.058\,xy \quad (3)$$

The positive sign of the coefficients refers to an increasing effect while the negative sign indicates a decreasing effect on the corresponding response. It was found that both the gel-forming polymer and chlorine dioxide concentration increase the residual chlorine dioxide concentration of the system. The positive sign of the main coefficients refers to this tendency.

Although the main coefficient of the polymer concentration is almost three times higher than that of the chlorine dioxide, the negative coefficient of its quadratic effect decreases its chlorine dioxide loading capacity. The negative coefficient of the interaction effect ($f = -0.058$) also reduces the remaining chlorine dioxide content. The obtained results are in good agreement with the results of the analytical measurements and the microstructural evaluation with PALS study.

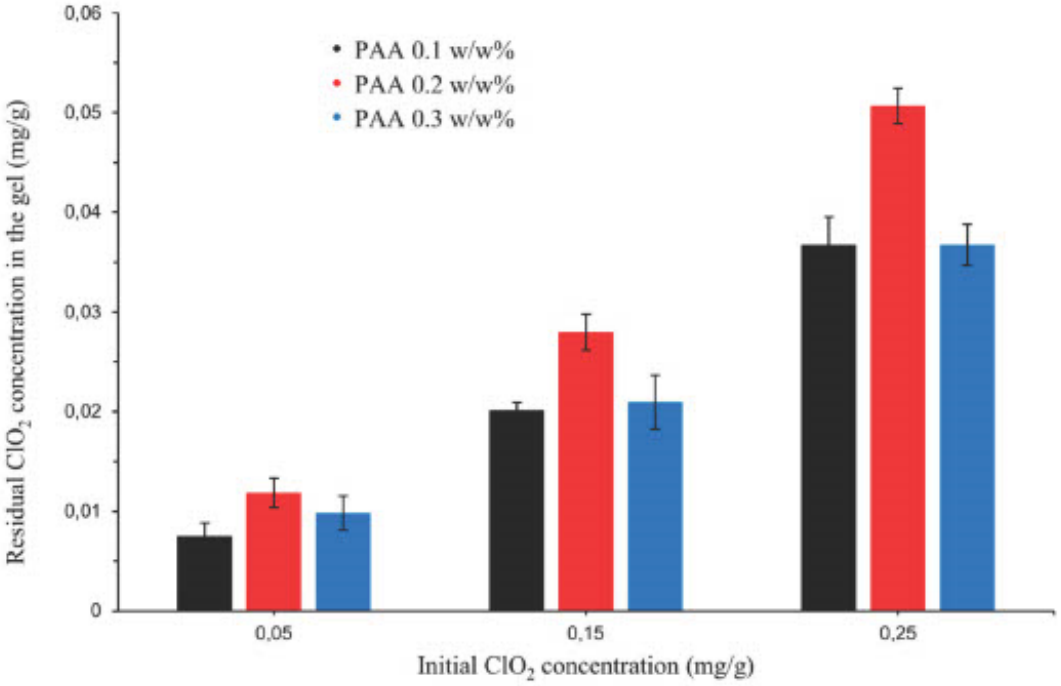

Fig. 2. Residual ClO_2 concentrations in gels after two weeks of storage at room temperature in open containers.

DOI:10.14753/SE.2022.2766

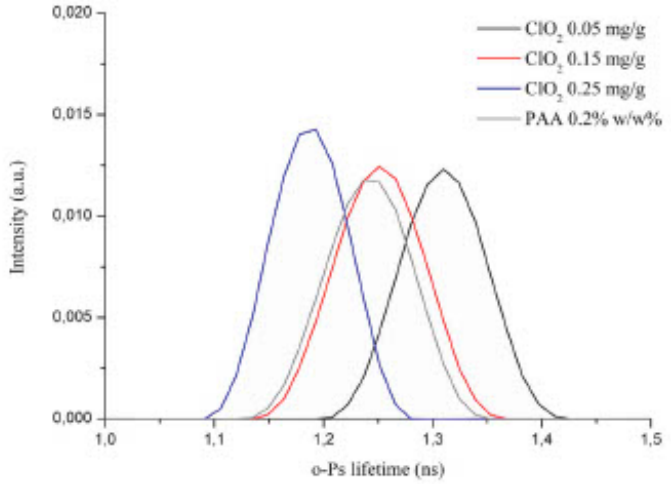

Fig. 3. Effect of ClO_2 concentration on the o-Ps lifetime distribution in PAA 0.2% w/w gels.

3.3. o-Ps lifetime in gels

The tracking of the o-Ps lifetime values of polymer gels is an effective method for the supramolecular characterization of a system. The data of the spectrum enabled the determination of the size distribution of the free volume holes of the gels, thus characterizing the structural arrangement of the system. In PAA-based gels, o-Ps lifetime values typically ranged between 1 and 1.5 ns. In the samples of various polymer concentrations, the supramolecular structure of the gel matrix is formed by the distance and relative position of the polymer chains. Shifting the lifetime distribution to lower values indicates a smaller hole size and a more ordered structure.

Fig. 3 demonstrates that the presence of chlorine dioxide in the gels modified the microstructure of the system. The bigger the chlorine dioxide concentration of the gel, the smaller the o-Ps lifetime value of the system, thus resulting in smaller free volumes. Interestingly at 0.2% w/w PAA content the polymer unloaded gel and the 0.15 mg/g chlorine dioxide-containing gel show similar distribution, which refers to the similar molecularly dissolved gas-loaded system. Fig. 4 represents the o-Ps lifetime distribution of 0.25 mg/g chlorine dioxide-containing gels of various PAA concentrations. The o-Ps lifetime distribution curves of 0.1 and 0.3% w/w polymer concentrations almost overlap each other, only their intensity is different, while the curve belongs to 0.2% w/w PAA concentration was shifted to lower lifetime values. The latter indicates that there exists a polymer concentration where PAA forms an arranged supramolecular structure with the hydrated chlorine dioxide thus loading more active ingredient in its free volume holes. The decreased o-Ps lifetime values refer to the loaded free volume holes of the polymer. This phenomenon is in good agreement with the results of the residual chlorine dioxide concentrations of the samples and the following statistical evaluation.

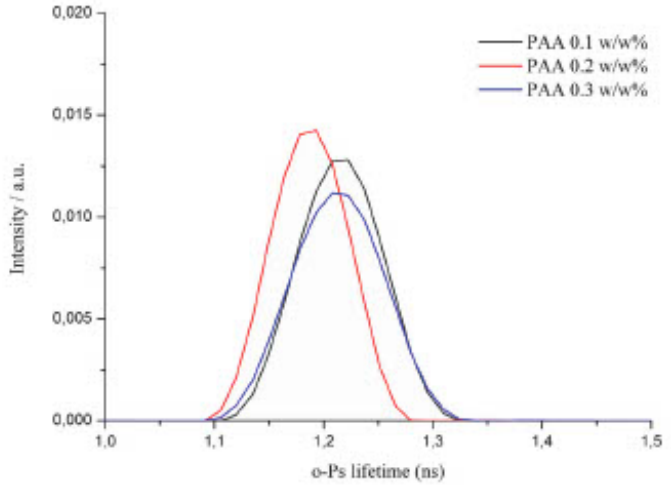

Fig. 4. o-Ps lifetime distribution of 0.1, 0.2 and 0.3% w/w PAA gels containing 0.25 mg/g ClO_2.

3.4. Microbiological evaluation

The antibacterial activities of chlorine dioxide-containing gels of different compositions were studied using *Enterococcus faecalis* strains. Fig. 5 shows the results of the experiments. In the case of gels containing 0.15 and 0.25 mg/g of chlorine dioxide, there is no development of a bacterial colony in the culture medium after two weeks of storage at room temperature in open containers. Each of the gels containing 0.1, 0.2 and 0.3% w/w PAA was able to maintain their antibacterial activity until the end of the storage time, and 100 µl of 6.9×10^8 CFU were killed after three contaminations. In the control samples it can be observed that as a result of the first infection, a significant bacterial culture was formed on the media, which is in good agreement with the results of the analytical measurements.

Control solutions, regardless of the concentration of chlorine dioxide, have lost the total amount of the drug dissolved during the first few days of the study. In the case of antimicrobial activity, a difference can only be observed with gels containing chlorine dioxide of 0.05 m/g. It can be seen that the addition of the first dose of bacterial suspension resulted in extensive bacterial colonies from each parallel of the 0.1% w/w PAA gel, which indicates that the chlorine dioxide of 0.0075 mg/g concentration determined by the analytical assay was not sufficient against of such an amount of bacteria. In the case of the most concentrated PAA gel, some colonies can be observed, so samples containing 0.3% w/w PAA destroyed most of the bacteria. The additions of another dose of bacterial suspension, this composition also lost of its antibacterial activity thus associated colonies were formed. Gels of medium PAA concentrations had adequate chlorine dioxide content at the end of the storage period, as all bacteria were destroyed during the first infection. The addition of the second dose of bacterial suspension, the presence of surviving bacteria can already be detected from one of the parallel ones; thus the antibacterial activity was only partially retained. The results of the microbiological study are in good agreement with the analytical and statistical examinations since the chlorine dioxide concentration, and the antibacterial activity of the samples are closely related. Among the gels, the composition containing 0.2% w/w PAA was found to be the most effective, it reserved its chlorine dioxide content for a prolonged time and consequently showed the best antimicrobial activity. The result correlates with the findings of the PALS study that the most homogeneous chlorine dioxide distribution and filled free volume holes can be observed in the case of medium PAA content.

4. Conclusion

Poly(acrylic acid)-based gels, containing chlorine dioxide as active components, were successfully prepared in 9 different compositions. During the storage period, the gels containing 0.2% w/w poly(acrylic acid) had a significantly enhanced chlorine dioxide loading capacity than the 0.1 and 0.3% w/w samples, which were also confirmed by statistical and analytical studies. The samples containing 0.2% w/w poly(acrylic acid) indicated a more complex molecular packing due to the supramolecular ordering of the polymeric chains. To sum up, poly (acrylic acid)-based gels enabled the loading and release of chlorine dioxide at effective antimicrobial concentrations, so their application can be therapeutically promising. The applicability and toxicity profile of the gels on human tissues requires further testing.

DOI:10.14753/SE.2022.2766

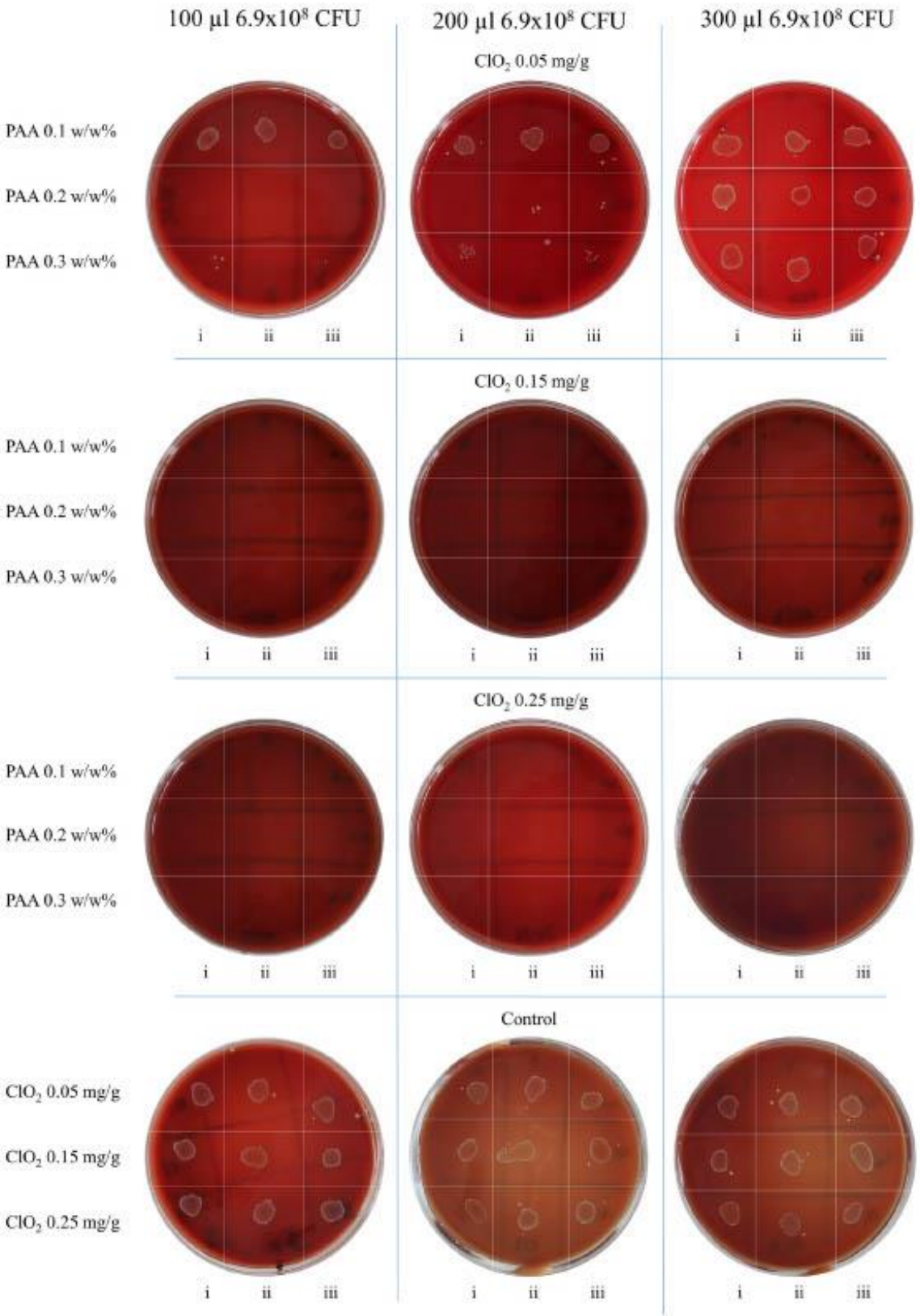

Fig. 5. Antibacterial activity of ClO_2 containing PAA gels after infecting three times with 100 µl 6.9 × 10^8 CFU *E. faecalis* suspension. Samples were cultured on blood agar plates. Three parallels (i, ii, iii) of each gel and the control sample were examined. Each row represents one concentration of ClO_2 and the control samples, while columns represent the addition of 100 µl bacterial suspension.

DOI:10.14753/SE.2022.2766

References

[1] G.D. Simpson, R.F. Miller, G.D. Laxton, W.R. Clements, A focus on chlorine dioxide: the "ideal" biocide, Corrosion 93: New Orleans, LA, Paper No. 472, 1993.

[2] D.F. Bridges, B. Rane, V.C. Wu, The effectiveness of closed-circulation gaseous chlorine dioxide or ozone treatment against bacterial pathogens on produce food control, Food Control 91 (2018) 261–267.

[3] T. Sanekata, T. Fukuda, T. Miura, H. Morino, C. Lee, K. Maeda, K. Araki, T. Otake, T. Kawahata, T. Shibata, Evaluation of the antiviral activity of chlorine dioxide and sodium hypochlorite against feline calicivirus, human influenza virus, measles virus, canine distemper virus, human herpesvirus, human adenovirus, canine adenovirus and canine parvovirus, Biocontrol Sci. 15 (2010) 45–49.

[4] G. Wen, X. Xu, T. Huang, H. Zhu, J. Ma, Inactivation of three genera of dominant fungal spores in groundwater using chlorine dioxide: effectiveness, influencing factors, and mechanisms, Water Res. 125 (2017) 132–140.

[5] S. Venkatnarayanan, P. Sriyutha Murthy, R. Kirubagaran, V.P. Venugopalan, Chlorine dioxide as an alternative antifouling biocide for cooling water systems: toxicity to larval barnacle *Amphibalanus reticulatus* (Utinomi), Mar. Pollut. Bull. 124 (2) (2017) 803–810.

[6] I. Ofori, S. Maddila, J. Lin, S.B. Jonnalagadda, Chlorine dioxide inactivation of *Pseudomonas aeruginosa* and *Staphylococcus aureus* in water: the kinetics and mechanism, J. Water Process Eng. 26 (2018) 46–54.

[7] A. Degrossoli, A. Müller, K. Xie, J.F. Schneider, V. Bader, K.F. Winklhofer, A.J. Meyer, L.I. Leichert, Neutrophil-generated HOCl leads to non-specific thiol oxidation in phagocytized bacteria, elife 7 (2018) e32288.

[8] D.R. Jenkins, Nosocomial infections and infection control, Medicine 45 (10) (2017) 629–633.

[9] M.L. Casey, B. Hawley, N. Edwards, J.M. Cox-Ganser, K.J. Cummings, Health problems and disinfectant product exposure among staff at a large multispecialty hospital, Am. J. Infect. Control 45 (10) (2017) 1133–1138.

[10] J.W. Ma, B.S. Huang, C.W. Hsu, C.W. Peng, M.L. Cheng, J.Y. Kao, T.D. Way, H.C. Yin, S. Wang, Efficacy and safety evaluation of a chlorine dioxide solution, Int. J. Environ. Res. Public Health 14 (3) (2017) 329.

[11] Z. Noszticzius, M. Wittmann, K. Kály-Kullai, Z. Beregvári, I. Kiss, L. Rosivall, J. Szegedi, Chlorine dioxide is a size-selective antimicrobial agent, PLoS One 8 (11) (2013) e79157.

[12] M.S. Hsu, M.Y. Wu, Y.T. Huang, C.H. Liao, Efficacy of chlorine dioxide disinfection to non-fermentative Gram-negative bacilli and non-tuberculous mycobacteria in a hospital water system, J. Hosp. Infect. 93 (1) (2016) 22–28.

[13] J.J. Lowe, S.G. Gibbs, P.C. Iwen, P.W. Smith, A.L. Hewlett, Impact of chlorine dioxide gas sterilization on nosocomial organism viability in a hospital room, Int. J. Environ. Res. Public Health 10 (6) (2013) 2596–2605.

[14] **Z. Noszticzius, S. Balogh, W.M. Gyökémé, K. Kály-Kullai, M. Megyesi, A. Volford, Permeation method and apparatus for preparing fluids containing high purity chlorine dioxide,** https://patentscope.wipo.int/search/en/detail.jsf?docId=WO2008035130, **(2008) (D.P.A.L.O. LLC, Editor).**

[15] A. Herczegh, M. Gyurkovics, H. Agababyan, Á. Ghidán, Z. Lohinai, Comparing the efficacy of hyper-pure chlorine-dioxide with other oral antiseptics on oral pathogen microorganisms and biofilm in vitro, Acta Microbiol. Immunol. Hung. 60 (3) (2013) 359–373.

[16] R.M. Franz, J.E. Browne, A.R. Lewis, Experimental design, modeling, and optimization strategies for product and process development, in: H.A. Lieberman, M.M. Rieger, G.S. Banker (Eds.), Pharmaceutical Dosage Forms. Disperse Systems, Marcel Dekker, New York, 1988.

[17] B. Szabó, K. Süvegh, R. Zelkó, Real time positron annihilation lifetime spectroscopy for the detection of the hydrocolloid gel-film transition of polymers, Polym. Test. 31 (2012) 546–549.

[18] I.K. MacKenzie, Experimental methods of annihilation time and energy spectrometry, in: W. Brandt, A. Dupasquier (Eds.), Positron Solid-State Physics, North-Holland, 1983.

[19] P. Kirkegaard, M. Eldrup, O.E. Mogensen, N.J. Pedersen, Program system for analysing positron lifetime spectra and angular correlation curves, Comput. Phys. Commun. 23 (1981) 307–335.

[20] A. Shukla, M. Peter, L. Hoffmann, Analysis of positron lifetime spectra using quantified maximum entropy and a general linear filter, Nucl. Instrum. Methods Phys. Res. A 335 (1993) 310–317.

Barnabás Palcsó PharmD, is a PhD student at Semmelweis University, Budapest. He graduated summa cum laude from the Faculty of Pharmacy of Semmelweis University in 2017. During his college years, he took part in undergraduate research projects in the field of polymeric drug delivery systems under the supervision of Romána Zelkó. He participated in Semmelweis Annual Scientific Conference and gained 3rd place in his section. Currently, his research work focuses on antibacterial gels and drug-loaded nanofibers.

Zsófia Moldován is a fifth-year dental student of Semmelweis University Budapest. Her primary interests are Conservative, Preventive dentistry and Orthodontics. She participates in Kerpel-Pronius Talent Support Programme at Semmelweis University Department of Community Dentistry and does research activities for Students' Scientific Associations at Conservative Department. Her scientific studies deal with the possibilities of reducing oral pathogen microorganisms and the dental use of hyper-pure chlorine dioxide. She gained the 1st place at Semmelweis Annual Scientific Conference in her section and the special award at Scientific Conference of Targu Mures.

Károly Süvegh, PhD, CSc. is an associate professor of the Institute of Chemistry and a full-time member of the Laboratory of Nuclear Chemistry of Eötvös Lóránd University, Budapest. He received his PhD from the Hungarian Academy of Sciences in 1995. His research work includes positron annihilation studies of liquids, molecular crystals, and polymers and defect structure analysis of metals. He authored or co-authored over 100 journal articles. He is a member of the Division of Nuclear and Resonance Spectroscopies of the Hungarian Academy of Sciences.

Anna Herczegh PhD, DMD is an assistant professor of the Department of Conservative Dentistry of Semmelweis University, Budapest. Her principal works are giving clinical practical training and lectures of Conservative, Endodontic and Preventive Dentistry. She is an examiner, tutor and mentor of students and residents and responsible for the research of Scientific Associations students. Her research focuses on the possibilities of reducing oral pathogen microorganisms and the dental use of hyper-pure chlorine dioxide. She is the author of 11 journal papers. She is a peer reviewer for two scientific journals. Patient care is also an essential part of her work.

Romána Zelkó PhD, D.Sc. is a full-time professor and the present dean of the Faculty of Pharmacy of the Semmelweis University, Budapest. Her research work focuses on polymeric delivery systems, physical ageing of polymers, microstructural characterization of dosage forms associated with their functionality-related characteristics. She is the author of several scientific (200 journal papers, 5 patents) and expert works. She is a member of the editorial boards of internationally recognized journals and a peer reviewer for more than 25 scientific journals with impact factor ranking. Her expertise covers the planning, development and solid state characterization of different dosage forms.

DOI:10.14753/SE.2022.2766

nanomaterials

MDPI

Article

Formulation of Chlorine-Dioxide-Releasing Nanofibers for Disinfection in Humid and CO_2-Rich Environment

Barnabás Palcsó [1], Adrienn Kazsoki [1], Anna Herczegh [2], Ágoston Ghidán [3], Balázs Pinke [4], László Mészáros [4,5] and Romána Zelkó [1,*]

1 University Pharmacy Department of Pharmacy Administration, Faculty of Pharmaceutical Sciences, Semmelweis University, Hőgyes Endre utca 7-9, H-1092 Budapest, Hungary; palcso.barnabas@pharma.semmelweis-univ.hu (B.P.); kazsoki.adrienn@pharma.semmelweis-univ.hu (A.K.)
2 Department of Conservative Dentistry, Faculty of Dentistry, Semmelweis University, Szentkirályi utca 47, H-1088 Budapest, Hungary; herczegh.anna@dent.semmelweis-univ.hu
3 Institute of Medical Microbiology, Faculty of Medicine, Semmelweis University, Nagyvárad tér 4, H-1089 Budapest, Hungary; ghidan.agoston@med.semmelweis-univ.hu
4 Department of Polymer Engineering, Faculty of Mechanical Engineering, Budapest University of Technology and Economics, Műegyetem rkp. 3, H-1111 Budapest, Hungary; pinke@pt.bme.hu (B.P.); meszaros@pt.bme.hu (L.M.)
5 MTA-BME Research Group for Composite Science and Technology, Műegyetem rkp. 3, H-1111 Budapest, Hungary
* Correspondence: zelko.romana@pharma.semmelweis-univ.hu; Tel.: +36-1-2170927

Abstract: Background: Preventing infectious diseases has become particularly relevant in the past few years. Therefore, antiseptics that are harmless and insusceptible to microbial resistance mechanisms are desired in medicine and public health. In our recent work, a poly(ethylene oxide)-based nanofibrous mat loaded with sodium chlorite was formulated. Methods: We tested the chlorine dioxide production and bacterial inactivation of the fibers in a medium, modeling the parameters of human exhaled air (ca. 5% (*v/v*) CO_2, T = 37 °C, RH > 95%). The morphology and microstructure of the fibers were investigated via scanning electron microscopy and infrared spectroscopy. Results: Smooth-surfaced, nanoscale fibers were produced. The ClO_2-producing ability of the fibers decreased from 65.8 ppm/mg to 4.8 ppm/mg with the increase of the sample weight from 1 to 30 mg. The effect of CO_2 concentration and exposure time was also evaluated. The antibacterial activity of the fibers was tested in a 24 h experiment. The sodium-chlorite-loaded fibers showed substantial antibacterial activity. Conclusions: Chlorine dioxide was liberated into the gas phase in the presence of CO_2 and water vapor, eliminating the bacteria. Sodium-chlorite-loaded nanofibers can be sources of prolonged chlorine dioxide production and subsequent pathogen inactivation in a CO_2-rich and humid environment. Based on the results, further evaluation of the possible application of the formulation in face-mask filters as medical devices is encouraged.

Keywords: electrospinning; nanofibers; poly(ethylene oxide); sodium chlorite; chlorine dioxide; antibacterial; disinfection

Citation: Palcsó, B.; Kazsoki, A.; Herczegh, A.; Ghidán, Á.; Pinke, B.; Mészáros, L.; Zelkó, R. Formulation of Chlorine-Dioxide-Releasing Nanofibers for Disinfection in Humid and CO_2-Rich Environment. *Nanomaterials* 2022, *12*, 1481. https://doi.org/10.3390/nano12091481

Academic Editor: Takuya Kitaoka

Received: 31 March 2022
Accepted: 26 April 2022
Published: 27 April 2022

1. Introduction

In the age of antimicrobial resistance, eliminating pathogens such as bacteria or viruses remains a grueling challenge in public and clinical health care. Preventing infections is a vital aspect of any successful antimicrobial management program. With the help of broad-spectrum antiseptics and disinfectants, the overuse of antibiotics and antiviral substances can be reduced [1]. To maintain adequate antibiotic stewardship, the use of effective, relatively harmless antiseptics and disinfectants that are insusceptible to microbial resistance mechanisms is desired. However, the rise of antiseptic-resistant pathogens is also a long-known phenomenon, especially in the hospital environment [2]. In the case of two common antiseptic agents, chlorhexidine and octenidine, it has been shown that by

DOI:10.14753/SE.2022.2766

increasing the usage of these substances in practice, a significant reduction in susceptibility can be observed in isolated *Staphylococcus aureus* strains [3]. Increased minimum inhibitory concentrations (MICs) for both antiseptics in *Staphylococcus* spp. strains have also been reported [4]. Several reports have also been published regarding the acquired microbial resistance against disinfectants [5–7]. Therefore, other alternative antimicrobial substances should be examined to address the emerging issue of the wide spread of antibiotic and antiseptic-resistant pathogens. Chlorine dioxide (ClO_2) is a gaseous oxidizing agent with good water solubility, used as a disinfectant mostly in water treatment and the food industry. Due to its unique molecular structure, the reactivity of ClO_2 is limited mainly to thiol-group-containing amino acids. Other organic macromolecules are also potential substrates of ClO_2, but the reaction rate is several magnitudes lower than in the case of thiol groups. The result of the chemical reaction and the mechanism of action of ClO_2 are the change in protein structure and subsequent loss of function. Several reports claimed the effectiveness of chlorine dioxide against all kinds of microbes, including bacteria, fungi, protozoa and viruses. The gaseous substance has a remarkable penetrating ability, enabling it to decontaminate areas considered impervious, such as biofilms [8–13]. The safety of ClO_2 relies not on the difference in macromolecules or metabolism of pathogens and human cells but on the difference in their size and the protecting factors existing in human tissue. Bacteria and viruses can be susceptible to a given concentration of ClO_2 that does not represent any harm to human or animal cells [14]. It has been shown in several animal studies that a certain level of ClO_2 exposure does not do any damage to the examined animals [15,16]. Although chlorine dioxide convincingly satisfies the requirements of an ideal biocide, it has not become a widely used compound in everyday practice. Reports have already been published considering the use of ClO_2 in the disinfection of hospital environments such as water systems, air, rooms and even ambulance vehicles [17–20]. However, in medical practice, the use of ClO_2 is mainly limited to dental applications such as root canal irrigation and mouth rinse [21,22]. The relatively small use of chlorine dioxide can be due to its cumbersome transportation and storage. The gaseous substance cannot be transported due to safety issues; therefore, chlorine dioxide is usually generated in aqueous solution at the site of application. One of the most common methods of chlorine dioxide production is the decomposition reaction of sodium chlorite ($NaClO_2$) in the presence of acid, which results in chlorine dioxide and other byproducts. The dissolved gas has high volatility that causes a rapid decrease in the concentration of the solution limiting its shelf life.

Polymer-based formulations represent promising solutions to the issues related to the practical use of ClO_2. Using polymer-based viscous solutions, the residence time of ClO_2 can be prolonged [23]. Electrospun nanofibers loaded with sodium chlorite produce ClO_2 under acidic conditions. Due to their high porosity and surface area to volume ratio, they can serve as efficient production sites for chlorine dioxide. Such nanosystems can enable ClO_2 gas production and liberation at the site of use [24]. Polyethylene oxide is a water-soluble polymer that is relatively easy to process by electrospinning [25]. Sodium chlorite is also water-soluble; thus, there is a good chance of producing sodium chlorite nanofibers based on a common solvent. In our recent work, we present a polymer-based, nanofiber-based formulation with ClO_2-generating ability. The nanofiber-based formulation is subjected to morphological and antibacterial examination. The ClO_2-generating ability and the rate of chlorine dioxide liberation were also evaluated.

2. Materials and Methods

2.1. Materials

Poly(ethylene oxide) (PEO, average M_w = 600,000 g·mol^{-1}) was obtained from Sigma-Aldrich (Budapest, Hungary). We used analytical-grade sodium chlorite ($NaClO_2$, Sigma-Aldrich, Budapest, Hungary) as the active ingredient. Distilled water was filtered on a 0.22 µm PES filter before preparing the precursor polymer solution. The materials did not undergo any further purification.

DOI:10.14753/SE.2022.2766

2.2. Precursor Polymer Solutions and Electrospinning

Aqueous polymer solutions were prepared by dissolving 5% (*w*/*w*) PEO in boiling water with continuous stirring. The samples were cooled down to room temperature and stirred overnight at 23 °C by magnetic stirring until homogenous solutions were obtained. Finally, sodium chlorite 20% (*w*/*w*) aqueous solution was added to the PEO solution to reach a concentration of 0.1% (*w*/*w*). Control PEO samples without active ingredients were prepared accordingly. Nanofiber production was carried out on lab-scale electrospinning equipment (SpinSplit Ltd., Budapest, Hungary). Precursor solutions were placed into plastic syringes (Luer lock, Sigma-Aldrich Ltd., Budapest, Hungary) with a volume of 3 mL and mounted to the pumping system of the instrument. The syringes were connected to a 22-gauge needle through Teflon tubes. The feeding rate for PEO control samples was 0.08 µL/s, with an applied voltage of 10.5 kV. The $NaClO_2$-loaded PEO samples were prepared with a 0.07 µL/s feeding rate and 14.8 kV of applied voltage. The samples were collected on aluminum foil, and the needle-collector distance was set to 21.5 cm. The experiments were performed in a well-controlled room, the temperature was set to 23 ± 1 °C and the relative humidity was 25 ± 5% (Figure 1).

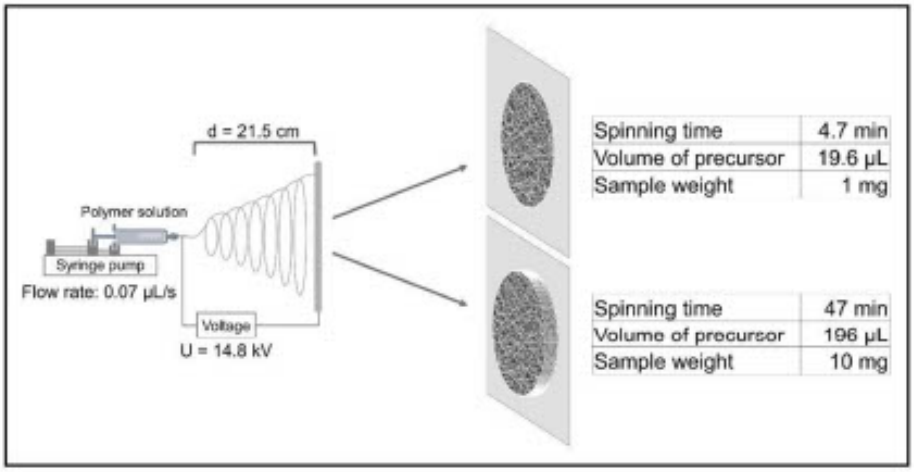

Figure 1. Electrospinning setup and preparation of two samples of different weights for illustration.

2.3. Fourier-Transform Infrared (FTIR) Spectroscopy

Infrared spectra of the components and the fibers were recorded with a Jasco FT/IR-4200 spectrophotometer, equipped with Jasco ATR PRO470-H single reflection accessory. Measurements were performed in absorbance mode, and spectra were collected over a wavenumber range of 4000 and 500 cm^{-1}. For each spectrum, 100 scans were performed at a resolution of 4 cm^{-1}. Spectra were evaluated with the software Spectra Manager-II (Jasco, Easton, MD, USA).

2.4. Scanning Electron Microscopy

Samples were fixed on a metal stub by conductive double-sided adhesive carbon discs and coated with a gold layer using a JEOL JFC-1200 Fine Coater (JEOL Ltd., Tokyo, Japan). Scanning electron microscopy (SEM) images were taken with a JEOL JSM-6380LA instrument (JEOL Ltd., Tokyo, Japan). The acceleration voltage and the working distance were 10 kV and 10 mm, respectively. For fiber diameter evaluation and distribution calculations, we measured the diameter of 100 random fibers using ImageJ (National Institutes of Health, Bethesda, MD, USA) software and prepared the histograms via Origin(Pro) software (Version 2018, OriginLab Corporation, Northampton, MA, USA).

DOI:10.14753/SE.2022.2766

2.5. Chlorine Dioxide Production of the Fibrous Samples

2.5.1. Experimental Setup

The ClO_2 production from $NaClO_2$-loaded PEO fibers was carried out in 60 mL amber glass bottles. First, a 0.5 mL container was placed into the bottle, and 300 µL of distilled water was measured into the container to maintain a humid environment of RH > 95%. The water in the 0.5 mL container also served as a source for ClO_2 concentration measurement. Next, the fibrous sample was stuck onto the inner wall of the bottle using double-sided adhesive tape, and CO_2 was slowly injected into the glass to reach a concentration of 5, 10 or 15% (*v*/*v*). Bottles fitted with special caps, impermeable to ClO_2, were kindly donated by Zoltán Noszticzius (Department of Physics, Budapest University of Technology and Economics, Budapest, Hungary). The suitable amount of CO_2 gas was monitored and determined beforehand using a Ventis Pro5 multi-gas detector. Lastly, bottles were placed into an incubator and stored at 37 °C. To measure the concentration of chlorine dioxide generated from the fibers, the bottles were opened, and 100 µL was taken instantly from the distilled water placed in the 0.5 mL container. The 100 µL ClO_2 aqueous solution was injected into a cuvette containing 2.9 mL of distilled water and measured using a Jasco V-750 UV-Visible spectrophotometer. The absorbance of the chlorine dioxide aqueous solution was recorded at 360 nm, where ClO_2 has its characteristic absorption maximum. The molar absorptivity of ClO_2 at 360 nm is 1250 cm^{-1} M^{-1} [26].

2.5.2. Measurements and Data Analysis

To calculate the ClO_2 concentration in the gas phase from concentrations measured in the aqueous solution, the following equation was used:

$$c(ClO_2)_g = k \cdot K_\theta \cdot V_m \cdot c(ClO_2)_{aq} \quad (1)$$

where k is a constant, K_θ is the distribution constant of ClO_2, V_m is the molar volume of the gas, $c(ClO_2)_g$ is the chlorine dioxide concentration in the gas phase in ppm (µL/L) and $c(ClO_2)_{aq}$ is the chlorine dioxide concentration in the aqueous solution in mol/L. At 37 °C, the value of the distribution constant is K_θ = 0.053 and the molar volume is V_m = 25.45 dm^3/mol. The k constant is derived from the conversion of the units and its value is $k = 1 \times 10^6$ [27]. To evaluate the chlorine dioxide production of the samples the following measurements were carried out:

1. To measure the total amount of ClO_2 generated in 24 h by fibers of various weights, we used 1, 5, 10, 15, 20 and 30 mg samples. Using these data, we calculated the ClO_2-generating ability per weight and the ClO_2 yield of the samples compared to the theoretical values. In this experiment, the CO_2 concentration was set to 5%.
2. We examined the effect of different CO_2 concentrations (5, 10, 15%) on the ClO_2 production of 5 mg samples in a 24 h measurement.
3. The effect of residence time of fibers in the medium was evaluated by measuring the ClO_2 production of 5 mg samples after 24, 48 and 72 h.

During all experiments, temperature was set to 37 °C, and RH was kept above 95%, as described above.

2.6. Bacterial Inactivation Study

To evaluate the antibacterial effect of the $NaClO_2$-loaded PEO fiber mats, we used a nonhazardous bacterium, Enterococcus faecalis, as a model organism. Enterococcus faecalis was chosen due to its resilience and undemanding nature in terms of growth requirements, which ensured that bacterial inactivation could be attributed to the effect of the generated chlorine dioxide [28]. The setup and reaction conditions were analogous to those described in the ClO_2 production study. Bacteria were added to the system via disposable inoculating loops, which were cut to make ca. 4 cm long pieces with the loop on their end. Each piece was glued into the inner part of the cap of an amber glass bottle, immersed into a bacterial suspension containing 2.8×10^9 CFU/mL of E. faecalis, then sealed. Each inoculating loop

DOI:10.14753/SE.2022.2766

contained approximately 1 µL of bacterial suspension. Sealed bottles were placed into an incubator and stored at 37 °C for 24 h. A medium similar to the composition of the air was prepared by setting the humidity and CO_2 concentration in the glass containers to >95% and 5%, respectively [29]. After 24 h, we opened the bottles and immersed the inoculating loops into 100 µL of saline and stirred thoroughly to suspend the remaining bacteria. Finally, the entire 100 µL of suspension was streaked on a blood agar plate. The blood agar plates were incubated at 37 °C for another 24 h, and the surviving colonies were counted. Control samples with unloaded PEO fibers were also prepared accordingly.

3. Results

3.1. Morphological Characterization

Scanning electron microscopy images show randomly oriented, smooth-surfaced, nanoscale polymer fibers (Figure 2). Bead-like structures could not be observed throughout the samples. The average fiber diameter value for unloaded PEO fibers was 315 ± 27 nm, and the fiber diameters showed normal distribution (Figure 2a). Adding salt to the polymer solution and the subsequent changes in spinning parameters altered the average fiber diameter substantially, as the average fiber diameter value was 193 ± 23 nm in the case of $NaClO_2$-loaded PEO fibers (Figure 2b). The fiber diameters of the $NaClO_2$-loaded sample also showed normal distribution.

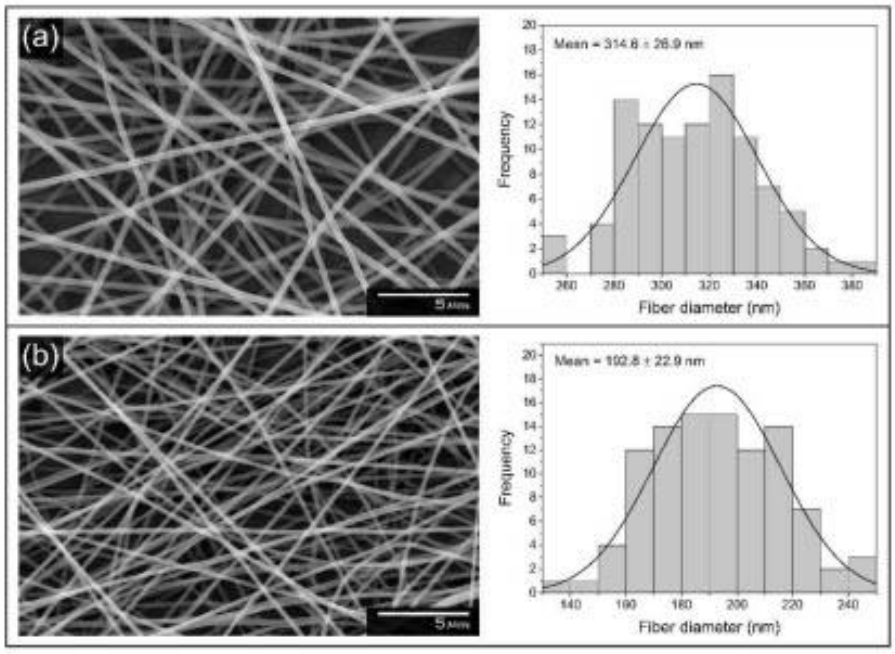

Figure 2. SEM images and histograms of the fiber diameter distribution of unloaded PEO (**a**) and $NaClO_2$-loaded PEO (**b**) fibers.

3.2. FTIR Analysis

To investigate the potential structural changes of the polymer macromolecules, FTIR spectra were recorded. Figure 3 shows the FTIR spectra of sodium chlorite, PEO and $NaClO_2$-loaded PEO fibers. On the spectrum of PEO fibers, the peak at the band observed at 2890 cm^{-1} was assigned to the symmetrical C–H stretching (Figure 3b). The peaks at 1467, 1341, 1280 and 842 cm^{-1} represent the scissoring, wagging, twisting and rocking of the CH_2 group. The sharp and intense band at 1095 cm^{-1}, along with the peaks at 1145 and 1061 cm^{-1}, is assigned to the asymmetric stretching vibration of the C–O–C bonds. The smaller, sharp peak at 960 cm^{-1} is due to C–C skeletal stretching vibrations [30]. The FTIR spectrum of the $NaClO_2$-loaded fibers shows similar bands and intensities to that of the unloaded PEO sample (Figure 3a). A slight difference between the two spectra can be seen

DOI:10.14753/SE.2022.2766

around the base of the peak at 842 cm^{-1} on the $NaClO_2$-loaded PEO spectrum. Sodium chlorite has its sharp and intense peaks at 800 and 823 cm^{-1} (Figure 3c).

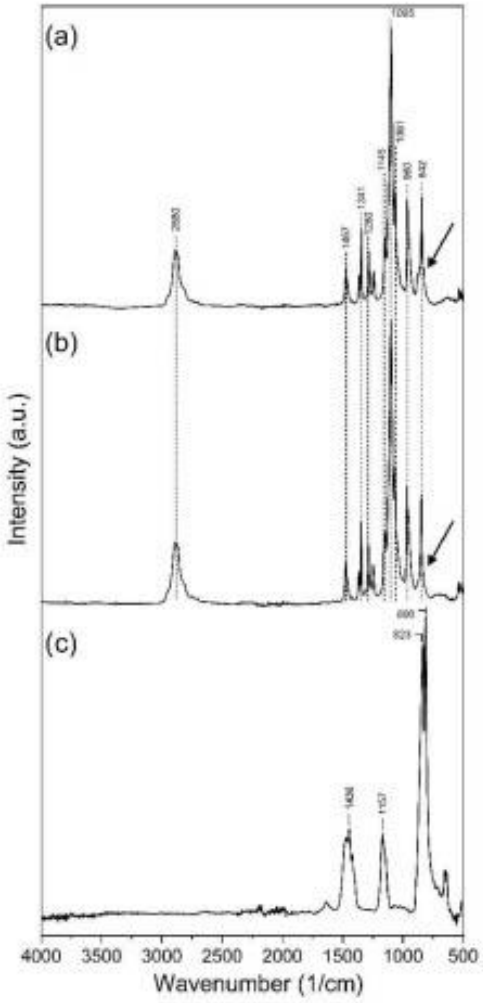

Figure 3. FTIR spectra of $NaClO_2$-loaded PEO fibers (**a**), unloaded PEO fibers (**b**) and sodium chlorite (**c**).

3.3. Chlorine Dioxide Production

The amount of chlorine dioxide generated by samples of different weights, along with the ClO_2-producing ability per weight of these samples, is shown in Figure 4. When placing 1 mg of $NaClO_2$-loaded PEO fiber into the medium, the ClO_2 concentration in the gas phase reached 65.8 ppm (μL/L) after 24 h. Larger weights of samples resulted in higher ClO_2 concentrations, but the rate of growth of the generated ClO_2 remained substantially lower than expected. There was no significant difference in the produced sodium chlorite of samples of higher weights. The ClO_2 production per weight data, however, show a gradual decrease in the ClO_2 generation ability with increasing fiber weights, along with the yield of generated ClO_2 compared to the theoretical values calculated from the $NaClO_2$–acid reaction [31]. During the 24 h experiment, the ClO_2 production ability and yield of 1 mg samples reached 65.8 ppm/mg and 89%, respectively, while the 30 mg samples could produce only 4.8 ppm/mg and 6.58% of the potential ClO_2 yield (Figure 4, Table 1).

Figure 5a shows the effect of carbon dioxide concentration on the ClO_2 production ability of the $NaClO_2$-loaded PEO fibers. We placed 5 mg of $NaClO_2$-loaded PEO samples into amber glass bottles containing 5, 10 and 15% (*v*/*v*) of CO_2, while humidity was kept above 95% and the temperature was set to 37 °C. After 24 h, there was no substantial difference in the produced ClO_2. However, the time of exposure to CO_2 in a humid environment resulted in significantly higher CO_2 concentrations after 48 and 72 h (Figure 5b).

DOI:10.14753/SE.2022.2766

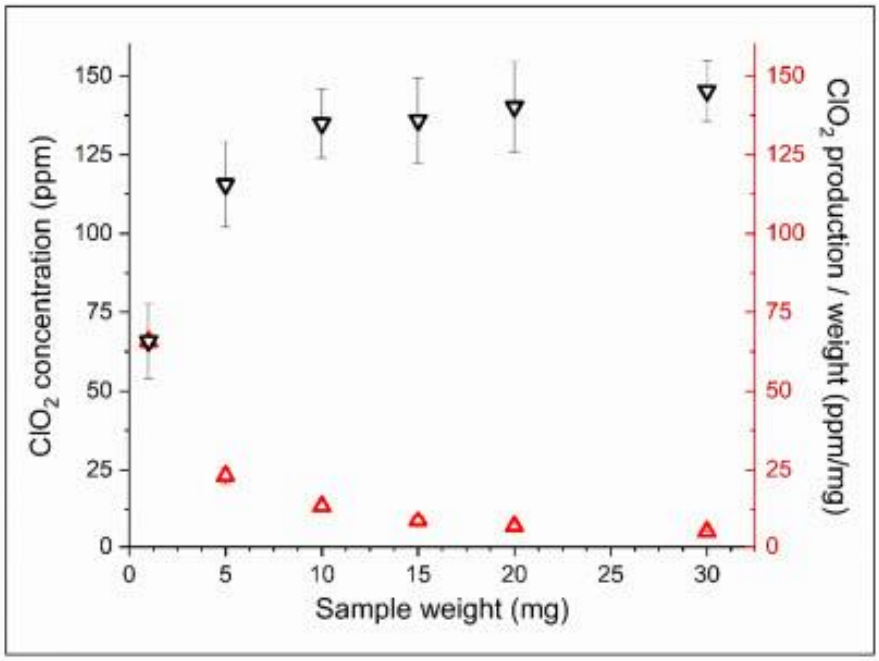

Figure 4. Chlorine dioxide production and chlorine dioxide production per weight of 1, 5, 10, 15, 20 and 30 mg samples.

Table 1. Yield of generated ClO_2 by samples of different weights calculated from the theoretical ClO_2 production of sodium chlorite in acidic environment.

m_{sample} (mg)	n_{NaClO_2} (mmol)	$c(ClO_2)_g$ (ppm)	$c(ClO_2)_g$ Theoretical (ppm) [1]	Yield (%)
1	0.217	65.79	73.57	89.43
5	1.084	115.54	367.85	31.41
10	2.168	134.93	735.69	18.34
15	3.252	135.91	1103.54	12.32
20	4.336	141.16	1471.38	9.59
30	6.504	145.23	2207.07	6.58

[1] Equations used to calculate the theoretical ClO_2 concentration are shown in the Supplementary Materials.

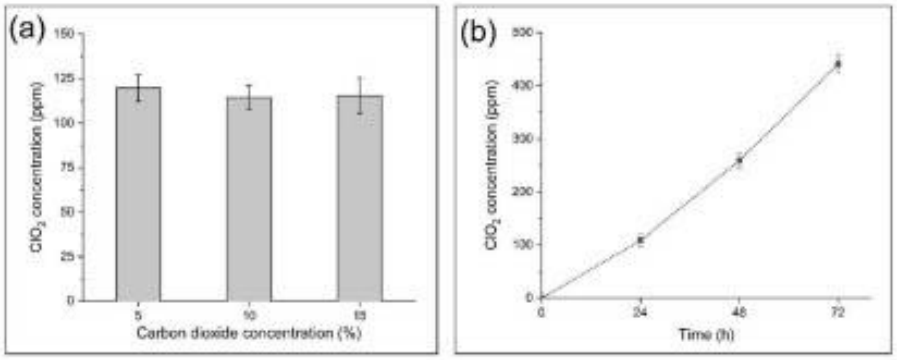

Figure 5. Effect of carbon dioxide concentration (**a**) and time (**b**) on ClO_2-generating ability of 5 mg $NaClO_2$-loaded PEO fibers.

3.4. Bacterial Inactivation Study

Figure 6a shows the setup of the bacterial inactivation experiment, while in Figure 6b, plates are shown after incubation and counting. We investigated the microorganism eliminating capacity of $NaClO_2$-loaded PEO fibers of 1, 5 and 10 mg, along with unloaded PEO fibers. The average number of surviving colonies per plate is shown in Figure 7. In the case

DOI:10.14753/SE.2022.2766

of unloaded PEO control samples, the number of colonies was too numerous to be counted in every parallel experiment, indicating that the reaction medium was optimal for bacterial growth (Figures 6b and 7). As the weight of $NaClO_2$-loaded PEO samples increased, the average survival decreased to zero. Only in one of the three parallels could surviving colonies be counted in the case of 1 and 5 mg $NaClO_2$-loaded PEO samples, indicated by arrows (Figure 6b). Bacterial growth did not occur with 10 mg of $NaClO_2$-loaded fibers.

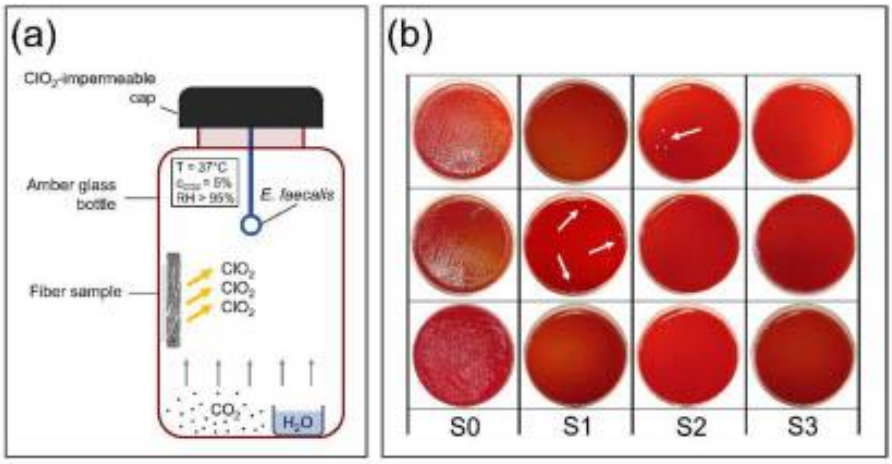

Figure 6. Experimental setup for bacterial inactivation study (a) and surviving colonies after incubation and counting (b) (S0: unloaded PEO fibers—control, S1: 1 mg $NaClO_2$-loaded PEO, S2: 5 mg $NaClO_2$-loaded PEO, S3: 10 mg $NaClO_2$-loaded PEO fibers).

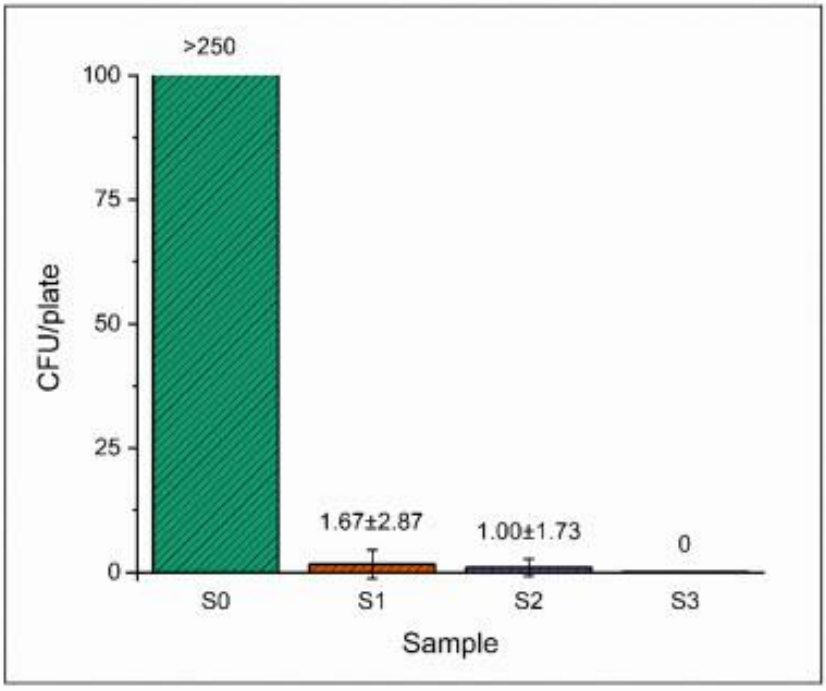

Figure 7. Average surviving colonies per plate of control (S0) and $NaClO_2$-loaded PEO fibers (S1: 1 mg, S2: 5 mg, S3: 10 mg).

4. Discussion

Scanning electron microscopy was used to evaluate the morphology of neat and $NaClO_2$-loaded PEO-based samples prepared by electrospinning. The spinning process resulted in smooth and uniform fibers both in the case of unloaded PEO and $NaClO_2$-loaded PEO samples; however, there was a substantial difference in the average fiber diameters.

DOI:10.14753/SE.2022.2766

The applied voltage was 10.5 kV during the spinning of PEO fibers, which appeared to be insufficient when spinning $NaClO_2$-loaded PEO samples; thus, the electric field needed to be increased. Generally, higher voltages result in lower fiber diameters, as the force pulling the fiber jet from the needle tip increases, resulting in the stretching and thinning of the ejected jet. However, studies have shown that the effect of higher voltages on fiber diameter may vary and depends on the composition of the precursor solution and other parameters of the electrospinning process [32,33]. The presence of inorganic salts increases the surface charge density and conductivity of the precursor polymer solution. The coulombic and electrostatic forces occurring between surface particles influence the stretching and thinning of the electrospun jet. Depending on the characteristics of the polymer macromolecule and the inorganic salt, the overall effect of the increasing salt concentration can result in either higher or lower average fiber diameter. In the case of polyvinylpyrrolidone (PVP), LiCl and $MgCl_2$ had an increasing effect on fiber diameter, while NaCl decreased the average diameter [34]. The average fiber diameter of LiCl-loaded PEO nanofibers increased with higher salt concentrations [35]. After a slight decrease in the lower concentration regions, $FeCl_3$ resulted in significantly thicker fibers when added to polyvinylidene fluoride. Lithium bromide, however, caused substantial thinning of the fibers when added to a styrene-based polymer system [36]. Figure 2 shows that $NaClO_2$ present in the $NaClO_2$-loaded PEO precursor solution and higher applied voltage together result in significantly thinner fibers compared to the PEO control sample.

Bands and intensities of the $NaClO_2$-loaded PEO and unloaded PEO spectra are similar, except for the region around the peak at 842 cm^{-1}, where a slight broadening can be observed on the $NaClO_2$-loaded PEO spectrum (Figure 3a). Sodium chlorite has its most intense bands at 800 and 823 cm^{-1} (Figure 3c). Due to the significant (ca. 50-fold) difference in the concentrations of PEO and $NaClO_2$, and the presence of the strong band at 842 cm^{-1} on the PEO spectrum, the intense peaks of $NaClO_2$ are covered on the $NaClO_2$-loaded PEO spectrum. The presence of $NaClO_2$ in the fibrous sample causes only a minor broadening at the base of the peak at 842 cm^{-1} on the $NaClO_2$-loaded PEO spectrum. Figure 3a,b also suggests that major changes did not occur in the structure and functional groups of PEO after loading $NaClO_2$.

To evaluate the sodium chlorite generating ability of $NaClO_2$-loaded PEO fibers, we placed samples into humid medium containing 5% (*v*/*v*) of CO_2 and incubated them at 37 °C for 24 h. One of the common methods of ClO_2 production is based on the reaction of sodium chlorite and acid (see Supplementary Materials). This phenomenon occurred in the fibrous mesh where carbonic acid, formed by water vapor and CO_2 gas in situ, was the reactant. The high surface-to-volume ratio of nanofibers provides enough reaction sites for $NaClO_2$ to form chlorine dioxide in the presence of H_2CO_3. A given portion of the generated chlorine dioxide dissolves in the excess of water placed in the 0.5 mL container. The concentration in the gas phase can be calculated from the data measured in the aqueous solution (see Supplementary Materials). In the case of the 1 mg $NaClO_2$-loaded PEO sample, the yield was above 89% after 24 h of incubation (Table 1). However, higher amounts of $NaClO_2$-loaded fibers did not result in proportionally higher ClO_2 concentrations in the same experiment (Figure 4). This phenomenon could be attributed to the chemical reaction limited by the low concentration of carbon dioxide. Therefore, to test our hypothesis, we investigated the effect of higher CO_2 concentrations on the ClO_2-producing ability of the $NaClO_2$-loaded fibers. The evaluation of the effect of carbon dioxide on ClO_2 production showed that the limiting factor was not the concentration of the acidic reactant, as the ClO_2 production did not change significantly after a two- and a three-fold increase in CO_2 concentration (Figure 5a). It has also been shown that the time of exposure has a substantial impact on ClO_2 production. Data suggest that the chlorine dioxide production in fiber samples is determined not only by the concentration of the reactants. When placing PEO nanofibers in a humid environment or fibers in contact with water directly, rapid dissolution and swelling of the mesh occur, resulting in a gel-like structure [37]. In our experiment, similar sizes were cut from the electrospun sample, but the thickness of the sample varied

DOI:10.14753/SE.2022.2766

with spinning time (Figure 1). When preparing larger weights, the spinning time extended, resulting in an increase in the thickness of the fiber mesh. As swelling occurs in the outer layers of the sample, the fibrous texture disintegrates, the surface-to-volume ratio decreases and the gel-like layer acts as a barrier for diffusion, resulting in a reduced number of reaction sites and slower ClO_2 production. The bacteria-eliminating ability of $NaClO_2$-loaded PEO samples was tested in humid medium (RH > 95%) containing 5% CO_2, similar to human breath. The overall ClO_2 production in the 24 h experiment led to substantial bacterial inactivation with only slight deviations occurring in the average CFU/plate values of 1 and 5 mg samples. The inoculating loops placed into the bottles contained ca. 2.8×10^6 CFUs, as their volume was 1 µL. The number of surviving colonies was too large to be counted regarding unloaded PEO fibers, while 1 and 5 mg of $NaClO_2$-loaded PEO fibers reduced the average CFU/plate to 1.67 ± 2.87 and 1.00 ± 1.73 after 24 h, respectively. Chlorine dioxide emitted into the gas phase from samples weighing 10 mg killed all bacteria placed on the inoculating loops.

The dissolution and gelation of the nanofibers in humid media can be a source of prolonged ClO_2 production; however, the structural changes may impair the usability of the fibrous mesh in certain conditions. The possible modifications and tailoring of the formulation by various polymers and compositions should be a matter of further investigation. A deeper understanding and investigation of the ClO_2 production kinetics is also desirable.

5. Conclusions

Chlorine-dioxide-emitting, $NaClO_2$-loaded PEO nanofibers were prepared via electrospinning. Chlorine dioxide generated from $NaClO_2$-loaded PEO samples eliminated bacteria from the gas phase successfully in 5% (*v*/*v*) CO_2 and RH > 95% in 24 h. The presence of the active ingredient did not result in major structural changes in the FTIR spectrum of the polymer. Chlorine dioxide production ability was measured from different weights of fibrous samples, and ClO_2 yield was calculated. Exposing smaller fibrous samples to CO_2 and humidity resulted in an increased ClO_2 production ability and higher yield, while a higher mass of fibrous layer of nearly equal surface area could not produce proportionally higher amounts of chlorine dioxide. The concentration of CO_2 did not alter the ClO_2 production of the samples, while time of exposure increased the concentration of the generated chlorine dioxide. Fibrous $NaClO_2$-loaded PEO samples present a substantial antimicrobial effect in conditions similar to exhaled air, as chlorine dioxide is formed in situ via the chlorite ion–acid reaction and emitted to the gas phase. One of the possible applications of the formulation discussed in our work may be the filters used in face masks, as the exhaled air is disinfected by chlorine dioxide generated from the fibers. Preventing the possible inhalation of ClO_2 and providing one-way flow may be achieved by using breathing valves; however, toxicological evaluation is required. Electrospinning represents an effective and continuous method in the preparation of nanofibers. Industrial implementation and upscaling of the technique are also widely studied [38]. Electrospun, nanofiber-based formulations equipped with effective antimicrobial agents can serve as suitable tools in the protection against the wide spread of pathogens.

Supplementary Materials: The following supporting information can be downloaded at: https://www.mdpi.com/article/10.3390/nano12091481/s1, Equations (S1)–(S3): Chlorine dioxide production via the chlorite ion—acid system, Table S1: $[ClO_2]_g$ (M)/$[ClO_2]_{aq}$ (M) distribution constant (K_θ) at different temperatures, Figure S1: Distribution constant at different temperatures along with the fitted polynomial equation [27,31].

Author Contributions: Conceptualization, B.P. (Barnabás Palcsó); methodology, B.P. (Barnabás Palcsó) and A.K.; formal analysis, B.P. (Barnabás Palcsó); investigation, B.P. (Barnabás Palcsó); resources, B.P. (Barnabás Palcsó), A.H., Á.G., B.P. (Balázs Pinke) and L.M.; data curation, B.P. (Barnabás Palcsó); writing—original draft preparation, B.P. (Barnabás Palcsó); writing—review and editing, A.K., A.H., Á.G., B.P. (Balázs Pinke), L.M. and R.Z.; visualization, B.P. (Barnabás Palcsó) and B.P. (Balázs Pinke); supervision, R.Z.; project administration, B.P. (Barnabás Palcsó); funding acquisition,

DOI:10.14753/SE.2022.2766

B.P. (Barnabás Palcsó), A.K. and R.Z. All authors have read and agreed to the published version of the manuscript.

Funding: This research was supported by ÚNKP-20-3-II-SE-35 and ÚNKP-20-4-I-SE-27 New National Excellence Program of the Ministry for Innovation and Technology, Hungary.

Institutional Review Board Statement: Not applicable.

Informed Consent Statement: Not applicable.

Data Availability Statement: Not applicable.

Acknowledgments: The authors would like to thank the Ministry for Innovation and Technology, Hungary for the financial support.

Conflicts of Interest: The authors declare no conflict of interest. The funders had no role in the design of the study; in the collection, analyses, or interpretation of data; in the writing of the manuscript, or in the decision to publish the results.

References

1. Messler, S.; Klare, I.; Wappler, F.; Werner, G.; Ligges, U.; Sakka, S.G.; Mattner, F. Reduction of nosocomial bloodstream infections and nosocomial vancomycin-resistant Enterococcus faecium on an intensive care unit after introduction of antiseptic octenidine-based bathing. *J. Hosp. Infect.* **2019**, *101*, 264–271. [CrossRef] [PubMed]
2. McDonnell, G.; Russell, A.D. Antiseptics and disinfectants: Activity, action, and resistance. *Clin. Microbiol. Rev.* **1999**, *12*, 147–179. [CrossRef] [PubMed]
3. Hardy, K.; Sunnucks, K.; Gil, H.; Shabir, S.; Trampari, E.; Hawkey, P.; Webber, M. Increased Usage of Antiseptics Is Associated with Reduced Susceptibility in Clinical Isolates of *Staphylococcus aureus*. *mBio* **2018**, *9*, Issue 3. e00894–e00918. [CrossRef]
4. Nicolae Dopcea, G.; Dopcea, I.; Nanu, A.E.; Diguta, C.F.; Matei, F. Resistance and cross-resistance in *Staphylococcus* spp. strains following prolonged exposure to different antiseptics. *J. Glob. Antimicrob. Resist.* **2020**, *21*, 399–404. [CrossRef] [PubMed]
5. Kampf, G. Antibiotic Resistance Can Be Enhanced in Gram-Positive Species by Some Biocidal Agents Used for Disinfection. *Antibiotics* **2019**, *8*, 15. [CrossRef]
6. Zhang, Y.Z.; Zhao, Y.J.; Xu, C.Q.; Zhang, X.C.; Li, J.H.; Dong, G.F.; Cao, J.M.; Zhou, T.L. Chlorhexidine exposure of clinical Klebsiella pneumoniae strains leads to acquired resistance to this disinfectant and to colistin. *Int. J. Antimicrob. Agents* **2019**, *53*, 864–867. [CrossRef]
7. Liu, W.J.; Fu, L.; Huang, M.; Zhang, J.P.; Wu, Y.; Zhou, Y.S.; Zeng, J.; Wang, G.X. Frequency of antiseptic resistance genes and reduced susceptibility to biocides in carbapenem-resistant Acinetobacter baumannii. *J. Med. Microbiol.* **2017**, *66*, 13–17. [CrossRef]
8. Herczegh, A.; Gyurkovics, M.; Agababyan, H.; Ghidán, Á.; Lohinai, Z. Comparing the efficacy of hyper-pure chlorine-dioxide with other oral antiseptics on oral pathogen microorganisms and biofilm in vitro. *Acta Microbiol. Immunol. Hung.* **2013**, *60*, 359–373. [CrossRef]
9. Wen, G.; Xu, X.; Huang, T.; Zhu, H.; Ma, J. Inactivation of three genera of dominant fungal spores in groundwater using chlorine dioxide: Effectiveness, influencing factors, and mechanisms. *Water Res.* **2017**, *125*, 132–140. [CrossRef]
10. Venkatnarayanan, S.; Sriyutha Murthy, P.; Kirubagaran, R.; Venugopalan, V.P. Chlorine dioxide as an alternative antifouling biocide for cooling water systems: Toxicity to larval barnacle Amphibalanus reticulatus (Utinomi). *Mar. Pollut. Bull.* **2017**, *124*, 803–810. [CrossRef]
11. Ofori, I.; Maddila, S.; Lin, J.; Jonnalagadda, S.B. Chlorine dioxide inactivation of Pseudomonas aeruginosa and *Staphylococcus aureus* in water: The kinetics and mechanism. *J. Water Process. Eng.* **2018**, *26*, 46–54. [CrossRef]
12. Stratilo, C.W.; Crichton, M.K.; Sawyer, T.W. Decontamination Efficacy and Skin Toxicity of Two Decontaminants against Bacillus anthracis. *PLoS ONE* **2015**, *10*, e0138491. [CrossRef] [PubMed]
13. Wei, R.; Wang, X.; Cao, Y.; Gong, L.; Liu, X.; Zhang, G.; Guo, C. Chlorine Dioxide Inhibits African Swine Fever Virus by Blocking Viral Attachment and Destroying Viral Nucleic Acids and Proteins. *Front. Vet. Sci.* **2022**, *9*, 844058. [CrossRef] [PubMed]
14. Noszticzius, Z.; Wittmann, M.; Kály-Kullai, K.; Beregvári, Z.; Kiss, I.; Rosivall, L.; Szegedi, J. Chlorine dioxide is a size-selective antimicrobial agent. *PLoS ONE* **2013**, *8*, e79157. [CrossRef] [PubMed]
15. Akamatsu, A.; Lee, C.; Morino, H.; Miura, T.; Ogata, N.; Shibata, T. Six-month low level chlorine dioxide gas inhalation toxicity study with two-week recovery period in rats. *J. Occup. Med. Toxicol.* **2012**, *7*, 8. [CrossRef] [PubMed]
16. Ma, J.W.; Huang, B.S.; Hsu, C.W.; Peng, C.W.; Cheng, M.L.; Kao, J.Y.; Way, T.D.; Yin, H.C.; Wang, S.S. Efficacy and Safety Evaluation of a Chlorine Dioxide Solution. *Int. J. Environ. Res. Public. Health* **2017**, *14*, 329. [CrossRef]
17. Vincenti, S.; de Waure, C.; Raponi, M.; Teleman, A.A.; Boninti, F.; Bruno, S.; Boccia, S.; Damiani, G.; Laurenti, P. Environmental surveillance of *Legionella* spp. colonization in the water system of a large academic hospital: Analysis of the four-year results on the effectiveness of the chlorine dioxide disinfection method. *Sci. Total Environ.* **2019**, *657*, 248–253. [CrossRef]
18. Trinh, V.M.; Yuan, M.-H.; Chen, Y.-H.; Wu, C.-Y.; Kang, S.-C.; Chiang, P.-C.; Hsiao, T.-C.; Huang, H.-P.; Zhao, Y.-L.; Lin, J.-F.; et al. Chlorine dioxide gas generation using rotating packed bed for air disinfection in a hospital. *J. Clean. Prod.* **2021**, *320*, 128885. [CrossRef]

DOI:10.14753/SE.2022.2766

19. Lowe, J.J.; Gibbs, S.G.; Iwen, P.C.; Smith, P.W.; Hewlett, A.L. Impact of Chlorine Dioxide Gas Sterilization on Nosocomial Organism Viability in a Hospital Room. *Int. J. Environ. Res. Public. Health* **2013**, *10*, 2596–2605. [CrossRef]
20. Lowe, J.J.; Hewlett, A.L.; Iwen, P.C.; Smith, P.W.; Gibbs, S.G. Evaluation of ambulance decontamination using gaseous chlorine dioxide. *Prehosp. Emerg. Care* **2013**, *17*, 401–408. [CrossRef]
21. Saini, R. Efficacy of preprocedural mouth rinse containing chlorine dioxide in reduction of viable bacterial count in dental aerosols during ultrasonic scaling: A double-blind, placebo-controlled clinical trial. *Dent. Hypotheses* **2015**, *6*, 65–71. [CrossRef]
22. Yeturu, S.K.; Acharya, S.; Urala, A.S.; Pentapati, K.C. Effect of Aloe vera, chlorine dioxide, and chlorhexidine mouth rinses on plaque and gingivitis: A randomized controlled trial. *J. Oral Biol. Craniofac. Res.* **2016**, *6*, 54–58. [CrossRef]
23. Palcso, B.; Moldovan, Z.; Suvegh, K.; Herczegh, A.; Zelko, R. Chlorine dioxide-loaded poly(acrylic acid) gels for prolonged antimicrobial effect. *Mater. Sci. Eng. C Mater. Biol. Appl.* **2019**, *98*, 782–788. [CrossRef] [PubMed]
24. Zhou, S.; Hu, C.; Zhao, G.; Jin, T.; Sheen, S.; Han, L.; Liu, L.; Yam, K.L. Novel generation systems of gaseous chlorine dioxide for Salmonella inactivation on fresh tomato. *Food Control* **2018**, *92*, 479–487. [CrossRef]
25. Son, W.K.; Youk, J.H.; Lee, T.S.; Park, W.H. The effects of solution properties and polyelectrolyte on electrospinning of ultrafine poly(ethylene oxide) fibers. *Polymer* **2004**, *45*, 2959–2966. [CrossRef]
26. Chuang, Y.-H.; Wu, K.-L.; Lin, W.-C.; Shi, H.-J. Photolysis of Chlorine Dioxide under UVA Irradiation: Radical Formation, Application in Treating Micropollutants, Formation of Disinfection Byproducts, and Toxicity under Scenarios Relevant to Potable Reuse and Drinking Water. *Environ. Sci. Technol.* **2022**, *56*, 2593–2604. [CrossRef]
27. Kály-Kullai, K.; Wittmann, M.; Noszticzius, Z.; Rosivall, L. Can chlorine dioxide prevent the spreading of coronavirus or other viral infections? Medical hypotheses. *Physiol. Int.* **2020**, *107*, 1–11. [CrossRef]
28. Fiore, E.; Van Tyne, D.; Gilmore, M.S. Pathogenicity of Enterococci. *Microbiol. Spectr.* **2019**, *7*, 189–221. [CrossRef]
29. Shetty, S.S.; Jayarama, A.; Karunasagar, I.; Pinto, R. A review on chemi-resistive human exhaled breath biosensors for early diagnosis of disease. *Mater. Today: Proc.* **2022**, *55*, 122–126. [CrossRef]
30. Saravanan, L.; Subramanian, S. Surface Chemical Studies on Silicon Carbide Suspensions in the Presence of Poly (Ethylene Glycol) and Chitosan. *Colloid Surf. Sci.* **2017**, *2*, 6–20. [CrossRef]
31. Kieffer, R.G.; Gordon, G. Disproportionation of chlorous acid. II. Kinetics. *Inorg. Chem.* **1968**, *7*, 239–244. [CrossRef]
32. Cramariuc, B.; Cramariuc, R.; Scarlet, R.; Manea, L.R.; Lupu, I.G.; Cramariuc, O. Fiber diameter in electrospinning process. *J. Electrost.* **2013**, *71*, 189–198. [CrossRef]
33. Edikresnha, D.; Suciati, T.; Khairurrijal, K. Preliminary study of composite fibers polyvinylpyrrolidone/cellulose acetate loaded by garlic extract by means of electrospinning method. *Mater. Today: Proc.* **2021**, *44*, A1–A4. [CrossRef]
34. Nartetamrongsutt, K.; Chase, G.G. The influence of salt and solvent concentrations on electrospun polyvinylpyrrolidone fiber diameters and bead formation. *Polymer* **2013**, *54*, 2166–2173. [CrossRef]
35. Yalcinkaya, F.; Yalcinkaya, B.; Jirsak, O. Influence of Salts on Electrospinning of Aqueous and Nonaqueous Polymer Solutions. *J. Nanomater.* **2015**, *2015*, 134251. [CrossRef]
36. Fan, L.; Xu, Y.; Zhou, X.; Chen, F.; Fu, Q. Effect of salt concentration in spinning solution on fiber diameter and mechanical property of electrospun styrene-butadiene-styrene tri-block copolymer membrane. *Polymer* **2018**, *153*, 61–69. [CrossRef]
37. Chen, C.-K.; Liao, M.-G.; Wu, Y.-L.; Fang, Z.-Y.; Chen, J.-A. Preparation of Highly Swelling/Antibacterial Cross-Linked N-Maleoyl-Functional Chitosan/Polyethylene Oxide Nanofiber Meshes for Controlled Antibiotic Release. *Mol. Pharm.* **2020**, *17*, 3461–3476. [CrossRef]
38. Angel, N.; Li, S.; Yan, F.; Kong, L. Recent advances in electrospinning of nanofibers from bio-based carbohydrate polymers and their applications. *Trends Food Sci. Technol.* **2022**, *120*, 308–324. [CrossRef]

DOI:10.14753/SE.2022.2766

nanomaterials

MDPI

Supplementary Materials

Formulation of chlorine dioxide-releasing nanofibers for disinfection in humid and CO_2-rich environment

Barnabás Palcsó[1], Adrienn Kazsoki[1], Anna Herczegh[2], Ágoston Ghidán[3], Balázs Pinke[4], László Mészáros[4,5] and Romána Zelkó[1]*

[1] University Pharmacy Department of Pharmacy Administration, Semmelweis University, Hőgyes Endre utca 7-9, H-1092 Budapest, Hungary
[2] Department of Conservative Dentistry, Semmelweis University, Szentkirályi utca 47, H-1088 Budapest, Hungary
[3] Institute of Medical Microbiology, Faculty of Medicine, Semmelweis University, Nagyvárad tér 4, H-1089, Budapest, Hungary
[4] Department of Polymer Engineering, Faculty of Mechanical Engineering, Budapest University of Technology and Economics, Műegyetem rkp. 3., H-1111 Budapest, Hungary
[5] MTA–BME Research Group for Composite Science and Technology, Műegyetem rkp. 3., H-1111 Budapest, Hungary
* Correspondence: zelko.romana@pharma.semmelweis-univ.hu; Tel.: +36-1-2170927

Citation: Lastname, F.; Lastname, F.; Lastname, F. Title. *Nanomaterials* **2022**, *12*, x. https://doi.org/10.3390/xxxxx

Academic Editor: Firstname Lastname

Received: date
Accepted: date
Published: date

DOI:10.14753/SE.2022.2766

The production of chlorine dioxide from sodium chlorite under acidic conditions can be described with the following equations [1]:

$$H^+ + ClO_2^- \rightleftharpoons HClO_2 \quad (1)$$

$$4\ HClO_2 \rightarrow 2\ ClO_2 + ClO_3^- + Cl^- + 2\ H^+ + H_2O \quad (2)$$

$$5\ HClO_2 \rightarrow 4\ ClO_2 + Cl^- + H^+ + H_2O \quad (3)$$

The first step is the protonation of chlorous acid with a pK_a of 1.72 (Equation 1). Chlorous acid then undergoes a self-decomposition reaction and chlorine dioxide is formed. There are two limiting cases of this process, and the stoichiometry can be calculated from the linear combination of Equation 2 and 3. First, an uncatalyzed reaction occurs, where the generated ClO_2:$HClO_2$ ratio is 1:2. In this reaction, chloride ion is produced, which acts a catalyzer and alters the process into Equation 3. Under ideal conditions, the ClO_2:$HClO_2$ ratio increases to 4:5. In our work we calculated the ClO_2 yield by Equation 3, assuming the ClO_2:$HClO_2$ ratio was 4:5.

The concentration of the produced chlorine dioxide in the gas phase was calculated from the absorbance measured in the water container placed into the glass bottles. Chlorine dioxide emitted from the fiber samples dissolves in the excess of water and a vapor-liquid equilibrium is reached. The distribution constant of ClO_2 between the two phases can be calculated from the concentrations measured in the gas and the aqueous phase (determined by Ishi) [2]. Using the data from Ishi's work we calculated the distribution constant regarding the parameters of our experiment.

Table 1. Table S1. $[ClO_2]_g$ (M)/$[ClO_2]_{aq}$ (M) distribution constant (K_θ) at different temperatures.

Temperature (°C)	Distribution constant
0	0.0155
5	0.0189
10	0.0222
15	0.0267
20	0.0316
30	0.0428
40	0.0578

Figure S1 shows the K_θ–temperature curve along with the fitted polynomial equation. Using the equation, the distribution constant at 37°C can be calculated. At 37°C the $[ClO_2]_g$ (M)/$[ClO_2]_{aq}$ (M) ratio was 0.053. Further calculation to determine $[ClO_2]_g$ form $[ClO_2]_{aq}$ values is described in the manuscript.

DOI:10.14753/SE.2022.2766

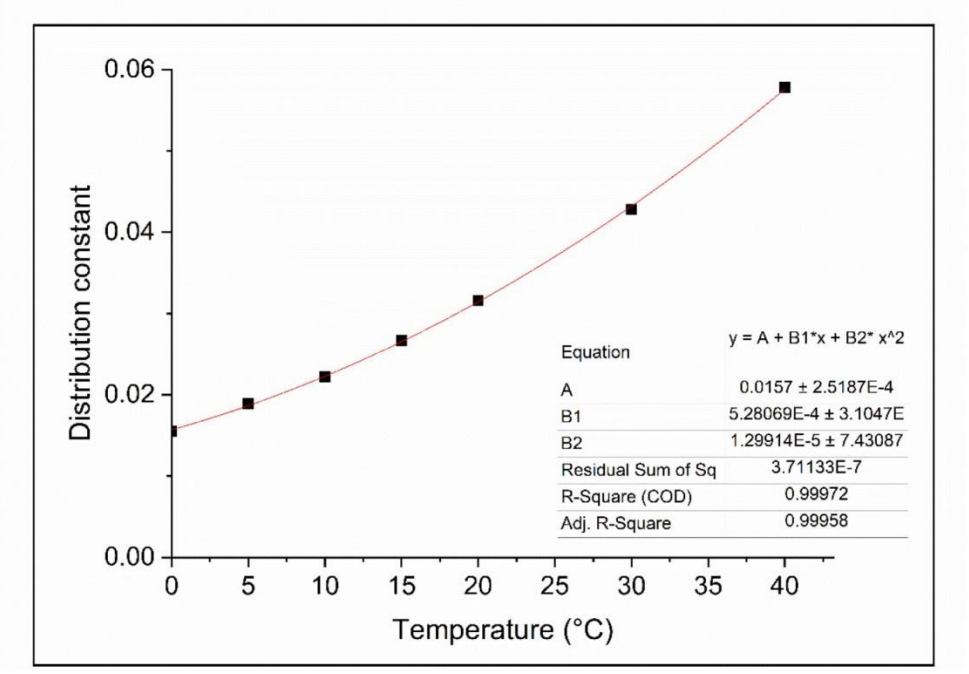

Figure S1. Distribution constant at different temperatures along with the fitted polynomial equation.

References

1 Kieffer, R. G. & Gordon, G. Disproportionation of chlorous acid. II. Kinetics. *Inorganic Chemistry* **7**, 239-244, doi:10.1021/ic50060a014 (1968).

2 Kály-Kullai, K., Wittmann, M., Noszticzius, Z. & Rosivall, L. Can chlorine dioxide prevent the spreading of coronavirus or other viral infections? Medical hypotheses. *Physiology International* **107**, 1-11, doi:10.1556/2060.2020.00015 (2020).